SLOPE FAILURE ALONG LOMSAK-CHUMPAE HIGHWAY

PHETCHABUN PROVINCE, THAILAND

Mr. Parinya Thongthiangdee

A Thesis Submitted in Partial Fulfillment of the Requirements for the Degree of

Master of Engineering in Geotechnology

Suranaree University of Technology

Academic Year 2003

ISBN 974-533-259-3

การพังทลายความลาดเอียงของมวลหินเส้นทางหล่มสัก-ชุมแพ จังหวัดเพชรบูรณ์ ประเทศไทย

นายปริญญา ทองเที่ยงดี

วิทยานิพนธ์นี้เป็นส่วนหนึ่งของการศึกษาตามหลักสูตรปริญญาวิศวกรรมศาสตรมหาบัณฑิต
สาขาวิชาเทคโนโลยีธรณี
มหาวิทยาลัยเทคโนโลยีสุรนารี
ปีการศึกษา 2546

ISBN 974-533-259-3

SLOPE FAILURE ALONG LOMSAK-CHUMPAE HIGHWAY,

PHETCHABUN PROVINCE, THAILAND

Suranaree University of Technology has approved this thesis submitted in partial fulfillment of the requirements for a Master's Degree.

Thesis examining committee

…….

(Dr. Chongpan Chonglakmani, Ph.D.)

Chairman

…….

(Assoc. Prof. Dr. Kittitep Fuenkajorn)

Member (Thesis Advisor)

…….

(Mr. Boonkarn Mongkonkarn)

Member

…….. ……..

(Assoc. Prof. Dr. Tawit Chitsomboon) (Assoc. Prof. Dr. Vorapot Khompis)

Vice Rector for Academic Affairs Dean of Institute of Engineering

ปริญญา ทองเที่ยงดี: การพังทลายความลาดเอียงของมวลหินเส้นทางหล่มสัก-ชุมแพ จังหวัดเพชรบูรณ์ ประเทศไทย
(SLOPE FAILURE ALONG LOMSAK-CHUMPAE HIGHWAY, PHETCHABUN PROVINCE, THAILAND) อาจารย์ที่ปรึกษา: รศ. ดร. กิตติเทพ เฟื่องขจร, 163 หน้า ISBN 974-533-259-3

หลวงสายหล่มสัก-ชุมแพและเสน วัตถุประสงค์ของงานวิจัยเพื่อศึกษาการพังทลายของความลาดเอียงของมวลหิน บนเส้นทางอวิธีการป้องกันการพังทลาย งานวิจัยเกี่ยวข้องกับการสำรวจภาคสนามและการคำนวณด้วยแบบจำลองทางคอมพิวเตอร์เพื่อศึกษาลักษณะการพังทลายความลาดเอียงของมวลหิน 11 แห่งตามเส้นทาง ข้อมูลที่ได้จากการสำรวจภาคสนามประกอบด้วย รูปร่างความลาดเอียงของมวลหิน สภาพรอยแตก รอยแยกในหิน อุปกรณ์ติดตั้งเพื่อป้องกันการพังทลาย รูปแบบการพังทลาย สภาพมวลหิน และน้ำใต้ดิน การประเมินค่าความแข็งของมวลหิน ใช้เกณฑ์การวิบัติของ Hoek-Brown และ Mohr-Coulomb ผลการสำรวจพบว่า ความลาดเอียงของมวลหินในปัจจุบัน มีเสถียรภาพ 3 แห่ง และไม่มีเสถียรภาพ 8 แห่ง ผลจากแบบจำลองทางคอมพิวเตอร์ ระบุว่าความแข็งของมวลหินจากวิธี Hoek-Brown มีค่าใกล้เคียงกับค่าความแข็งของมวลหินที่คำนวณโดยวิธีของ Mohr-Coulomb ในสภาวะอิ่มตัวด้วยน้ำ การหาค่าความแข็งแรงเฉือนของมวลดินและมวลหินโดยวิธีการสอบเทียบค่าจากโปรแกรมคอมพิวเตอร์ SLOPE/W เพื่อนำค่าเหล่านี้ไปคำนวณหาค่าปัจจัยความปลอดภัยความลาดเอียงของมวลหิน พบว่าค่าแรงยึดเหนี่ยวและค่ามุมเสียดทานของดินมีค่า 0.019 เมกกะปาสคาลและ 23 องศาตามลำดับ ค่าแรงยึดเหนี่ยวและค่ามุมเสียดทานของหินผุมีค่า 0.021 เมกกะปาสคาลและ 27 องศาตามลำดับ โดยทั่วไปความลาดเอียงของมวลหินในพื้นที่ศึกษา

มีแนวโน้มที่จะเกิดการพังทลายในช่วงที่ฝนตก เนื่องจากหน้าลาดเอียงมีความชันมาก งานวิจัยเสนอวิธีการป้องกันการพังทลายจากสองแนวคิดคือ (1) แนวคิดดั้งเดิมและ (2) แนวคิดของ Bieniawski การออกแบบวิธีการค้ำยันโดยแนวคิดดั้งเดิม พิจารณาลักษณะความลาดเอียงของมวลหินและรูปแบบการพังทลาย ในขณะที่การออกแบบวิธีการค้ำยันโดยแนวคิดของ Bieniawski พิจารณาค่า SMR ซึ่งใช้เป็นเกณฑ์กำหนดอุปกรณ์ค้ำยันความลาดเอียงของมวลหิน จากการศึกษาพบว่าการออกแบบวิธีการค้ำยันโดยแนวคิดดั้งเดิม เป็นวิธีการป้องกันการพังทลายที่สอดคล้องกับหน้างานจริง นอกจากนี้ยังประหยัดและสะดวกติดตั้งอุปกรณ์ค้ำยันมากกว่าวิธีการค้ำยันโดยแนวคิดของ Bieniawski

สาขาวิชาเทคโนโลยีธรณี ลายมือชื่อนักศึกษา.....

ปีการศึกษา 2546 ลายมือชื่ออาจารย์ที่ปรึกษา.....

PARINYA THONGTHIANGDEE: SLOPE FAILURE ALONG LOMSAK-CHUMPAE HIGHWAY, PHETCHABUN PROVINCE, THAILAND
THESIS ADVISOR: ASSOC. PROF. KITTITEP FUENKAJORN, Ph.D., P.E.
163 PP., ISBN 974-533-259-3

REMEDIAL MEASURES/SLOPE GEOMETRY/ROCK CONDITIONS/SHEAR STRENGTH PROPERTIES/ROCK SUPPORTS

The main objectives of this research are to investigate the slope failure and to propose remedial measures to prevent further failure along Lomsak-Chumpae highway, Thailand. The research involves field examination and computer modeling which has been performed to identify the failure characteristics of eleven rock slopes along the highway. The collected data are slope geometry, joint conditions and orientation, performance of the existing supports (if any), modes of failure, rock conditions, and groundwater conditions. The Hoek-Brown criterion and the Mohr-Coulomb criterion are used for estimating the shear strength properties of the rock mass. The results of field investigation indicate three stable slopes and eight unstable slopes. The results from computer modeling provide the shear strength estimates of Hoek and Brown criterion, which are in good agreement with the back-calculated strength under saturated condition. Calibrated shear strength parameters for calculating the safety factor of the rock slopes are performed by the SLOPE/W computer program. For soil, the obtained cohesion and friction angle are 0.019 MPa

and 23 degrees. For highly weathered rock, the obtained cohesion and friction angle are 0.021 MPa and 27 degrees. Most rock slopes along Lomsak-Chumpae highway pose the possibility of failure due to the slope face angle is great enough to initiate failures during rainfall. Two stabilization methods for each site are recommended: (1) the conventional approach and (2) the Bieniawski's approach. The conventional design process considers the slope characteristics and modes of failure. The Bieniawski's design process uses SMR values to design rock supports for each stability class. The rock supports of conventional approach are more specific uses, conservative, and convenient to install rock supports than those of Bieniawski's approach.

สาขาวิชาเทคโนโลยีธรณี ลายมือชื่อนักศึกษา.....

ปีการศึกษา 2546 ลายมือชื่ออาจารย์ที่ปรึกษา.....

ACKNOWLEDGEMENTS

The author is most grateful to the GMT Corporation Ltd for providing financial support throughout the study program.

The author also would like to thank Asst. Prof. Ladda Wannakao, Department of Geotechnology, Khon Kaen University and Mr. Somwang Changsuwan, Department of Highway, who provided the relevant reports.

Grateful thanks and appreciation are given to Assoc. Prof. Dr. Kittitep Fuenkajorn, thesis advisor, who allowed the author work independently, but gave a critical review of this research. Many thanks are also extended to Dr. Chongpan Chonglakmani and Mr. Boonkarn Mongkonkarn, who served on the thesis committee and commented on the manuscript.

Finally, the author extends his heartfelt gratitude to his parents who put him in the path of learning.

Mr. Parinya Thongthiangdee

TABLE OF CONTENTS

PAGE

TABLE OF CONTENTS (Continued)

PAGE

TABLE OF CONTENTS (Continued)

PAGE

TABLE OF CONTENTS (Continued)

PAGE

TABLE OF CONTENTS (Continued)

PAGE

TABLE OF CONTENTS (Continued)

PAGE

LIST OF TABLES

TABLE **PAGE**

LIST OF TABLES (Continued)

TABLE **PAGE**

LIST OF FIGURES

FIGURE **PAGE**

LIST OF FIGURES (Continued)

FIGURE **PAGE**

LIST OF FIGURES (Continued)

FIGURE **PAGE**

LIST OF FIGURES (Continued)

FIGURE **PAGE**

LIST OF SYMBOLS AND ABBREVIATIONS

C	=	Cohesion
D	=	Disturbance factor
F	=	Safety factor
F_1	=	Parallelism between joints and slope face strikes
F_2	=	Joint dip angle in the planar mode of failure
F_3	=	The relationship between the slope face and joint dip
F_4	=	The adjustment factor for the method of excavation
GSI	=	Geological strength index
H	=	Slope height
H_w	=	The height of water in slope
JRC	=	Joint roughness coefficient
L	=	Slope length
m_i	=	Material constant for the intact rock
P	=	Plane failure
Q	=	Tunneling quality
RMR	=	Rock mass rating
s	=	Material constant for the rock mass
S	=	Joint spacing
SMR	=	Slope mass rating
T	=	Toppling failure

LIST OF SYMBOLS AND ABBREVIATIONS (Continued)

T_{total}	=	Total tension of rock bolts
U	=	Uplift pore pressure
W	=	Weight of rock slope
σ_{ci}	=	Uniaxial compressive strength of intact rock
ϕ	=	Friction angle of soil or rock
γ	=	Unit weight of material
γ_{rock}	=	Unit weight of rock
γ_{water}	=	Unit weight of water
β	=	The angle of installed bolt parallel to the slope face
β_j	=	Joint dip direction
β_s	=	Slope dip direction
α_j	=	Joint dip direction
α_s	=	Slope dip direction
Ψ_f	=	Slope face angle
Ψ_p	=	Failure plane angle

CHAPTER I

INTRODUCTION

1.1 Background of problems and significance of the study

Lomsak-Chumpae highway was constructed over 20 years ago to shorten the distance from the north to the northeast of Thailand. It is 105 kilometers long, cutting across Phetchabun province and Khon Kaen province. The area is a part of Dong Phraya Yen Mountain range, which is a mountainous terrain. The problem of slope failures along the road cuts has repeatedly occurred on some locations. During the past five years, slope stabilization schemes had been repeatedly implemented which mainly involved various combinations of rock bolts, wire mesh, shotcrete, drained pipes, and gabion. Few years after the installation, it was proved that they could not effectively prevent the failures. The recent failures brought down both earthen and installed materials, and obstructed the traffic for several hours. This has posed severe economic impacts on the commercial and tourism of the regions. The present research involves an attempt at identifying the true mechanisms governing the instability, offering the reasons for the ineffectiveness of the previous stabilization methods, and proposing new remedial methods to prevent further failure.

1.2 Research objectives

The objectives of this research are to determine a potential slope failure and a remedial measure to prevent further failure along Lomsak-Chumsak highway, to

locate the potential of instability areas along the road cuts, and to study the engineering properties of the rocks by means of field investigation and computer simulation for predicting further slope failures.

1.3 Research hypothesis

a. The study uses the data from the Department of Highway (DOH) and the Department of Geotechnology, Khon Kaen University. It is assumed here that these data are correct and reliable.

b. The Hoek-Brown criterion is used for estimating the rock mass strength of some slopes that have no effects from the structural control.

c. The Mohr-Coulomb criterion is used for determining the shear strength parameters (cohesion and friction angle) of some structural controlled slopes.

d. The failed slopes are used for determining the shear strength parameters by back-calculated strength.

e. The friction angle and cohesion are assumed here that these parameters control rock slope stability. Therefore, Hoek-Brown and Mohr-Coulomb criterion that consist of cohesion and friction angle are applicable for the rock slope stability analysis here.

1.4 Research methodology

This research is divided into 8 tasks, as follows.

a. Task 1: Literature review

The objective of the literature review is to collect and examine the previous studies on the geological conditions of the sites (Wannakao et al., 1985; Changsuwan,

1984), and the case studies from the published papers (journals, proceedings, and conferences).

b. Task 2: Field investigation

Field investigation will be conducted along Lomsak-Chumpae highway, Amphoe Lomsak, Phetchabun province, Thailand. The purpose of field investigation is to obtain geological engineering data of the sites. The study criteria follow as much as practical the methods suggested by the International Society of Rock Mechanics (Brown, 1981). The data include slope geometry, joint conditions and orientation, intact rock strength, performance of the existing rock supports (if any), modes of failure, rock conditions, and groundwater conditions. The data obtained from fieldwork will be used for kinematics analysis and computer simulation.

c. Task 3: Kinematics analysis

The objective of the kinematics analysis is to determine the possibility of sliding by using a stereonet. The measurements of the strike and dip angle of joints and beddings are plotted on a stereonet. The stereonet provides pole plots and plane plots by using the computer program, “DIPS”, version 3 (Rock Engineering Group, 1989).

d. Task 4: Computer simulation

The objective of the computer simulation is to calibrate and back-calculate the shear strength parameters of soil and rock for predicting the slope failure. Several values of properties are assumed in the computer simulation, which eventually gives safety factors close to the actual field condition. The Hoek and Brown failure criterion (Hoek et al., 2002) will be used. The chosen input parameters follow as much as practical the methods suggested by Hoek et al. (2002). The dry condition

and fully saturated condition are used for back-calculated strength. The SLOPE/W (GEO-SLOPE International, 1995) will be used in the back analysis. The results will reveal the shear strength parameters and the safety factors of each site.

e. Task 5: Analysis

The analysis aims to predict the slope failures. Both Hoek-Brown and Coulomb criterion are compared. The analysis will reveal the similarity and the difference of their shear strength parameters. The expected results give the shear strength parameters and the safety factors for pre-failures and post-failures. The obtained shear strength parameters are used for predicting the slope failures, and failure characteristics.

f. Task 6: Verification of the results

The objective of the verification of the results is to examine the correctness of the computer simulation. It can be done by using the range of disturbed and undisturbed material properties from back analysis results (Hoek and Bray, 1981) for comparison with the obtained results (friction angle and cohesion). The obtained results are checked with the actual field conditions.

g. Task 7: Recommendation for remedial methods (support design)

The objective of this task is to suggest the suitable means for preventing slope failure at each site. The remedial measures such as unloading, rock bolt, wire mesh, shotcrete, gabion, and drained hole will be considered for each slope location.

h. Task 8: Thesis writing

All research activities, methods, and results will be documented and compiled in the thesis. The contents or findings may be published in the conference, proceedings, and journals.

1.5 Scope and limitations of the study

a. The study involves field investigation on the geological engineering aspects of the rock slopes along Lomsak-Chumpae highway, Amphoe Lomsak, Phetchaboon province, Thailand.

b. Significant slope locations from km 16+450 to km 78+680 are emphasized.

c. The study starts with desktop study and collection of existing information from the relevant books, reports, journals, conferences, and proceedings.

d. Field investigation will be conducted on stable and unstable slopes along the highway to understand their recent massive failures.

e. The collected data include slope geometry, joint condition and orientation, performance of the existing rock supports (if any), modes of failures, rock conditions, and groundwater conditions.

f. The methods of investigation follow as much as practical the methods suggested by the International Society of Rock Mechanics (Brown, 1981).

g. Drilling exploration, geophysical exploration, and laboratory testing are excluded.

h. Software used in the thesis is SLOPE/W (GEO-SLOPE International, 1995) and RocLab (Hoek et al., 2002).

i. Computer modeling divides the layer of slope into two layers such as soil layer and highly weathered shale.

j. Analysis method in the SLOPE/W is Bishop's simplified (Bishop, 1955).

k. Support design includes unloading, rock bolt, wire mesh, shotcrete, gabion, and drained hole.

l. Only two joint shear strength criteria are used in this study: Mohr-Coulomb criterion and Hoek-Brown criterion.

1.6 Thesis contents

The first chapter introduces the thesis, by briefly describing the background of problems and significance of the study, and identifying the research objectives, the research hypothesis, the research methodology, and the scope and limitations of the study. The second chapter describes the literature review. Detailed previous studies of the site, geology of the site, slope history, climate, transportation, discussion on slope failures, classification of slope failures, factors affecting slope stability, geological engineering aspects, and remedial measures are provided. Relevant literatures including those in journals, proceedings, and reports have been reviewed. Chapter three describes the field investigation. This chapter contains introduction, methods of field investigation, results of field investigation, and cause of massive failure. Computer modeling is presented in chapter four. This chapter contains the objective of the computer modeling, computer program and model construction, material properties, groundwater conditions, back analysis for shear strength properties, and calibrated shear strength parameters for computer modeling. Chapter five shows the analytical results obtained from field investigation and computer modeling that consist of failure characteristics, results of calibrated shear strength parameters and the back analysis. Chapter six describes the scheme of rock slope

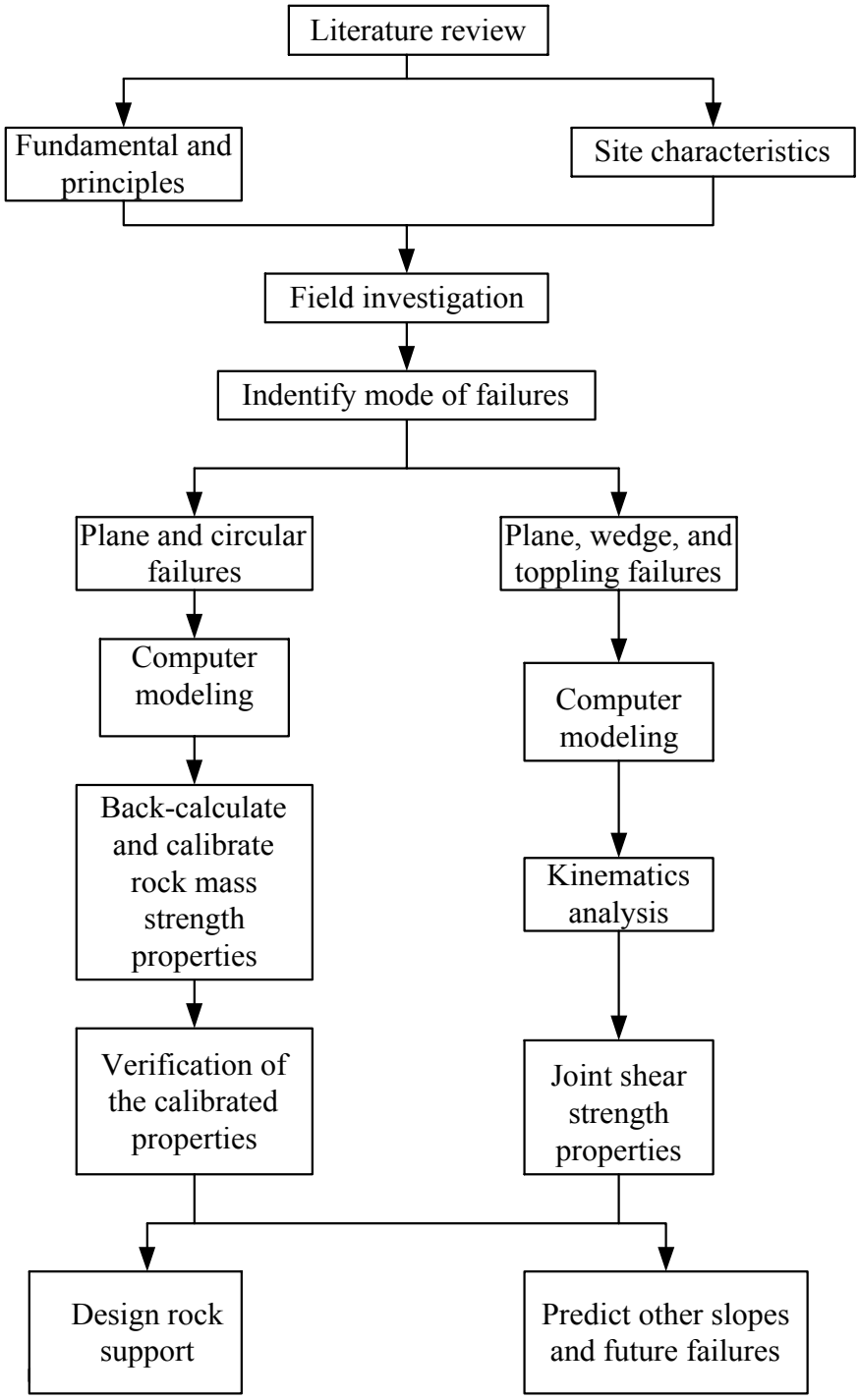

Figure 1.1 Flow chart of the study on slope failures along Lomsak-Chumpae highway, Thailand.

stabilization for each site. Chapter seven provides the conclusions, discussions, and recommendations for future studies.

CHAPTER II

LITERATURE REVIEW

2.1 Previous studies of the site

Changsuwan (1984) investigated all cut slopes along Lomsak-Chumpae highway, Amphoe Lomsak, Phetchabun province, Thailand. He used NGI tunneling quality index (Q-system) and assessed rock mass quality, i.e. poor or good quality. Wannakao et al. (1985) studied the cut slopes along Lomsak-Chumpae highway from km. 18 to 24 where the cut slopes intensely failed. They reported that the slope failures at the site could be classified into plane failure, circular failure, wedge failure, toppling failure, and rock falls. Figure 2.1 shows location map of the study area along Lomsak-Chumpae highway, Thailand.

2.1.1 Geology of the site

Regional rock strata of investigated and adjacent areas are in north-south trending. Fortunately the highway cuts thorough in the east-west trending, it reveals the geologic sections of the area clearly. The rock exposed along the road cuts is Paleozoic strata, which is a part of the Phetchabun fold-belt and Mesozoic strata of Khorat group. Many geologists have studied geological history of the area. The relevant published papers are of Chonglakmani and Sattayarak (1978) who study the Mesozoic and Paleozoic strata. Paleozoic strata are studied by Helmcke (1982). Figure 2.2 shows geologic map of the study area.

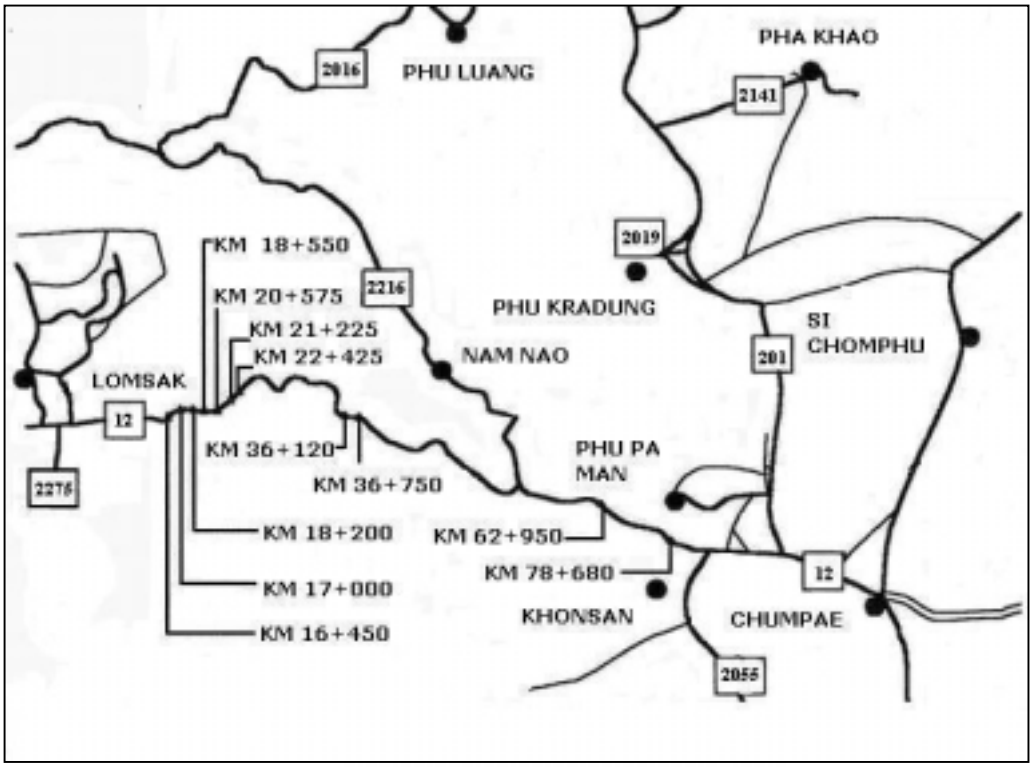

Figure 2.1 Location map of the study area along Lomsak-Chumpae highway, Thailand.

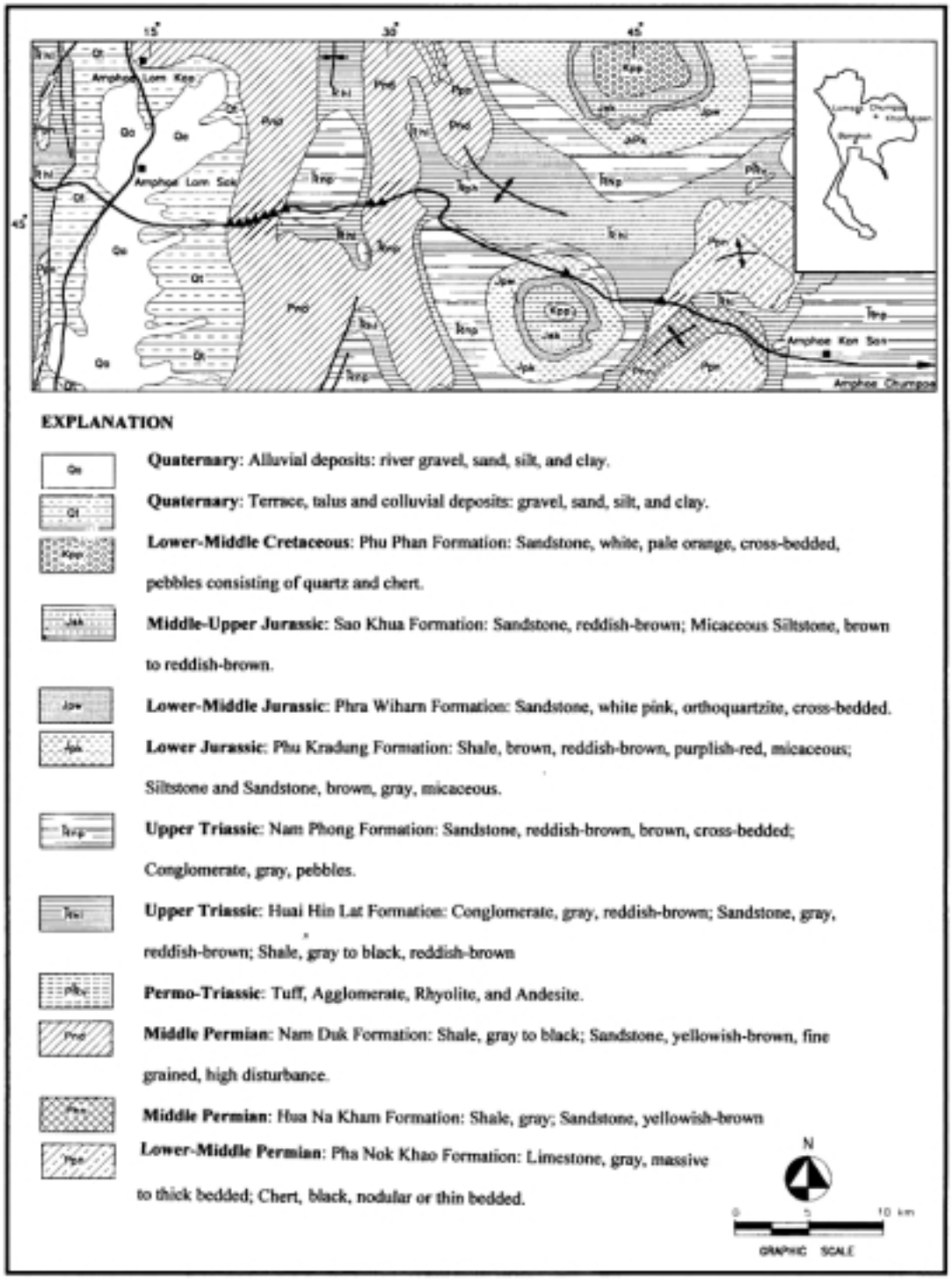

Figure 2.2 Geologic map of the study area (modified from Chonglakmani and Sattayarak, 1979).

Tightly folded and faulted Paleozoic strata are exposed at km. 16-21.5 and at km. 34-42. Chonglakmani and Sattayarak (1978) believe that these strata, which are called as Nam Duk formation, are of Lower Permian to Middle Permian. They state that this formation is geosynclinal sequence, consisting of limestone interbedded with sandstone and shale. Helmcke (1982) has divided these strata into molasse (post-orogenic stage), flysh (syn-orogenic stage), and pelagic (pre-orogenic stage) facies. He reports that the flysch strata and Molasse strata have different styles of deformation and belong to two different stock works. An upper stock work does not show cleavage and a lower stock work is characterized by slaty cleavage. He finds that Nam Duk formation at km.16-21.5 is pelagic facies with flysch facies at km.18.5-19.5, but at km.34-42 is molasses facies. He points out that folding of flysch strata inclines toward the east and shows monoclinic symmetry. Over thrusts are developed quite frequently; slaty cleavages are also well-developed in shape; kink bands incline towards the west are also developed. On the contrary, folding in the molasses strata tends to be upright and tight or slightly inclined toward the west. Faults are steep. Cleavages and kink bands are not developed. Deformation of these strata is due to tectonic activities during Upper Permain-Middle Triassic, a major episode correlated with the Indosinian orogeny. Andesitic and dioritic dikes are commonly found in cutting through these strata.

Mesozoic strata, Khorat group, expose from km.21.5-34. These strata composed of reddish brown to brownish red competent sandstone interbedded with incompetent siltstone. Thick conglomeratic sandstone beds are also found in the unit. Permian rocks are thrusted over Mesozoic rocks at km.21.5. These thrust faults activities, during Cretaceous to Tertiary, cause slight deformation and tilting in

Mesozoic strata. Angular unconformity between Mesozoic and Paleozoic rocks is found at km.34. Andesitic, rhyolitic agglomerate and tuff, volcanic extrusion during Triassic-Lower Jurassic, expose at km.42-46. Conglomerate, sandstone, siltstone and mudstone of Mesozoic strata are found again at km.46-77.

Other Permian strata are found again at km 77 to Amphoe Khon San. However, these strata, Pha Nok Khao, are different from Nam Duk formation. They consist of gray limestone alternated with bedded chert and shale. These strata are less deformed and more calcareous than Nam Duk strata. Chonglakmani and Sattayarak (1978) believe that the Pha Nok Khao in the area belongs to shelf facies.

Geological structures from km 18-24 are investigated in details. Major structures are beddings, foldings, jointings, fractures, and cleavages. Attitudes of these structures are recorded and mapped. Geological structures of Paleozoic and Mesozoic strata are studied separately. Nam Duk formation is subjected to Indosinian activities; therefore, it shows more complicated structures than Mesozoic strata.

Major bedding planes and slaty cleavages in shale of the formation are in N-S trending and dipping westward. Shale and slaty shale strata are steeply dipping and easily deformed. Dipping of these strata varies from west to east.

Tight chevron folds are very common in the formation. Axes of folds are approximately in northeast-southwest direction. Tension fractures and fracture cleavages occur at the limbs and the crest of folds is filled with calcite. Tension fractures are also found where igneous dikes intruded through the formation. Thrust faults found in the area are in NE-SW directions with gentle dipping about 15-25 degrees to the west.

Mesozoic strata have simpler structures than Nam Duk formation. These rock units subject to less activity. Therefore, bedding planes of these strata are gentle dipped. Major trend of the bedding is N-S direction. However, steeply dipping of bedding planes is found near the contact with Nam Duk formation where faults thrust. These units form a broad open syncline.

2.1.2 Slope history

The highway was constructed in 1970. The excavation was made primarily by the drill-and-blast method. The design was relied on the benching concept, which resulted in relatively high slopes. The working slopes vary from 50 to 70 degrees, the bench height from 10 to 20 meters, and the total slope height from 10 to 70 meters. The slope toe is normally less than 1.5 meters from the edge of the pavement. This narrow gap later posed some difficulties in terms of the rock stabilization. A trench was excavated at the slope toe to catch the rock fragments and to drain the surface runoff. After excavation, the slope toe was generally overlain by clayey soil. Thickness of the soil layer was about 2-5 meters. Few years after in services, minor rock falls had been observed, particularly during and after heavy rainfall.

In 1984, Changsuwan used the NGI tunneling quality index to classify the rock mass forming the slopes along the highway. The objective of this geo-engineering classification is to assist in the stability evaluation, and the design of the rock support. It was reported that from km 16 to km 79, there were at least ten unstable rock slopes. The rock mass forming these slopes was classified as poor to very poor based on the quality index. The modes of failure included plane sliding and

circular failure. The failure resulted in minor debris flow, which usually associated with the heavy rainfall.

In 1985, Wannakao et al. (1985) investigated the rock slopes along the highway from km 18 to km 24 where the failures were frequent. It was reported that large-scale plane failure occurred at km 19. The bedding planes of slaty-shale were nearly parallel to the slope faces, and were daylighted at some parts of the slope. This resulted in a progressive failure on the slope face. Circular failures were also found on the slopes between km 19 and km 21.5. It was concluded that small spacing and low shear strength of the rock joints caused by the weathering and erosion processes contributed to the observed circular failure. These investigators also concluded that even though most of the failures were progressive, the failure processes appear to be only minor rockfall and relatively small-scale debris flow. In addition, they took the rock samples to perform tilt test. The obtained results give the friction angle from 30 to 65 degrees. The trenches and gabion had been effective in trapping the rock debris. The rock fragments rolling onto the pavement were quickly removed by the on-site workers.

In 1987, an attempt was made by the Department of Highway (DOH) to improve the stability of several slopes along the highway. Shotcrete (2-7 cm thick) and wire mesh were vastly applied onto the entire slope face for at least ten locations along the highway. Short drained pipes, made of 50 cm long perforated PVC, were installed on the slope face to drain water behind the shotcrete. The drained pipes had a square pattern with an average spacing of 1.5 meters.

Since the year 2000, massive failure had repeatedly occurred on some slopes where the shotcrete has been installed. The massive slope failures brought

down both the earthen and the supported materials. The remaining rock mass on the slopes also appears to be very unstable. Until then, through the service life of the highway, such massive failure had never occurred.

2.1.3 Climate

Rainfall data of Amphoe Lomsak are obtained from the Highway District of Phetchabun province (2002). They show continuously yearly rainfall from 1995 to 2001. In 1995, the maximum monthly rainfall during 12 months was 319.5 mm on August, 276.7 mm on July, and 121.2 mm on September. The maximum monthly rainfall in 1996 was 400.2 mm on September, 277.1 mm on August, and 186.5 mm on April. It can be clearly seen that the three maximum monthly rainfalls in 1997 were 266.3 mm on August, 243.1 mm on July, and 222.4 mm on September. The three maximum monthly rainfalls in 1998 were 200.8 mm on May, 171.8 mm on August, and 143.3 mm on July. Cumulative rainfall in 1999 showed the maximum monthly rainfall was 215.3 mm on May, 201.2 mm on August, and 253.8 mm on September. In 2000, the maximum monthly rainfall was 322.2 mm on August, 253.8 mm on September, and 227.8 mm on May. The maximum monthly rainfall was 194 mm on May, 156.6 mm on August, and 155.5 mm on July 2001. Recently, the rainfall data recorded in 2002 from January to June does not show the maximum monthly rainfall due to lack of data. Generally, the maximum monthly rainfall during the past 8 years is likely occurred in May, July, August, and September.

2.1.4 Transportation

The Lomsak-Chumpae highway is named highway no. 12. The transportation data are from the Highway District of Phetchabun province (2002). From 1995 to 1999, the Department of Highway recorded an average annual traffic by

type such a pickup, a sedan, a light bus, a heavy bus, a light truck, a medium truck, and a heavy truck. The transportation of total vehicles from Ban Pak Chong-Namnao National Park at km 27+500 was 1972 cars in 1995. In 1996, the total vehicles from Ban Pak Chong-Namnao National Park were 1547. The amount of the traffic in 1997 was 1734. An average annual traffic in 1998 was 2023 cars. In 1999, the amount of traffic was 2407. The average annual daily traffic on highway in 2000 from Ban Pak Chong to Namnao National Park was 1555.

2.2 Discussions on slope failures

Popescu (2002) mentioned that each major rock slope failure is a case history in itself because factors causing the instabilities differ from former events. That is the reason why case studies will continue to be of paramount importance in developing effective procedures to minimize the rock slope instabilities by optimizing the balance between safety and economy. Each event will contribute new observations and conclusions from which we can gain experience and which progressively improve our knowledge.

Much progress has been made in developing techniques to minimize the impact of slope instabilities, although new, more efficient, quicker and cheaper methods could well emerge in the future. Rock slope instabilities may be corrected by one or any combination of four principle measures: modification of slope geometry, drainage, retaining structures, and internal slope reinforcement. There are a number of levels of effectiveness and levels of acceptability that may be applied in the use of these measures, for while one slide may require an immediate and absolute long-term correction, another may only require minimal control for a short period.

Whatever the measure chosen, and whatever the level of effectiveness required, the geotechnical engineer and engineering geologist have to be combined their talents and energies to solve the problem. Solving slope failure related problems is changing from what has been predominantly an art to what may be termed an art-science. The continual collaboration and sharing of experience by engineers and engineering geologists will no doubt move the field as a whole closer toward the science end of the art-science spectrum than it is at present.

2.3 Classification of slope failures

Slope failures can be classified according to an interest and the modes of failure. A brief review of such classification system is presented here.

2.3.1 Classification according to an interest

Slope failures can be classified into three categories according to the interest: mass movement along natural slopes, open pit slope failures, and slope failure associated with civil engineering works (Bhatta, 1992).

- Natural slopes

Flatter rock slopes in nature have been formed by erosion and weathering processes e.g. air, water, and glacier erosion, while steeper slopes have been formed by orogenic activities (like mountain building and igneous intrusion). Large masses of rock have been moved during the centuries to obtain more stable position. Natural slides on structural planes and other of weakness have been common phenomena. Deep-seated rockslides have been common phenomena in canyons through centuries. High Mountain dissected by deep canyons is subjected to

undercutting of their toe. Excessive shear stresses are created greater than the shearing resistance, resulting in failure and movement of large intact masses.

- Open pit slope failures

Open pit slopes are designed in such a manner that the slope angle is as steep as possible to extract the maximum amount of mineral from the mine at the lowest possible cost. Excavated slope is mostly temporary because excavation proceeds continuously into greater depths and widths. The excavated slope becomes final at the end of the lifetime of the project so that only temporary remedial measures for slope stability are taken.

- Civil engineering works slides

Excavation for civil engineering works includes highway or railway cuts, the structural buildings on rock, and tunnel portals. The excavated slope is the final slope for the lifetime of the project, so that permanent remedial measures design must be applied directly after the exposure of the work.

2.3.2 Classification according to modes of failure

The methods of Hoek and Bray (1981) are used widely for rock slope classification. The classification of rock slope is as belows:

- Plane failure

Plane failure occurs when a geological discontinuity, such as bedding planes, strikes parallel or nearly parallel (within approximately ± 20 degrees) to slope face. The plane must daylight in the slope face that means the dip of the plane is smaller than the dip of the slope face. Moreover, the dip of the failure plane must be greater than the friction angle of the plane.

-Circular failure

A rock body is divided into a discontinuous mass. The failure path is normally defined by one or more discontinuity. In case of soil slope, the individual particles are very small compared with the size of the slope, and a strongly defined structural no longer existed. Then the failure paths are in the circular form.

-Wedge failure

Wedge failure occurs when two discontinuities strike obliquely across the slope face, their line of intersection daylights in the slope face, and the line of intersection inclines at an angle larger than the angle of internal friction of the rock.

-Toppling failure

The toppling may result in an abrupt falling or sliding, but the form of movement is tilting without collapse. Toppling failure has traditionally been regarded as occurring in two modes: block toppling and flexural toppling. The former occurs when the center of gravity of a block of rock lies outside the outline of the base of the block, with the result that a critical overturning moment develops. The latter occurs under certain circumstance when a layered rock mass outcrop at a rock slopes, and the principal stress parallel to the slope face. Apart from these, inter-layer slip causes the intact rock to fracture and the resulting blocks to overturn.

-Rock falls

Rock falls are different from previous mentioned above. The path of moving does not follow any planes, but move through the air. These occur when two joint sets in competent rocks form various block sizes ranging from a few centimeters to large boulders.

2.4 Factor affecting slope stability

It is of primary importance to recognize the conditions that cause the slope to be hazardous for sliding and trigger the slope movement. Abramson et al. (1995) mentioned that slope stability is affected by the following:

2.4.1 Soil/rock fabric

Soil and rock have their own individual fabric. Mineral fabric may be sufficiently developed in some rocks to influence their engineering characteristics and properties. Examples of this are the fabric of schists, slates, shales, and laminated clays, which can cause marked anisotropy in their strength and deformation characteristics. In some cases, the decay of the mineral fabric could result in complete loss of strength upon disturbance e.g., quick clays. Both micro and macro fabric (major joints and beddings) are important features related to slopes. Details such as mineral orientation, stratification, fracture, faulting, shear zones, and joints must be gathered and assembled for a meaningful slope stability model to be developed.

Kitagawa (1999) studied genetical between the mechanisms of decomposition of granitic rocks. He reported that decomposed granitic rocks have been strongly fractures and characterized by remarkable alteration to clay minerals at hydrothermal stage before weathering. The clay veins were generally developed in the granitic rocks, in particular in the decomposed parts. The existence of clay veins had significant effect upon occurrence of slope failures. The slope failures were often occurred in some areas where smectite formed by hydrothermal activity was formed remarkably in granitic rocks.

Fujita (1999) discussed many landslides of the soft rock type and found that the fine clastic sediments were generally soft and weak. They were easily form-sliding surfaces for landslides. Ishii et al. (1999) studied the influence of the clay minerals on strength characteristics of the landslide clay. They reported that the strength of clay containing chlorite or montmorillonite was small.

2.4.2 Geological structures

Faquhar (1980) presented geological processes affecting the stability of rock slopes along Massachusetts Highways. Concurrent tasks were identification and measurement of slope parameters, review of technological constraints, description of testing programs, and survey of modeling capabilities, overlapping with refinement of geotechnical methods, improvement of slope technology, liaison with operating agencies, and research dissemination.

Geological structures of the slope-forming materials were a dominant feature in the slope behavior. For example, an attitude of beds was of direct relevance to consideration of potential instability in sedimentary rocks. These structures played an important role in understanding slope development processes, formation of valleys, ridges, escarpments, and the development of residual soils, talus, and colluvial deposits. Other major and minor structural discontinuities, such as faults, folds, and joints were carefully studied and mapped. In order to predict slope stability accurately, it was essential to recognize features such as a sequence of weak and a strong beds, thin marker beds, old failure surfaces, fault zones, and hydrogeological effects.

Omar et al. (2002) show case studies of geological factors contributing to slope failure along Selim highway, Malaysia. Based on the study, eight geological

factors contributing to cut slope failures are identified. The factors are geology, weathering, joints, faults, orientation, aperture, persistence, and spacing. Fiorillo (2003) analysed a slope along a stretch of the Adriatic coast, near Petacciato (Molise, Italy). He reported that several re-activations occurred in the past century, involving the zone between the build-up area and the sea, along a coastal slope over 2000 m long and 200 m high.

- Sequence of weak and strong beds

Weak rocks like shales and claystones that may be slickensided due to alteration are often critical in the development of slope instability. Elleboudy (1999) tried to assess the factors adverse to weaken and loosen the rock formation, comprising limestone interbedded with shale. He identified that the most adverse geo-environmental factors threaten the stability of the slope in order to adopt the appropriate preventive measures.

- Thin marker beds

Such beds may consist of coal, bentonite, or clay seams, or carbonaceous shale. These beds are easily missed during routine investigations.

-Old failure surfaces or shear planes

These surfaces and planes often lead to slope instability if they reactivate by weathering process, human activities such as over-falling, or undercutting by rivers and streams.

-Fault-related geologic features

Features such as the presence of ground-up materials near fault zones are often remolded, which may result in less resistance to sliding because of loss in shear strength. Groundwater is attracted to fault zone. Faults can act as conduits for flow

of water, which explains why rocks adjacent to them are often found to be hydro-thermally altered. Replacement of original minerals by clays, zeolites, and silica or calcite in void spaces, changes the character of the rocks near the fault zone, as a result of which stability problems may ensure.

In the case of soluble rocks, a fault usually localizes solution in them, leading to planar caverns developed along the fault zone. Caverns may develop along faults even in no soluble rocks as a result of washing out of gouge and crushed rock, and the opening of extension fractures oblique to the fault plane as a by-product of movement along the fault (Abramson et al., 1995). Fuenkajorn and Thongthiangdee (2002) indicate that the Mesozoic strata are subject to less tectonic activity than the Paleozoic strata. These effects result in fault and initiate complex structural geology in the study area such as gentle dip and steep dip angle in bedding. Suorineni et al. (1999) studied open stope mining affected by fault-related geological features. They indicate that faults increase the risk for slough in stopes near a fault.

-Hydrogeologic features

Such a feature may be a competent water bearing stratum, for example, sandstone, limestone, gravel, or sand, overlying a much less permeable cohesive or a highly weathered shale. The excess water in the pervious stratum contributes to slope failure in a number of ways-by creating high pore pressures in the materials forming the slope, by a washout of fines at the interface of the two layers of contrasting permeability, and by softening the underlying cohesive soils that make up the lower slope (Abramson et al., 1995). Enoki and Kokubu (1999) analyzed slope failure due to rainfall along the base rock and found that the result of permeability along the base rock had a marked influence in the conditions of slope failure. They suggested that

determination of permeability along the base rock meant of large-scale field tests that improved the accuracy of the measurements should be developed.

2.4.3 Groundwater

The ways of groundwater flow depend on the local geology. Water plays a very important role in slope stability, which is discussed at length. In brief terms, water can influence the strength of slope-forming materials by chemical and hydrothermal alteration, and increase pore water pressures. It subsequently decreases in shear strength, reduction of apparent cohesion due to capillary forces (soil suction) upon saturation, and softening of stiff fissured clays and shales (Abramson et al., 1995).

2.4.4 Ground stresses

All slope-forming materials are subjected to initial stress as a result of gravitational loading, tectonic activity, weathering, erosion, and other processes. Stresses produced by these processes are embodied in the materials themselves, remaining there after the stimulus that generates them is removed. For this reason, they are called residual stresses. Stress relief produces many structural features. Stress release activity is an important feature in many rock formations. High lateral stresses play a crucial role in initiating landslides in over consolidated clay and clay-shale. The stress history of slope-forming material is very important and is often used to differentiate normally consolidated soil. There are significant differences in terms of engineering properties between these two types of soils (Abramson et al., 1995). Nawari and Liang (1999) researched the fuzzy-based stability investigation of sliding rock masses. They mentioned that gravities, tectonics, weathering and erosion brought about the environment were factors contributing eventually to the instabilities

of rock slopes. Such factors are generally difficult to quantify with the present approaches. They presented a new procedure to estimate the risk of instabilities of sliding rock masses, using fuzzy-safety techniques.

2.4.5 Weathering

There are two types of weathering: one is the chemical weathering due to chemical changes. The other is the mechanical weathering as a result of wind, temperature changes, freeze-thaw cycles, and erosion by streams and rivers. The rate of chemical weathering ranges from a few days to many years and can affect both the short term and long term stability of slopes. On the other hand, mechanical weathering may take years before it has any adverse effect on slopes. Chemical weathering is the breakdown of minerals into new compounds by the action of chemical agents: acid in air, in rain, and in river water. Mechanical weathering is a process by which rock is broken into small fragments as a result of energy developed by physical forces. These examples are freeze-thaw cycles and temperature changes (Abramson, 1995). Maharaj (1999) presented the results of literature review and site investigations on the effects of weathering on slope stability in mud rocks and its implications for slope stabilization. He found that the weathering of mud rocks and the reaction of derivative acidic leaches with calcareous lithologies could cause the precipitation of gypsum. The precipitation of gypsum can increase potential of the susceptibility of weathered mud rock slopes to failure during rainfall. Lan et al. (2002) present a summary of the weathering profiles in south China and discuss their engineering and geological properties. A five-grade scheme has been adopted in the zoning of a granite weathering profile. A majority of the physical and mechanical properties have good statistical correlations with the degree of weathering.

2.4.6 Seismic effects

The displacements of earth structures are subjected from seismic loads (Michalowski and You, 1999). Many major and minor landslides occurred during earthquakes in the past. Geological features, whether major or minor, have a significant influence on slope stability during earthquakes. Earthquake results in an increase of shear stresses and a reduction of shear strength by increasing pore pressures. Liquefaction of small-saturated sand and silt lenses within a slope can result in a progressive failure of materials that may be relatively intensive to seismic disturbances.

2.5 Geological engineering aspects

2.5.1 Joint shear strength

Rock mass is heterogeneous, anisotropic and discontinuous. For a realistic assessment of the stability of rock slopes, estimation of the shear resistance of a rock mass both along any desired plane of potential shear and along the weakest discontinuity is essential. The shear strength of rock joints is markedly influenced by the roughness of the joint surfaces, as well as by the nature of the rock material itself. Since over twenty years, various attempts have been to quantify these effects. Most of such attempts either relied on experimental testing to derive empirical parameters, or on numerical models based on a discontinuous approach. The difficult major in dealing with these latter models appears to be the proper choice of the input data set of parameters (joint stiffness and strength).

Patton (1966) quantified the roughness by defining the dilation angle and developed a theory for the shear strength of rock joints based on such a measure of

roughness. Ladanyi and Archambault (1970) develop a model for the shear strength of rock joints, assuming that two modes of failure occur simultaneously. Although the idea behind their model is excellent, it is difficult to determine the parameters used.

Barton and Choubey (1977) established an empirical law for the shear strength of rock joints, adopting a term, called the joint roughness coefficient (JRC), to evaluate the roughness contribution to the shear strength. Barton provided a chart, which gives the JRC values for a set of ten rough profiles. By comparing these ten characteristic profiles with those of the real joint, it is possible to estimate the JRC values. To determine the JRC, Tse and Cruden (1979) converted Barton's table into equations. In order to define the JRC value, many researchers have investigated the correlation between the statistical parameters (Reeves, 1985) or the fractal dimensions (Lee et al., 1990; Xie et al., 1997) of Barton's profiles and the JRC values.

However, it is important to notice that the shear strength of a joint depends on the direction of shearing (Huang and Doong, 1990; Jing et al., 1992), the statistical parameters and the fractal dimensions (Seidal and Haberfield, 1995) give no directional information. Movements along rock discontinuities in foundations, dams, tunnels, and slopes can occur in various directions depending on the external forces (e.g., external loads, water pressures, earthquake forces, etc.) acting on the structure and on the kinematic constraints. Therefore, it is important to estimate the strength of rock discontinuities in different directions. The peak shear strength of joints shows anisotropic values due to the roughness variation with shearing direction in direct shear tests.

Even along one particular direction, the shear strength of a natural joint can be different between the forward and backward movements. In any case, a precise and quick measurement of the rough joint surface is important to study the shearing mechanism and both the peak and the residual strength of the rock joint, as well as the amount of dilatation the discontinuity undergoes. Roughness is difficult to quantify and, even when quantified, the result strongly depends on the chosen method of representation. Due to technological limitations, many studies focused on two-dimensional characteristics of roughness, by studying cross-section profiles (2D).

Although these researches have indicated important properties of the joint surfaces, several authors have shown that the morphology must be handled in a three-dimensional manner, considering both anisotropy and volumetric features (Lanaro et al., 1998; Xie et al., 1999).

Grasselli and Egger (2000) studied the shear strength equation for rock joints, based on 3-D surface characterization. They described a new approach to characterize the three-dimensional morphology of rough joint surfaces and proposed a new equation to evaluate the peak shear strength. They conclude that this expression is valid for joints considered totally matched at the beginning and the proposed criterion fits well the test results. However, the suggested new equation is based on few experimental shear strength data. It is essential, for the future, to increase the database in order to verify the applicability of the proposed shear strength criterion to a variety of rock joints.

2.5.2 Rock mass strength

Hoek and Brown (1980) proposed a failure criterion for rock. The original failure criterion was developed during the preparation of the book

"Underground Excavation in Rock". The criterion was required in order to provide input information for the design of underground excavations. The significant contribution that Hoek and Brown made was to link the equation to geological observations in the form of Bieniawski' s Rock Mass Rating (Bieniawski, 1976). The original criterion, with its bias towards hard rock was based on the assumption that rock mass failure was controlled by translation and rotation of individual rock pieces, separated by numerous joint surfaces. Failure of the intact rock was assumed to play no significant role in the overall failure process and it was assumed that the joint pattern was chaotic so that there were no preferred failure directions and the rock mass could be treated as isotropic.

Hoek (1983) reports that giving trouble throughout the development of the criterion has been the relationship between Hoek-Brown criterion, with the non-linear parameters m_i and s, and the Mohr-Coulomb criterion, with the parameters C and ϕ. Practically all software for soil and rock mechanics is written in terms of the Mohr-Coulomb criterion and it is necessary to define the relationship between m_i and s and C and ϕ in order to allow the criterion to be used to provide input for this software.

By 1988, the Hoek and Brown criterion was widely used for a variety of rock engineering problems, including slope stability analyses. As mentioned earlier, the criterion was originally developed for the confined conditions surrounding underground excavations and it was recognised that it gave optimistic results near surfaces in slopes. Consequently, in 1988 the idea of undisturbed and disturbed rock masses (Hoek and Brown, 1988) was introduced to provide a method for downgrading the properties for near surface rock masses.

Hoek (1990) addressed the on-going debate on the relationship between the Hoek-Brown and the Mohr-Coulomb criterion. The Hoek-Brown criterion had become wide spread and because of the lack of suitable alternatives, it was used on very poor rock masses. These rock masses differed significantly from the tightly interlocked hard rock mass model used in the development of the original criteria. In particular, it was felt that the finite tensile strength predicted by the original Hoek-Brown criterion was too optimistic and that it needed to be revised.

Hoek et al. (1992) proposed parameters *a* that provided the means for changing the curvature of the failure envelope, particularly in the very low normal stress range. Basically, the modified Hoek and Brown criterion forces the failures envelope to produce zero tensile strength.

Hoek (1994) and Hoek et al. (1995) introduced the concept of the geological strength index (GSI) as a replacement of Bieniawski's RMR. It had become increasingly obvious that the Bieniawski's RMR was difficult to apply to very poor rock mass. In addition, the relationship between RMR and m_i and s was no longer linear in these very low ranges. It was also felt that a system based more heavily on fundamental geological observations and less on 'numbers' was needed.

Hoek and Brown (1997) incorporated all of the refinements described above. In addition, a method for estimating the equivalent Mohr-Coulomb cohesioin and friction was introduced. In this method, the Hoek and Brown criterion was used to generate a series of values relating axial strength to confining pressure (or shear strength to normal stress) and these were treated as the results of a hypothetical large scale in situ tiaxial or shear test. A linear regression was used to find the average

slope and intercept and these were then transformed into a cohesive strength C and a friction angle ϕ.

Hoek et al. (1998) extend the range of the geological strength index (GSI) down to 5 to include extremely poor quality schistose rock masses such as the 'schist' encountered in the excavations for the Athens Metro and the graphitic phyllites encountered in some of the tunnels in Venezuela. This extension to GSI is based largely on work of Marie Benissi on the Athens Metro.

Afterwards, many papers of Hoek-Brown criterion put more geology in the failure criterion (Sonmez and Ulusay, 1999; Hoek and Marinos, 2000; Marinos and Hoek, 2000; Marinos and Hoek, 2001; Hoek, 2000). In particular, the properties of very weak rocks are addressed in detail for the first time. A new GSI chart for heterogeneous weak rock mass is introduced in these papers.

Currently, Hoek et al. (2002) address the long running issue of the relationship between the Hoek-Brown and Mohr-Coulomb criteria. An exact method for calculating the cohesive strength and friction angle is presented and appropriate stress ranges for tunnels and slopes are given. A rock mass damage criterion is introduced to account for the strength reduction due to stress relaxation and blast damage in slope stability and foundation problems. A windows program called "RocLab" is developed to accompany this paper.

However, the wide spread use of the Hoek and Brown criterion has not been complemented by equally increasing efforts to verify the same. There are very few reported cases in which the application of the Hoek-Brown failure criterion has been verified against actual observations of failure. It appears that many engineers have been busy applying the failure criterion, without taking the time to assess its

validity. Some verifications of the criterion are provided by Helgstedt (1997) that compared the predicted strengths with back-calculated value from a dam foundation and a large-scale natural slope, as well as from tests on rock filled. He concludes that the Hoek-Brown criterion consistently predicts too high shear strengths for these cases. All these cases are rock masses of poor to medium quality with GSI in the range of 22 to 55.

Kumar (1998) studies the effects on the shear failure envelope of Hoek-Brown criterion for rock mass. It is found that the change of material constant (a) affects both the shear envelope and the friction angle change.

Zhao (2000) studies the test of dynamic uniaxial and triaxial compression on granite of Singapore. The results are analyzed in this paper in order to examine the validity and applicability of the Mohr-Coulomb and the Hoek and Brown criterion to the rock material strength properties subjected to dynamic loads. The study indicates that rock material strength under dynamic loads can be approximately described by the Mohr-Coulomb criterion at low confining pressure range.

Sjoberg et al. (2001) and Pierce et al. (2001) have shown that the Hoek-Brown criterion for undisturbed in situ rock mass (D=0) results in rock mass properties that are too optimistic. The effects of heavy blast damage as well as stress relief due to removal of the overburden result in disturbance of the rock mass. It is considered that the "disturbed" rock mass properties (Hoek and Brown, 1988), D = 1 are more appropriate for these rock masses.

Lorig and Varona (2001) show that factors such as the lateral confinement produced by different radii of curvature of slopes (in plan) as compared with their height also have an influence on the degree of disturbance.

Cheng and Liu (1990) report the results of very careful back analysis of deformation measurements, from extensometers placed before the commencement of excavation, in the Mingtan power cavern in Taiwan. It is found that a zero of blast damage extended for a distance of approximately 2 m around all large excavations. The back-calculated strength and deformation properties of the damaged rock mass give an equivalent disturbance factor D = 0.7.

2.5.3 Determination of the strength parameters

The strength of rock masses is notoriously difficult to assess. Laboratory tests on core samples are not representative of a rock mass of significantly large volume. On the other hand, in situ strength testing of the rock mass is seldom practically or economically feasible. Back-analysis of observed failures can provide representative values for large-scale rock mass strength, but obviously, this is only possible for cases in which rock mass failure has occurred.

Sonmez et al. (1998) determine the strength of closely jointed rock. A computer program for the back determination of shear strength parameters mobilized in slope cut satisfies the Hoek and Brown criterion. The result has also been satisfactorily applied to slope failure in three open pit mines in Turkey.

Jiang et al. (1999) study a back analysis to determine unsaturated strength parameters. This method is based on the Bishop factor of safety equation. The result has the potential to determine the magnitude of residual cohesion and

friction angle from actual slope failures as long as the suction distribution along the slip surface at failure is known.

Sakurai and Nagayama (1999) deal with a back analysis method for assessing the stability of slopes which can determine not only a sliding plane, but also the strength parameters, such as cohesion and friction angle, by using displacements measured at the slope surface alone. This method is based on a concept of strain-induced anisotropic damage of rocks, and formulated by finite element method. They used conventional limit equilibrium for back analysis and reported cohesion and friction angle from measured displacements. The strength parameters are obtained; the factor safety can easily be evaluated.

Jiang and Yamagami (2002) study the slip surface within a failed slope that often involves a pre-existing interface or a weak layer. In such case, back analysis is extremely difficult to obtain Mohr-Coulomb shear strength parameters required for remedial work design because of heterogeneous. An artificial network model is developed for back-calculated strength parameters along the slip surface control by a weak layer. The neural networks could provide a useful tool for back-calculation of the strength parameters for a heterogeneous field surface controlled by a weak layer.

Schaefer (2002) studies the residual strength and back analysis of slopes in Pierre shale. A key to understanding the behaviour of slopes is its geologic history resulting in the information of fissures and old slide scars. Unloading and weathering have produced heavily consolidated clay shale that readily fails due to minor disturbances. Numerous studies have demonstrated that the peak strength of the layers may be represented by a friction angle of 10 to 12 degrees and residual

strengths are often only 5 or 6 degrees, with laboratory measured values as low as 3 degrees.

2.6 Remedial measures

Slope stabilization methods generally reduce driving forces; increase resisting forces, or both. Driving forces can be reduced by excavation of material from the appropriate part of the unstable ground and drainage of water to reduce the hydrostatic pressures acting on the unstable zone. Resisting forces can be increased by the followings. Water drained increases the shear strength of the ground, eliminates of weak strata or other potential failure zones, builds of retaining structures or other supports, provides in situ reinforcement of the ground, and treats by chemical treatment (hardening of soils) to increase shear strength of the ground. As an alternative to slope stabilization, adjusting the location of construction or selecting a different site all together can avoid the unstable slope.

Jamaludin and Hussein (1999) presented some experiences on method of stabilization and remedial works that carried on some fail fill slopes along the highway. They received the geotechnical data for remedial solution of the fill slope. Kabir and Hamid (1999) presented an anchored slope and gabion wall. Performance of the structure during last five monsoons was reported.

Al-Homoud et al. (1997) conducted geological and geotechnical investigation along a highway embankment landslide. They concluded the most appropriate remedial measure for road design and stabilization of the sliding area that it was found to be a combination of vertical reduction in embankment height and horizontal realignment. The remediation was implemented in the field successfully.

2.6.1 Unloading

Unloading is a technique to reduce the driving forces within a slide mass. The most common type of unloading is excavation of the head of a slide. In the case where the construction of a conventional embankment can lead to slope instability, lightweight fill materials can be used to lessen the driving forces caused by the embankment.

- Excavation

Excavation is a common method for increasing the stability of a slope by reducing the driving forces that contribute to movements. This can include removing weight from the upper part of the slope, removing all unstable or potentially unstable materials, flattering slopes, and benching. Some disadvantages associated with excavation are cost linked to accessibility (as the slope must usually be excavated from the top downward). The main advantage of excavation is typically low cost (Abramson et al., 1995).

-Lightweight fill

In embankment construction, lightweight fill reduced the driving force of the slope e.g., reducing the effect of land cutting in road (Nakano et al., 1999) and thereby increased the stability. Lightweight materials, such as slag, encapsulated sawdust, expended shale, cinders, shredded rubber tires, polystyrene foam, and seashells, were used successfully. Selection of the type of lightweight material depended on its cost and availability in local areas (Abramson, 1995).

2.6.2 Rock bolt

Reinforced rock becomes a competent structural entity either on its own or as part of the composite rock-steel or rock-concrete structure. Rock bolts perform

their task by one or a combination of several mechanisms. The simplest of suspension, a loose block, is secured in the slope face. Much more often, bolts act to increase the stress and the friction strength across joints, encouraging loose blocks or thinly stratified beds to bind together. Stillborg (1994) carries out a series of tests in which bolts are installed across simulated joints and subjected to tensile loading. This type of test gives more accurate representation of conditions encountered underground than does a standard "pull-out" test.

2.6.3 Wire mesh

The wire mesh, also called screen, used in ground support applications can be made from either woven or welded wire. Its main purpose is to support the rock between bolts, which is particularly necessary when the rock is closely jointed and the rock bolts are moderately to widely space. The wire mesh can also serve as reinforcement for shotcrete. Hoek (2000) describes remedial works, consisting of shotcrete, rock bolt, and wire mesh in Hong Kong. He reports that a chain link fence is very effective for minor rock falls as long as it is properly maintained.

2.6.4 Shotcrete

Shotcrete is concrete applied by spraying. Just like concrete, it contains fine and coarse gravel aggregate (sand and gravel), cement, water, and sometimes additives to accelerate setting or to improve flow (Lorman, 1968; Reading, 1966). It is applied pneumatically and is compacted dynamically under high velocity.

2.6.5 Gabions

Gabions are an alternative for toe protection where slopes are undercut by fast flowing water, along riverbanks and the tailrace channels of generating stations. They are constructed by filling wire baskets with durable crushed rock or

cobbles. The baskets, made of hexagonal woven-steel galvanized wire mesh, are wired together and filled in-groups. They are placed to overlap each other, forming a buttress wall that is rapidly and inexpensively constructed and has the further advantage of being able to tolerate substantial settlements and deformation.

2.6.6 Drainage

Of all stabilization techniques considered for the correction or prevention of landslides, proper water drainage is the most important. Drainage reduces the destabilizing hydrostatic and seepage forces on a slope as well as the risk of erosion and piping. Various drainage techniques are discussed below. Hoek (2000) describes the drained holes that thay are installed in Hong Kong. He comments inadequate drainage is the key factor in most failures. For drainage, to be efficient, special attention must be given to high transient groundwater pressure. Raking drains are used in occasionally, but problems can result from blockage due to poor design and lack of maintenance. Surface drains are usually constructed to intercept up-slope runoff, but they often similarly suffer from poor design and lack of maintenance.

-Surface drainage

Carefully planned surface drainage is essential for treatment of any slide or potential slide. Every effort must be made to ensure that surface runoff is carried away from and not seeping downwards into the slope. Such considerations are always made and are extremely important when evaluating a failure. Temporary remedial measures are usually considered after a landslide. They include using sandbags to divert water runoff away from the failure zone. The cracks are sealed with surface coatings such as shotcrete, lean concrete, or bitumen to reduce water

infiltration. The slope surface is covered with plastic sheets or the like to reduce the risk of movement during construction.

-Subsurface drainage

The factor of safety against failure on any potential slip surface that passes below the phreatic surface can be improved by subsurface drainage. Methods that can be used to be accomplishing subsurface drainage are drainage blankets, trenches, cut-off drains, horizontal drains, relief drains, and drainage tunnels.

CHAPTER III

FIELD INVESTIGATION

3.1 Introduction

The objective of the field investigation is to examine the rock slope characteristics along Lomsak-Chumpae highway, Amphoe Lomsak, Phetchabun province. The obtained data provide basis for identifying mode of failure and shear strength estimates, which are used in the kinematics analysis. This chapter describes the methods and results of the investigation.

3.2 Methods

Field investigation has been conducted on 11 unstable and stable rock slopes along the highway during November 2001 (winter season) and during May 2002 (rainy season). Equipment for the investigation includes global positional system (GPS), geological hammer, geological compass, measuring tape, and geological map with a scale 1:250,000, Phetchabun province. A route map of Thailand highway with a scale 1:1,000,000 is also used to locate the examined rock slopes. The study route ranges from 16^{o} 30' to 16^{o} 45' northern latitude and 101^{o} 15' to 102^{o} eastern longitude. The collected data include slope geometry, joint conditions and orientation, intact rock strength, performance of the existing rock supports (if any), modes of failures, and groundwater conditions. The method and criteria follow as much as practical those suggested by the International Society of Rock Mechanics (Brown, 1981).

3.3 Results

Table 3.1 summarizes the slope characteristics along Lomsak-Chumpae highway, Thailand. These include location number, rock type, slope height, slope orientation, number of joint sets, joint orientation, joint spacing, joint aperture, types of filled material, joint roughness coefficient (JRC), groundwater condition, existing supports, field determined intact rock strength, and stability condition. The slope characteristics are described as follows.

The slope location from km 16+450 to km 16+489 is on the left side of Lomsak-Chumpae highway. The rock is reddish-brown shale of Nam Duk Formation in Middle Permian. It is highly and heavily fractured. The uniaxial compressive strength of the intact rock is between 5 and 25 MPa. The slope height is 25 m. The orientation of the slope face is 70/60 degrees. The joints are dry. Soil and highly weathered shale appear on top of the slope. The existing supports include rock bolt and wire mesh. The length or rock bolt is 50 cm, with 2.5 cm diameter. Wire mesh is 6x7 cm in opening. Gabion wall consists of rock pieces of andesite, which is wrapped by wire mesh or chain link. The gabion wall is 50 cm wide and 50 cm high. Figure 3.1 shows the rock slope at km 16+450. The ravelling of soil/rock debris on the slope face was found from the upper to the lower slope faces.

The slope location from km 17+000 to km 17+200 is on the left side of Lomsak-Chumpae highway. The rock is gray shale of Nam Duk Formation of Middle Permian. It is highly weathered shale. The uniaxial compressive strength of the intact rock is between 25 and 50 MPa. The slope height is 25 m. The orientation of the slope face is 75/72 degrees. There are three joint sets having the representative orientation (strike/dip angle) 167/81 degrees, 81/77 degrees, and 306/74 degrees. The

Table 3.1 Slope characteristics obtained from field investigation.

Slope location	Rock Type	Slope Height (m)	Slope Orientation (Strike/dip) (Degrees)	Number of Joint Set	Joint Orientation (Strike/dip) (Degrees)	Joint Spacing (cm)	Joint Aperture (cm)	Filled Material	JRC	Ground-water condition	Existing Supports	Estimated Intact Rock Strength (MPa)
Km 16+450	Shale	25	70/60	N/A	N/A	N/A	N/A	N/A	N/A	Dry	Wire mesh, rock bolt	5-25
Km 17+000	Shale	25	75/72	3	J1: 167/81, J2: 81/77, J3: 306/74	5-10	0.5-1	Clay	5	Dry	No existing supports	25-50
Km 18+200	Shale	20	85/62	No joint sets	N/A	N/A	N/A	N/A	N/A	Dry	Shotcrete	5-25
Km 18+550	Slaty shale	35 .	190/48	3	J1: 115/81, J2: 14/38, J3: 185/60	5-20	0.1-1	Calcite	3-5	Dry	No existing supports	5-25
Km 20+575	Shale	15	225/45 (slope face), 225/64 (upper slope face)	3	J1: 80/64, J2: 198/56, J3: 334/53	5-15	0.1-1	Clay	1	Dry	Shotcrete, drained holes, and gabion	5-25
Km 21+225	Shale	15	55/57	3	J1: 86/64, J2: 225/36, J3: 311/82	5-15	0.1-1.5	Clay	1	Dry	Shotcrete and drained holes	5-25

Table 3.1 Slope characteristics obtained from field investigation (continued).

Slope location	Rock Type	Slope Height (m)	Slope Orientation (Strike/dip) (Degrees)	Number of Joint Set	Joint Orientation (Strike/dip) (Degrees)	Joint Spacing (cm)	Joint Aperture (cm)	Filled Material	JRC	Ground-water condition	Existing Supports	Estimated Intact Rock Strength (MPa)
Km 22+425	Sandstone	17	40/71	4	J1: 180/78, J2: 276/66, J3: 34/34, J4: 91/44	5-10	0.3-1	Clay	5	Dry	Rock bolt, wire mesh, gabion	50-100
Km 36+120	Shale	20	321/50	3	J1: 25/83, J2: 294/51, J3: 284/82	5-10	0.5-1	Clay	1-3	Dry	Shotcrete and drained holes	5-25
Km 36+750	Shale	15	303/48 (slope face), 300/60 (upper slope face)	N/A	N/A	N/A	N/A	N/A	N/A	Dry	Shotcrete and Drained holes	5-25
Km 62+950	Sandstone interbedded siltstone	15	156/55	4	J1: 99/24, J2: 135/80, J3: 165/64, J4: 216/61	5-15	0.1-0.8	Clay	5	Dry	No existing supports	25-50
Km 78+680	Limestone	20	265/60	5	J1: 65/48, J2: 133/71, J3: 107/26, J4: 203/74 J5: 256/63	10-30	0.5-1	Clay	3-5	Dry	No existing supports	50-100

Figure 3.1 Rock slope at km 16+450 (looking east). The rock is shale of Nam Duk Formation Middle Permian. Ravelling of soil/rock debris on the slope face found from the upper to the lower slope faces.

joint spacing is between 5 and 10 cm. Persistence of rock discontinuity is about 70 %. The JRC is estimated as 5. The joint aperture is between 0.5 and 1 cm. Filled material is clay. The joints are dry. The rock slope is unstable from rock falls. Figure 3.2a shows high variation of the folding of shale at km 17+000. Figure 3.2b shows the rock slope at km 17+000 at side view. Figure 3.2c shows rock falls found during rainy season on the slope surface and the ditch.

The slope location from km 18+200 to km 18+400 is on the right side of Lomsak-Chumpae highway. The rock is yellowish-brown shale of Nam Duk Formation in Middle Permian. The uniaxial compressive strength of the intact rock is between 5 and 25 MPa.The slope height is 20 m. The slope face is covered by shotcrete. However, the lithology of the rock can be deduced from the slope location nearby. The orientation of the slope face is 85/62 degrees. The existing supports include shotcrete, wire mesh, rock bolt, and gabion wall. The shotcrete is between 2 and 5 cm in thickness. Wire mesh is 6x7 cm in opening. The length of rock bolt is 50 cm, with 2.5 cm in diameter. The gabion wall of limestone is wrapped by wire mesh that consists of two layers of limestone. The upper layer wall comprises 80 cm wide and 80 cm high and the lower layer wall contains 50 cm wide and 50 cm high. Figurre 3.3 shows the rock slope at km 18+200, which is covered by shotcrete.

The slope location from km 18+550 to km 18+650 is on the right side of Lomsak-Chumpae highway, near Huai Tong Bridge. The rock is yellowish-brown slaty shale of Nam Duk Formation in Middle Permian. It is highly weathered and heavily fractured. The uniaxial compressive strength of the intact rock is estimated between 5 and 25 MPa. The slope height is 35 m. The orientation of the slope face is 190/48 degrees. There are three joint sets having the representative orientations

Figure 3.2a Rock slope at km 17+000 (looking east). The rock is shale.

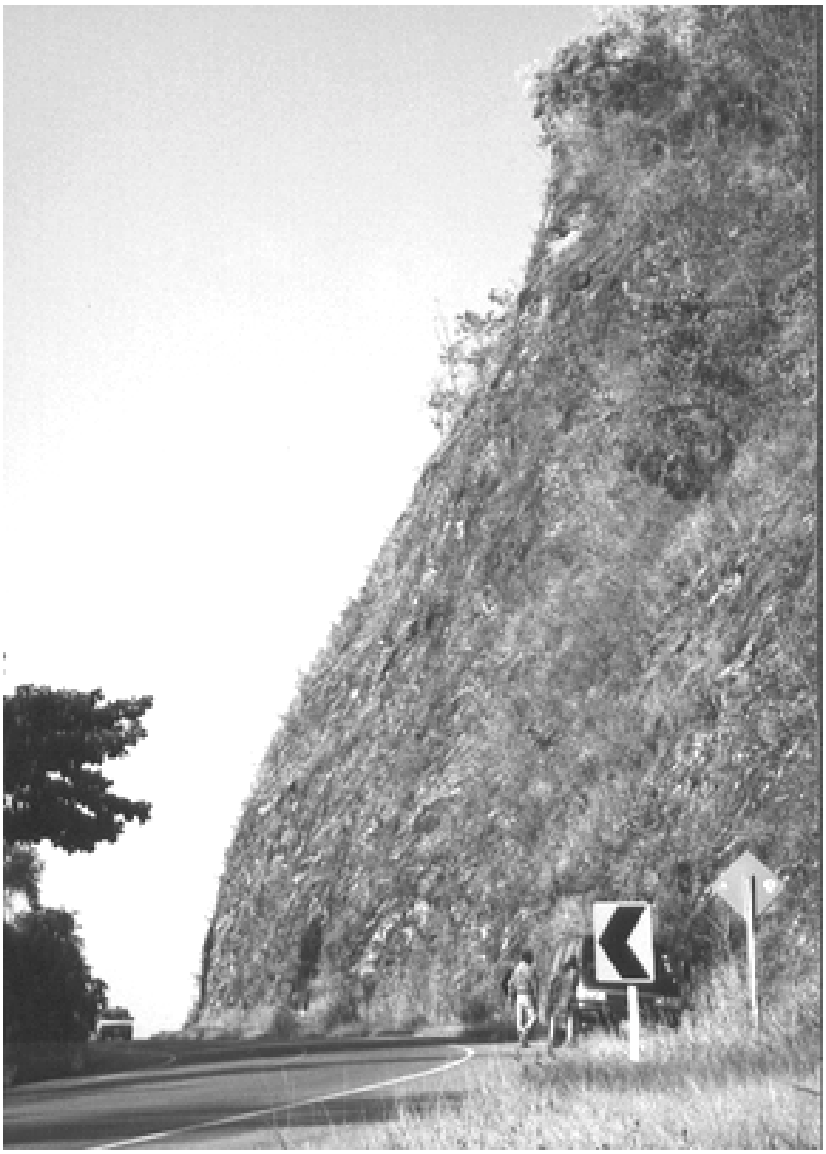

Figure 3.2b Rock slope at km 17+000 (looking east). The rock is shale of Nam Duk Formation in Middle Permian. The slope is stable.

Figure 3.2c Rock falls at km 17+000 (looking east) during Rainy Season. Various block sizes cover the ditch and roll off the ditch to the rim of the highway.

Figure 3.3 Rock slope at km 18+200 (looking east). Shotcrete covers the slope face.

(strike/dip angle) equal 115/81 degrees, 14/38 degrees, and 185/60 degrees. The average joint spacing is between 5 and 20 cm. Persistence of the rock discontinuities is about 90 %. The JRC is estimated as 3 to 5. The average width of the joint aperture is between 0.1 and 1 cm. Filled material in rock joints is calcite. The joints are dry. The rock slope is stable. Figure 3.4 shows the rock slope at km 18+550. The main discontinuity set forms the slope face.

The slope location from km 20+575 to km 20+650 is on the right side of Lomsak-Chumpae highway. The rock is yellowish-brown shale of Nam Duk Formation in Middle Permian. It is heavily fractured and highly weathered shale. The uniaxial compressive strength of the intact rock is between 5 and 25 MPa. The slope height is 15 m. The orientation of the slope face is 225/45 degrees; the upper slope face is 225/64 degrees. There are three joint sets having the representative orientation (strike/dip angle) equal 80/64 degrees, 198/56 degrees, and 334/53 degrees. The average joint spacing is between 5 and 15 cm. Persistence of the rock discontinuities is about 100 %. The JRC is estimated as 1. The average width of the joint aperture is between 0.1 and 1 cm. Filled material in rock joints is clay. The joints are dry. The existing supports include shotcrete, drained holes, and gabion. Shotcrete is between 3 and 8 cm in thickness. The length of drained pipes is between 30 and 50 cm. The inner diameter of drained pipes is 6.5 cm and the outer diameter of drained pipes is 6.8 cm. Gabion wall consists of rock pieces of andesite, which is wrapped by wire mesh or chain link. The gabion wall is 50 cm wide and 50 cm high. The rock slope is unstable showing circular failure. Figure 3.5a shows the rock slope at km 20+575. The slope failure occurs on the upper slope. The failure brought down

Figure 3.4 Rock slope at km 18+550 (looking south). The rock is slaty shale of Nam Duk Formation in Middle Permian. The main discontinuity set forms the slope face.

Figure 3.5a Rock slope at km 20+575 (looking south). The rock is shale of Nam Duk Formation in Middle Permian.

both earthen and installed materials. Figure 3.5b shows the drained pipe in the pile of rock debris.

The slope location from km 21+225 to km 21+265 is on the left side of Lomsak-Chumpae highway. The rock is yellowish-brown shale of Nam Duk Formation in Middle Permian. It is highly weathered and heavily fracture shale. The uniaxial compressive strength of the intact rock is between 5 and 25 MPa. The slope height is 15 m. The orientation of the slope face is 55/57 degrees. There are three joint sets having the representative orientation (strike/dip angle) equal 86/64 degrees, 225/36 degrees, and 311/82 degrees. The average joint spacing is between 5 and 15 cm. Persistence of the rock discontinuities is about 100 %. The JRC is estimated as 1. The average width of the joint apertures is between 0.1 and 1.5 cm. Filled material in rock joints is clay. The joints are dry. The existing supports are shotcrete and drained holes. Shotcrete is between 2 and 7 cm in thickness. The length of drained pipes is between 30 and 50 cm. The inner diameter of drained pipes is 6.5 cm and the outer diameter of drained pipes is 6.8 cm. The rock slope is unstable showing circular failure. Figure 3.6 shows the rock slope at km 21+225. The massive slope failure occurs. The failure brought down earthen and installed materials. The remaining shotcrete appears on the lower slope face.

The slope location from km 22+425 to km 22+570 is on the left side of Lomsak-Chumpae highway. The rock is reddish-brown sandstone of Nam Phong Formation in Upper Triassic. It is slightly weathered to fresh rock. The uniaxial compressive strength of the intact rock is estimated between 50 and 100 MPa. The slope height is 17 m. The orientation of the slope face is 40/71 degrees. There are four joint sets having the representative orientations (strike/dip angle) equal 180/78

Figure 3.5b Drained pipe is found at km 20+575, in the pile of rock debris.

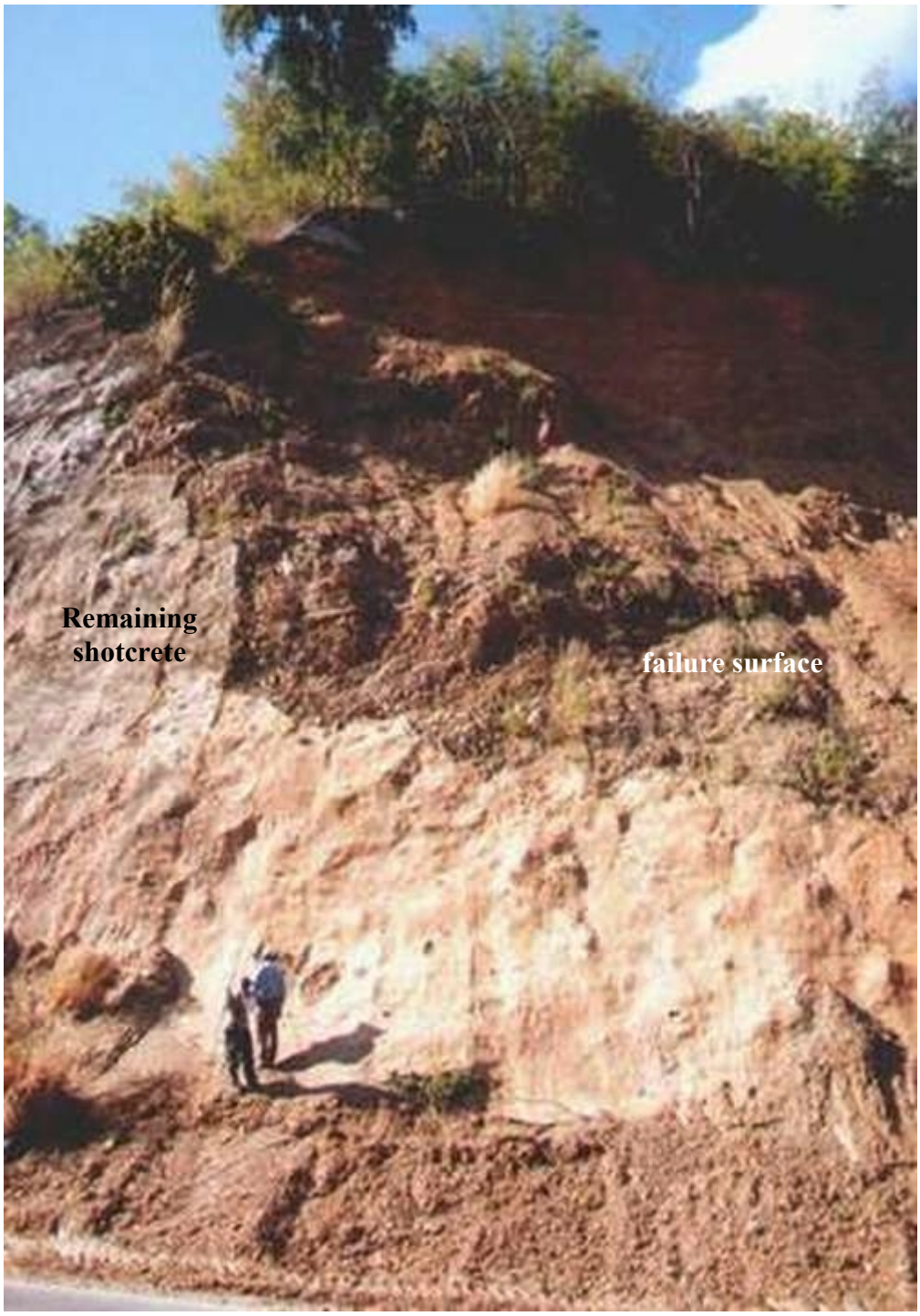

Figure 3.6 Rock slope at km 21+225 (looking northeast). Massive slope failure occurred after the installation of shotcrete. Failure surface cut from the upper slope through the mid-height of the slope face.

degrees, 276/66 degrees, 34/34 degrees and 91/44 degrees. The average joint spacing is between 5 and 10 cm. Persistence of the rock discontinuities is about 60 %. The JRC is estimated as 5. The average width of the joint aperture is between 0.3 and 1 cm. Filled material in rock joints is clay. The joints are dry. The existing supports include rock bolt, wire mesh, and gabion. The length or rock bolt 47 cm, with 2.5 cm diameter. Wire mesh is 6x7 cm in opening. Gabion wall consists of rock pieces of andesite, which is wrapped by wire mesh or chain link. The gabion wall is 50 cm wide and 50 cm high. The rock slope is stable. Figure 3.7 shows the rock slope at km 22+425. The slope is stable due to effective rock supports.

The slope location from km 36+120 to km 36+175 is on the right side of Lomsak-Chumpae highway. The rock is Nam Duk Formation in Middle Permian. It is highly weathered shale with yellowish-brown. The uniaxial compressive strength of the intact rock is estimated between 5 and 25 MPa. The slope height is 20 meter. The slope profile is very irregular. The orientation of the slope face is 321/50 degrees. There are three joint sets having the representative orientation (strike/dip angle) equal 25/83 degrees, 294/51 degrees, and 284/82 degrees. The average joint spacing is between 5 and 10 cm. The JRC is estimated as 1 to 3. The joint aperture is between 0.5 and 1 cm. Persistence of rock discontinuities is about 100 %. The filled material is clay. The joints are dry. The existing supports are shotcrete and drained holes. Shotcrete is between 2 and 8 cm in thickness. The length of drained pipes is between 30 and 50 cm. The inner diameter of drained pipes is 6.5 cm and the outer diameter of drained pipes is 6.8 cm. The rock slope is unstable. Figure 3.8 shows the massive slope failure along the slope face (the direction of the slope movement).

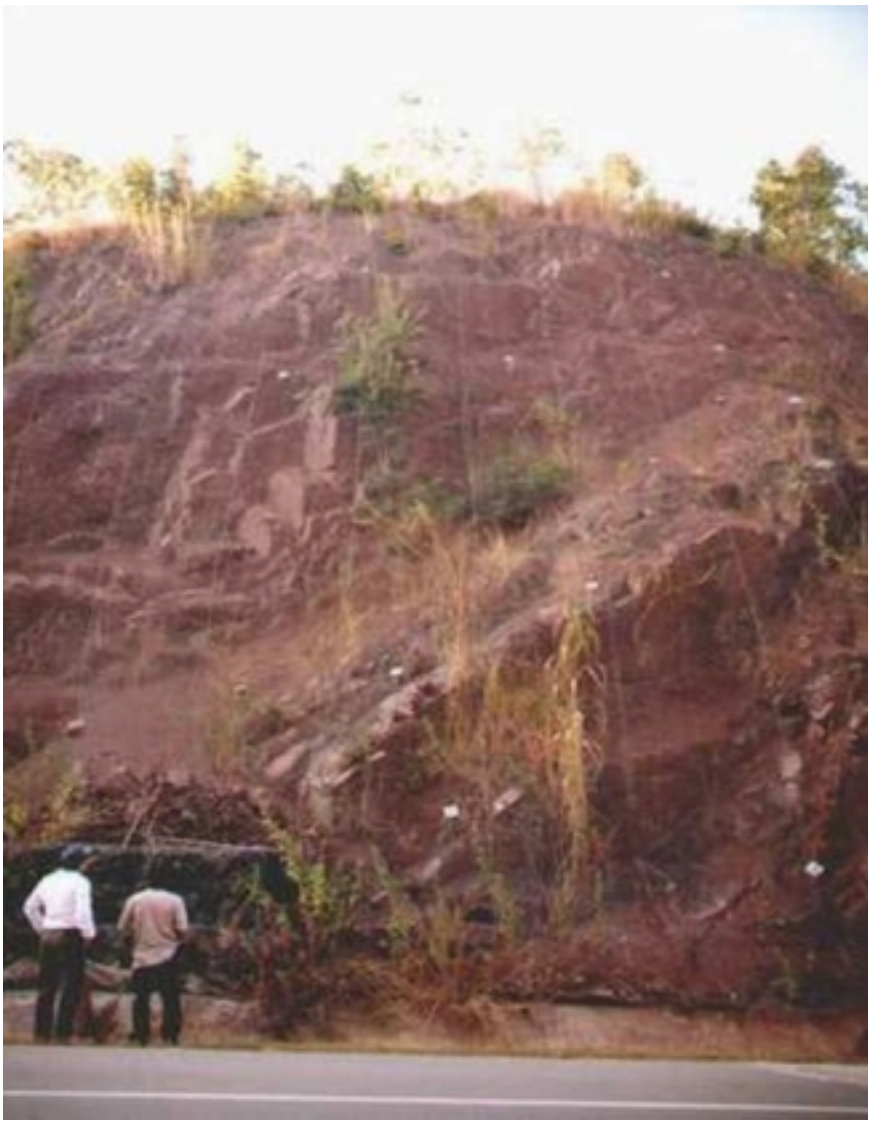

Figure 3.7 Rock slope at km 22+425 (looking east). The rock is sandstone of Nam Phong Formation in Upper Triassic. Wire mesh is covered the entire slope face in an attempt at preventing rock falls.

Figure 3.8 Rock slope at km 36+120 (looking southwest). Massive failure occurred.

The slope location from km 36+750 to km 36+825 is on the right side of Lomsak-Chumpae highway. The rock is yellowish-brown shale of Nam Duk Formation in Middle Permian. It is highly weathered and heavily fractured shale. The uniaxial compressive strength of the intact rock is between 5 and 25 MPa. The slope height is 15 meters high. The slope orientation is 303/48 degrees; the upper slope face is 300/60 degrees. The slope profile is very irregular. The rock mass characteristics are virtually identical to those at km 36+120. Filled material is clay. The joints are dry. The existing supports include shotcrete and drained holes. Shotcrete is between 2 and 8 cm in thickness. The length of drained pipes is between 30 and 50 cm. The inner diameter of drained pipes is 6.5 cm and the outer diameter of drained pipes is 6.8 cm. The shotcrete remains on the slope face. Figure 3.9 shows failure surface exposed after massive slope failure at km 36+750. The failure brought down earthen and installed materials. The remaining shotcrete appears on the left side of the slope face.

The slope location from km 62+950 to km 63+000 is on the right side of Lomsak-Chumpae highway. The rock is sandstone interbedded with siltstone of Phu Kradung Formation in Lower Jurassic. The uniaxial compressive strength of the intact rock is between 25 and 50 MPa. The slope height is 15 m. The joint orientation of the slope face is 156/55 degrees. There are four joint sets having the representative orientation equal 99/24 degrees, 135/80 degrees, 165/64 degrees, and 216/61 degrees. The average joint spacing is between 5 and 15 cm. The JRC is estimated as 5. The joint aperture is between 0.1 and 0.8 cm. Persistence of rock discontinuities is about 100 %. Filled material is clay. The joints are dry. Figure 3.10 shows the rock slope at km 62+950. The slope is stable.

Figure 3.9 Rock slope at km 36+750 (looking southwest). Failure surface exposed after massive slope failure. The failure brought down both earthen and installed materials. The remaining shotcrete appears on the left side of the slope face.

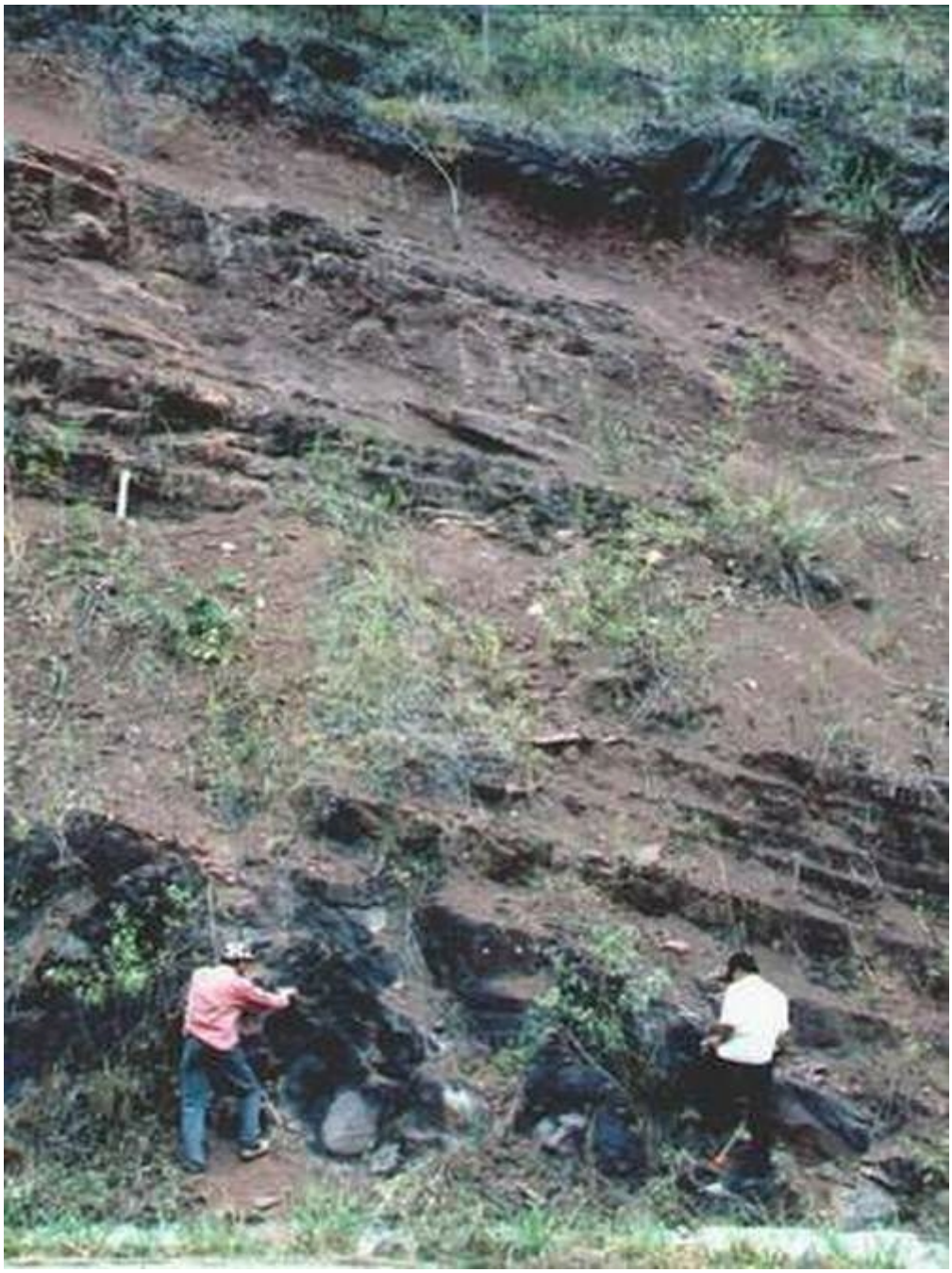

Figure 3.10 Rock slope at km 62+950 (looking south). Sandstone interbedded with siltstone appeared on the slope face. The rock is Phu Kradung Formation in Lower Jurassic.

The slope location from km 78+680 to km 78+890 is on the right side of Lomsak-Chumpae highway. The rock is gray limestone of Pha Nok Khao Formation in Lower Permian to Middle Permian. It is highly weathered to fresh rock. The estimated uniaxial compressive strength of the intact rock is between 50 and 100 MPa. The slope height is 20 m. The orientation of the slope face (strike/dip angle) is 265/60 degrees. There are five joint sets (Table 3.1) having the representative orientations (strike/dip) equal 65/48 degrees (J1: joint set 1), 133/71 degrees (J2: joint set 2), 107/26 degrees (J3: joint set 3), 203/74 degrees (J4: joint set 4), and 256/63 degrees (J5: joint set 5). The average joint spacing is between 10 and 30 cm. Persistence of the rock discontinuities is about 60%. The JRC is estimated as 3 to 5. The average width of the joint aperture is between 0.5 and 1 cm. Filled material in rock joints is clay. The joints are dry. The rock slope is unstable showing rock falls, especially during rainy season. Figure 3.11 shows the rock slope at km 78+680. Rock falls are observed on the slope surface and the ditch.

3.4 Cause of massive failure

The common cause and the sequence of the massive failure for these slopes are that the full-face shotcrete with inappropriate drained pipes prevented the infiltrated water from seeping out of the slope. The shotcrete was not effective in preventing the rock fragments from dislodging from the slope face. It is observed that slabs of shotcrete in many areas were detached from the surface of the weathered rocks. The drained pipes were poorly designed. They were too short and were not effective in reducing the pore pressure.

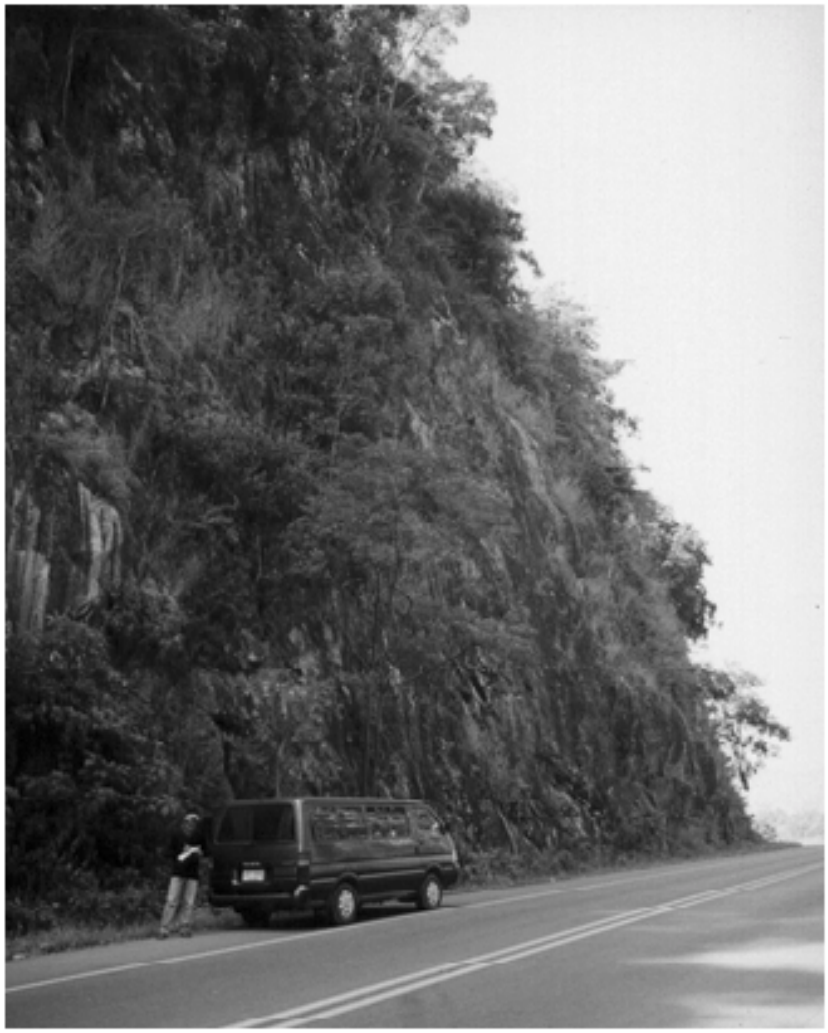

Figure 3.11 Rock slope at km 78+680 (looking west). The rock is limestone of Pha Nok Khao Formation in Lower to Middle Permian. Rock falls are observed on the slope surface and the ditch.

CHAPTER IV

COMPUTER MODELING

4.1 Objective

The objectives of the computer modeling are to determine the possibility of sliding by using the kinematics analysis, to back-calculate the shear strength properties of soil/rock by Mohr-Coulomb criterion, to calculate the shear strength properties of rock using Hoek-Brown failure criterion, and to determine the factor of safety for pre-failure and post-failure of the slope at each slope location. The obtained results are compared against the actual field conditions.

4.2 Computer modeling

4.2.1 Computer program

The computer program "DIPS", version 3 (Rock Engineering Grouop, 1989) is used to plot a stereonet. The stereonet provides pole plots and plane plots. RocLab is a program for determining the rock mass strength parameters, based on the generalized Hoek and Brown criterion (Hoek et al., 2002). The program provides a simple and intuitive implementation of the Hoek and Brown failure criterion, allowing the effects of changing rock mass parameters, by giving the equivalent cohesion and friction angle on the failure envelopes. Program GEO-SLOPE Office (GEO-SLOPE International, 1995), which is called "SLOPE/W", is used in this study to provide the limit equilibrium analysis for computing the factor of safety of soil slope and rock slope. It can also be calibrated on the shear strength properties of soil

and rock for computing the safety factor of each rock slope and back calculating some failed slopes.

4.2.2 Model construction

Scatterable poles are classified into three to five representative pole clusters on the stereonet. Representative plane plots are selected from the average maximum densities of representative poles to define the planes on the stereonet. The RocLab program determines the friction angle for comparing between the failure plane angles and the friction angles whether they have the possibility of slope failure or not.

The initial input parameter for determining the rock mass strength in RocLab is the uniaxial compressive strength (σ_{ci}), which is estimated by field technique. A material constant (m_i) is related to the frictional properties of the rock. These basic properties are determined from laboratory tests as described by Hoek and Bray (1997), but in many cases, the information is required before laboratory tests can be completed. To meet this need, guidelines that can be used to estimate these parameters are provided by Marinos and Hoek (2000).

The most important component of Hoek and Brown system for rock mass is the process of reducing the material constant σ_{ci} and m_i method selected from their "laboratory values" to appropriate in situ values. This is accomplished through the geological strength index (GSI). The disturbance factor (D) is the effect of blast damage as well as stress relief due to removal of the overburden. This results in disturbance of the rock mass.

The chosen analysis for SLOPE/W program is Bishop's simplified since this method is proper for circular failure. The soil and rock layers can be divided into

two layers, soil layer and highly weathered shale for analyzing circular failures. The slip surface is cut from the upper to the lower slope as circular failure. A grid of rotational centers is defined to specify and control the location of the slip surfaces. To control the location of the trial slip surfaces, it is necessary to define lines or points, which are used to compute the slip circle radii. Units used in the study are in metric system.

4.3 Material properties

4.3.1 Soil and rock properties

One of the most critical steps in any limit equilibrium analysis is the determination or the estimation of the shear strength properties (C and ϕ) for the surface along which it is anticipated that sliding takes place. Due to pre-existing slope failures on these rock slopes, residual shear strength parameters (cohesion and friction angle) are selected for computing the safety factor. Some slope locations, i.e. km 16+450, 18+550, 20+575, 21+225, 36+120, and 36+750 have shown slope failures. The slope locations at km 22+425 and 62+950 pose a stable condition. The slope locations at km 17+000 and 78+680 show minor failures (rock falls). The slope location at km 18+200 is covered by shotcrete.

The estimates of the shear strength parameters here are based on the previous researches. The published information from the back analysis (Hoek and Bray, 1981), the previous researches (Changsuwan, 1984; Wannakao, 1985), and the RocLab program (Hoek et al., 2002) are collected for trial calibrations of safety factors.

In choosing the range of soil properties, it is considered that the friction angle probably ranges from 15 to 25 degrees for disturbed material. The cohesion ranges from 0 to 0.04 MPa for soil and 0.04 to 0.1 MPa for weathered soft rock, 0.1 to 0.2 MPa for soft rock. For undisturbed materials, the cohesion can be estimated as 0.2 to 0.28 MPa for undisturbed rock masses with few structures, and over 0.28 MPa for undisturbed rock masses. The unit weight of the intact rock (γ) is between 22 and 26 kN/m^3 (Changsuwan, 1984). Wannakao et al. (1985) study the shear strength parameters by tilt test. The cohesion is very low that can be ignored. The friction angle is between 30 and 65 degrees. These parameters are fed into the RocLab program for the safety factor calculation and the SLOPE/W program for iterative shear strength process.

4.3.2 Groundwater conditions

There are two-groundwater conditions to analyze slopes: dry and fully saturated. Dry condition represents no pore pressure in the slope. Fully saturated condition having groundwater table at the slope top, which can cause pore pressure built up behind the slope face. The piezometric line defines these conditions. Both are used for back-calculated strength or back analysis of the shear strength properties. The groundwater conditions can therefore affect the stability conditions.

4.3.3 Back analysis for shear strength parameters

Back analysis determines the material properties under dry and fully saturated conditions. The estimating rock mass strength is compared among different locations. The input parameters (C, ϕ) are varied in an iterative process in order to give a safety factor close to 1 for slope failures at km 18+550, 20+575, 21+225, 36+120, and 36+750. At km 16+450, it does not fail as circular or plane failure.

Therefore, it cannot be back calculated. After a slope fails, it may repeatedly fail since the slope face angle is great enough to initiate subsequent failures during rainfall. The calculation is carried out for checking whether it is stable or not. Back analysis relies on the accurate input of data into SLOPE/W program, without which it would be not possible to create an accurate model.

4.3.4 Calibrated shear strength parameters

The calculation of safety factor needs to determine the shear strength properties of soil/rock for accounting for the slope stability. These must be good agreement with the actual slopes in the field. For examples, the FS less than 1, the slope must be unstable, and the FS over 1, the slope must be stable. The trial and error process is used for calibrated shear strength parameters by the SLOPE/W program. The input unit weight of each rock type must be fixed in the SLOPE/W program and then calibrates the friction angle and cohesion of each slope location.

CHAPTER V

ANALYTICAL RESULTS

5.1 Introduction

The objectives of analytical results are to analyze the results from field investigation and computer modeling. Failure characteristics such as kinematics analysis, limit equilibrium analysis, intact rock strength estimates are analyzed. Computer modelings such as the shear strength properties by RocLab program, back analysis for shear strength parameters by SLOPE/W program, and calibrated shear strength parameters by SLOPE/W program are analyzed.

5.2 Failure characteristics

The objective of failure analysis is to identify the modes of failure, which include plane failure, circular failure, wedge failure, toppling failure, and rock falls. The kinematics analysis and limit equilibrium provide the rock slope failure prediction and rock support design. The kinematics analysis uses the stereonet plotting to interpret plane failure, wedge failure, and toppling failure. Calibrated shear strength parameters provide the shear strength properties for the limit equilibrium analysis. The limit equilibrium analysis is used for determining the safety factor of rock slopes and back-calculating the shear strength properties of rock masses.

5.2.1 Kinematics analysis

Kinematics analysis uses stereographic projection to plot strike and dip angles of the discontinuities and slope face (free surface) from field measurements. The slope locations at km 16+450 through km 78+680 are analyzed because their joint orientation and the joint spacing have been determined quantitatively. The slope locations at km 16+450 and km 18+200 are excluded from the kinematics analysis because there is no joint measurement as shotcrete covered the slope face. These results are interpreted to identify whether the slope is stable or not.

The slope location at km 17+000 consists of 50 joint orientation measurements. There are three joint sets (Figure 5.1). From the representative planes in Figure 5.2, the dip of the slope face is less than the dip of failure plane (J2). Therefore, the plane failure cannot occur. However, rock falls have occurred which is probably from loose blocks of highly weathered rock. The sizes of rock falls are from few centimeters to boulders. Rock falls are found from the slope crest down to the slope toe. Some blocks roll off the ditch on the highway.

The slope location at km 18+550 consists of 21 joint orientation measurements. Figure 5.3 shows the poles, which have three pole clusters. Figure 5.4 shows the representative planes at km 18+550. The dip of the slope face is less than the dip of joint set 3 (J3) and less than the dip of intersection between planes (J1 and J3), which means that plane failure and wedge failure cannot occur. The plane of joint set 2 (J2) does not involve in the sliding, but it can give rise to toppling failure.

The slope location at km 20+575 consists of 60 joint orientation measurements. There are three joint sets. Figure 5.5 shows the pole plots at km

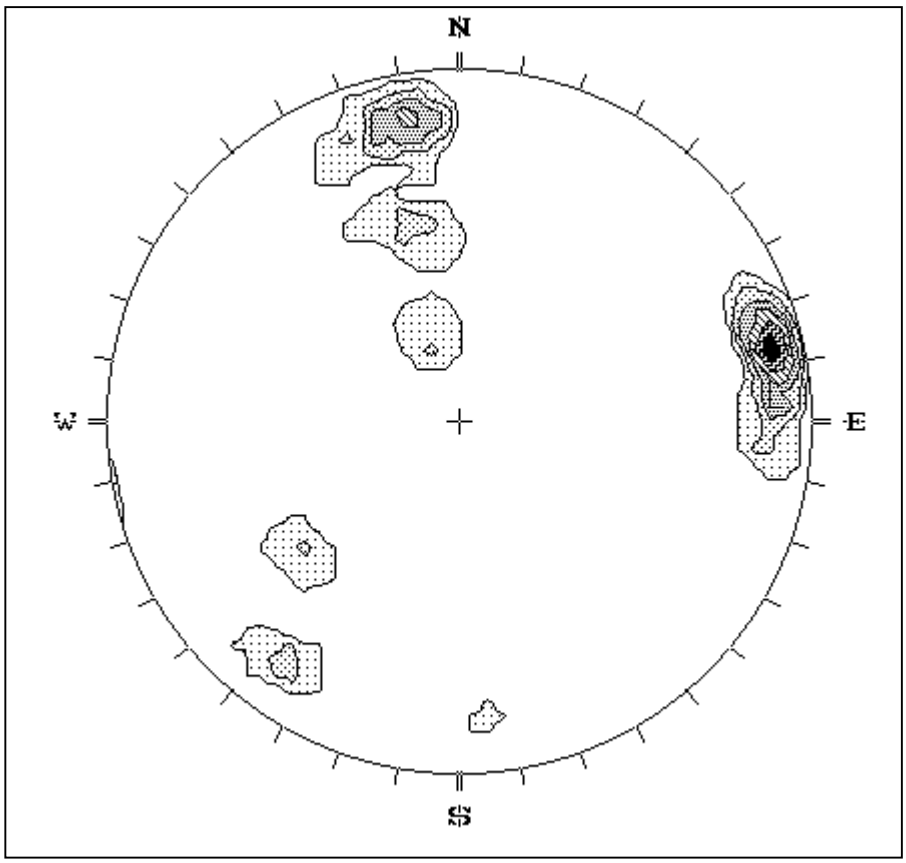

Figure 5.1 Pole plots at km 17+000. There are three representative pole clusters.

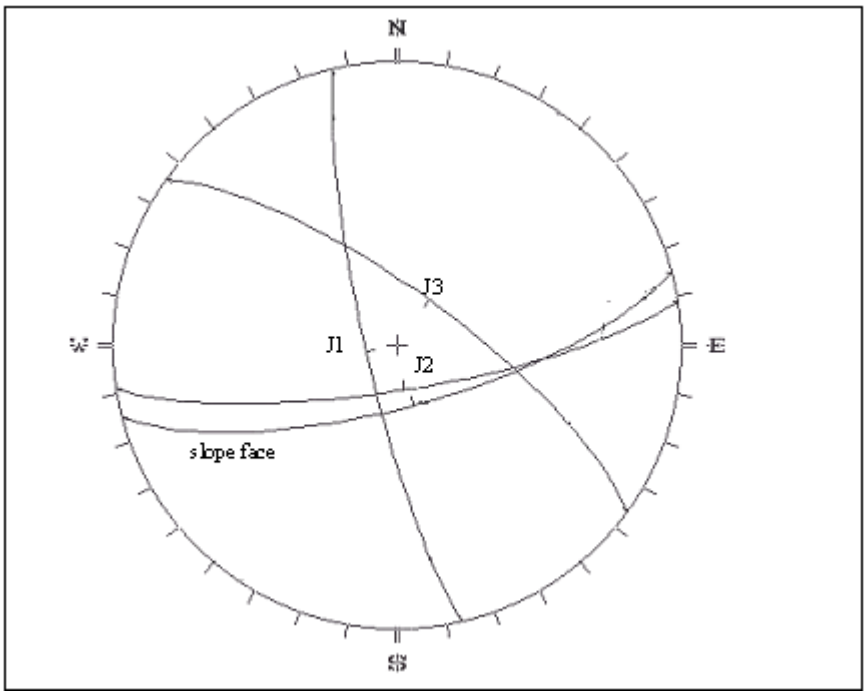

Figure 5.2 Representative plane plots at km 17+000. The dip of the slope face is less than the dip of failure plane (J2); plane failure cannot occur.

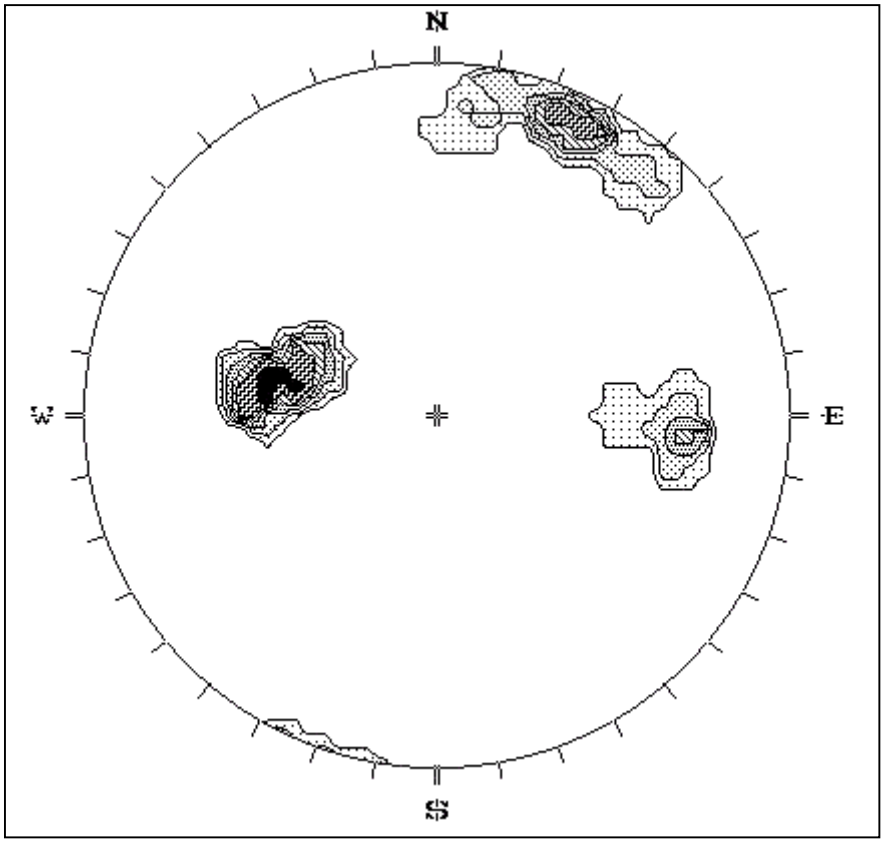

Figure 5.3 Pole plots at km 18+550. There are three representative pole clusters.

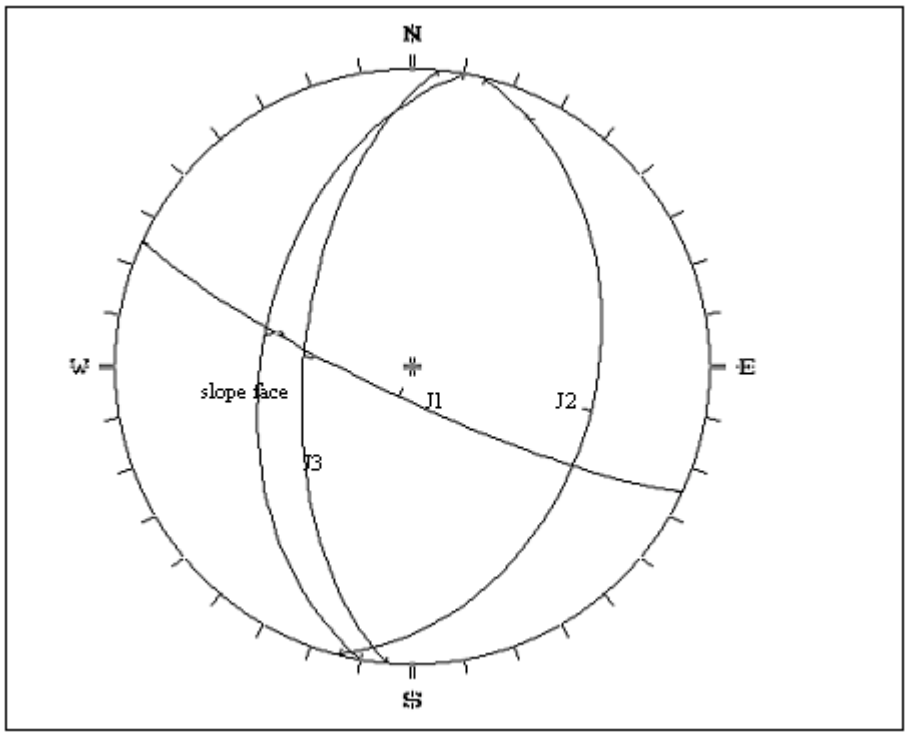

Figure 5.4 Representative plane plots at km 18+550. The dip of the slope face is less than the dip of the plane of J3 and less than the dip of intersection between planes (J1 and J3), which means that plane failure and wedge failures cannot occur. The plane of joint set 2 does not involve in sliding, but it can give rise to toppling failure.

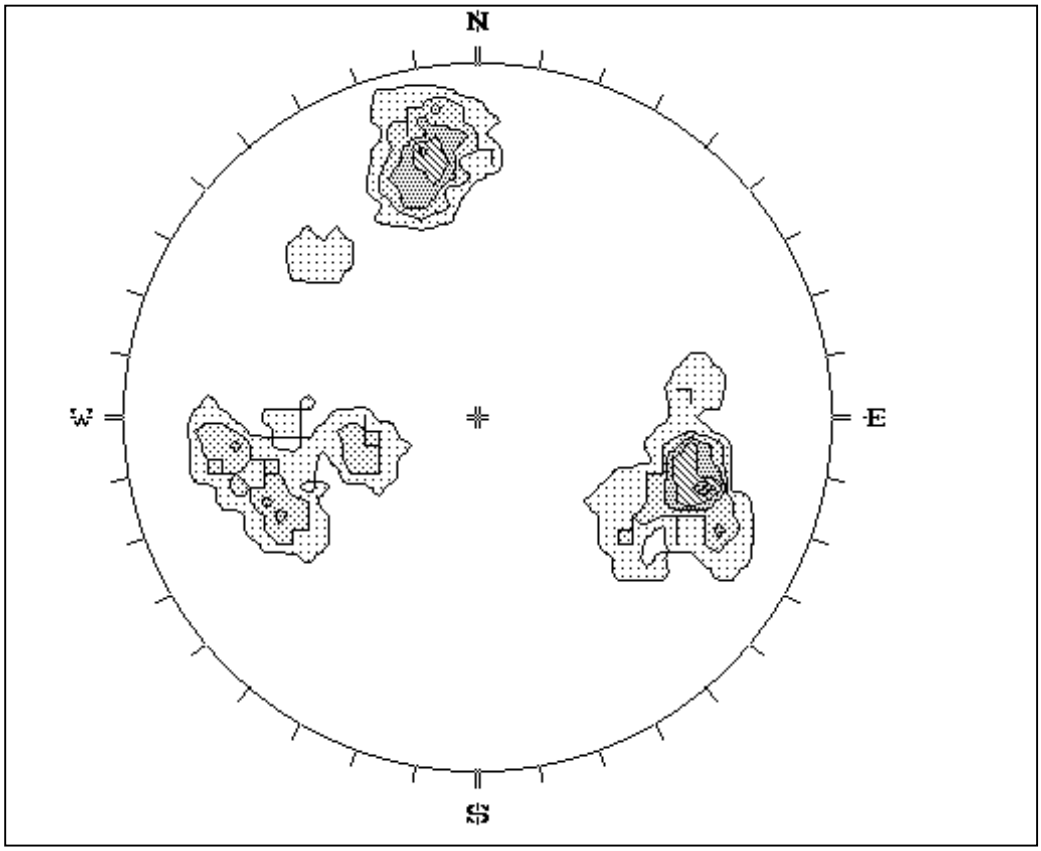

Figure 5.5 Pole plots at km 20+575. There are three pole clusters.

20+575. Figure 5.6 shows that the dip of the slope face is less than the dip of the failure plane (J2). However, the dip of the slope face is greater than the dip of intersection between planes (J2 and J3), which means that wedge failure can occur.

The slope location at km 21+225 consists of 51 joint orientation measurements. There are three joint sets. Figure 5.7 shows the pole plots at km 21+225. Figure 5.8 shows the representative planes at km 21+225 that the dip of the slope face is greater than the dip of intersection between planes (J1 and J3), which means that wedge failure can occur. The plane of J2 does not involve in sliding, but it can give rise to toppling.

The slope location at 22+425 consists of 74 joint orientation measurements. There are four joint sets (Figure 5.9). From the representative planes in Figure 5.10, the dip of intersections between J1 and J4, J2 and J3, J1 and J3, J4 and J2, and J3 and J4 is less than the dip of the slope face. However, the actual slope failure in the field has no wedge form due to the friction angle of sandstone is likely greater than the dip of the intersections between the planes.

The slope location at km 36+120 consists of 65 joint orientation measurements. Figure 5.11 shows the pole plots at km 36+120 having three joint sets. Figure 5.12 shows the dip of the slope face less than the dip of the plane of J2 and less than the dip of intersection between planes (J1 and J3), which means that plane failure and wedge failure cannot occur.

The slope location at km 62+950 consists of 60 joint orientation measurements. The geometry is complicated and the rock has a high strength (from field intact rock strength estimate). From the pole plots at km 62+950 (Figure 5.13),

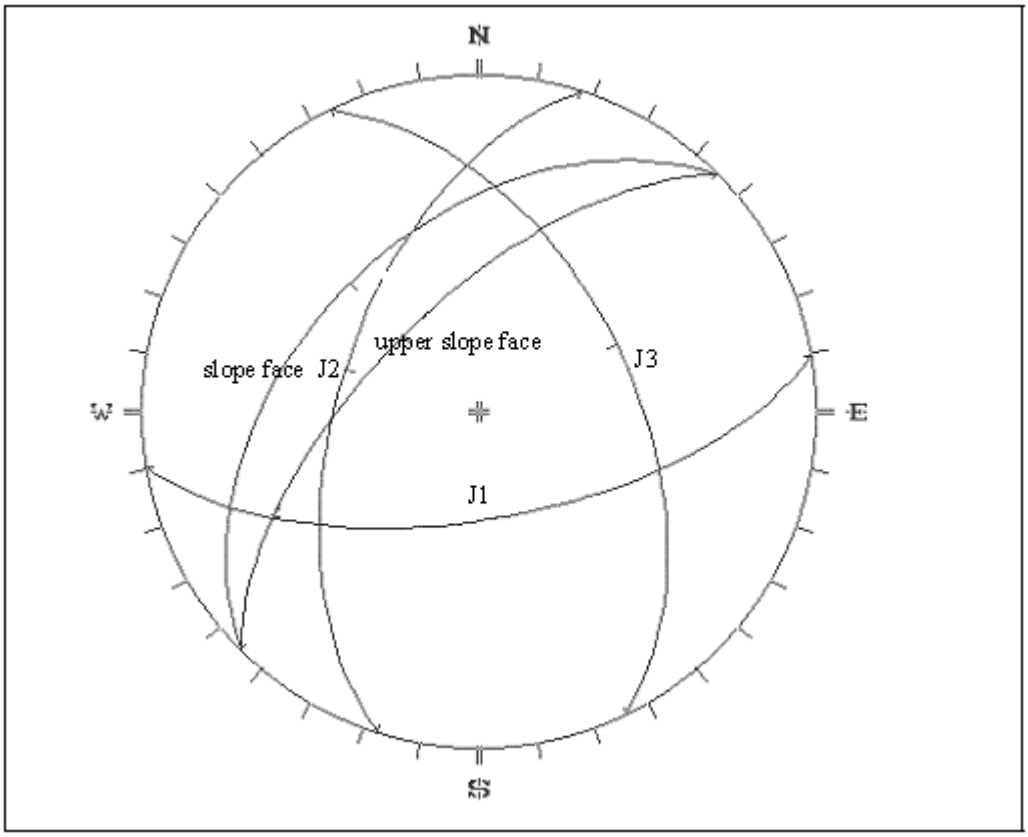

Figure 5.6 Representative plane plots at km 20+575. The dip of the slope face is less than the dip of the failure plane (J2) and less than the dip of intersection between planes (J1 and J2). However, the dip of slope face is greater than the dip of intersection line between planes (J2 and J3), which means that wedge failure can occur.

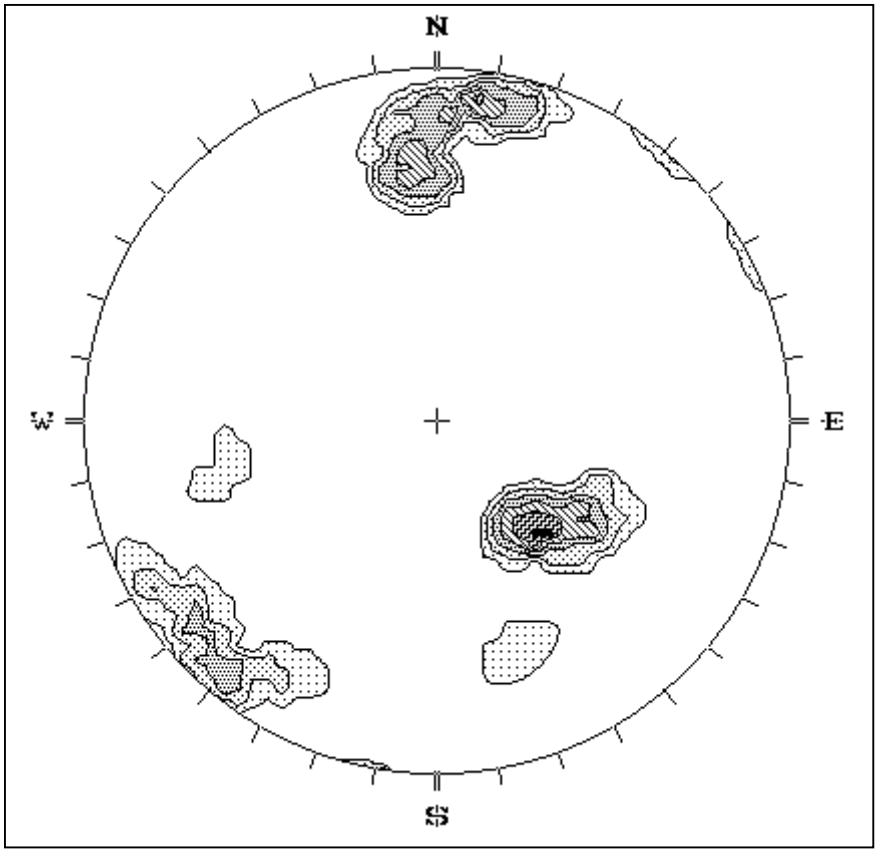

Figure 5.7 Pole plots at km 21+225. There are three representative pole clusters.

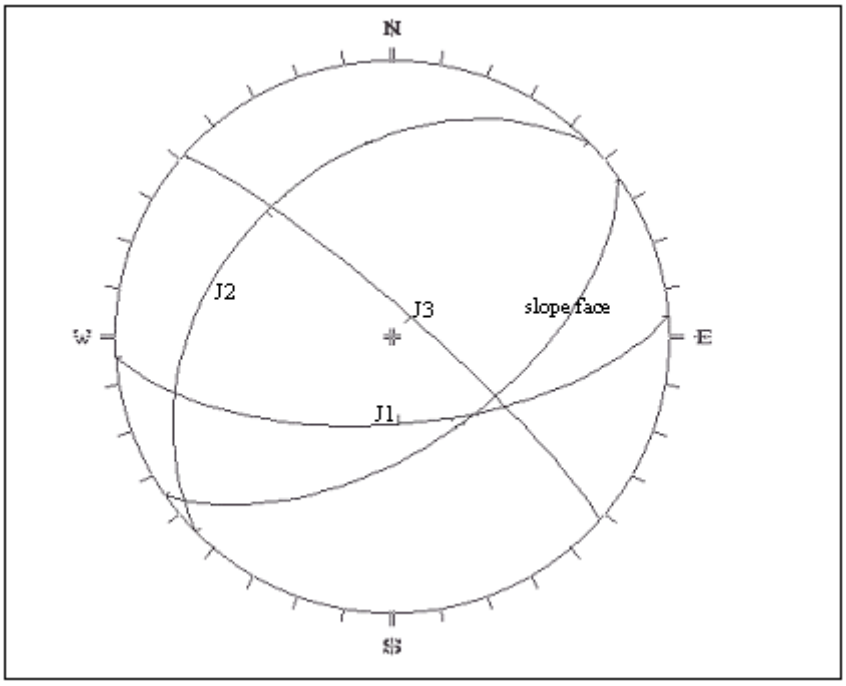

Figure 5.8 Representative plane plots at km 21+225. The dip of the slope face is greater than the dip of intersection between planes (J1 and J3), which means that wedge failure can occur. The plane of J2 can give rise to toppling failure.

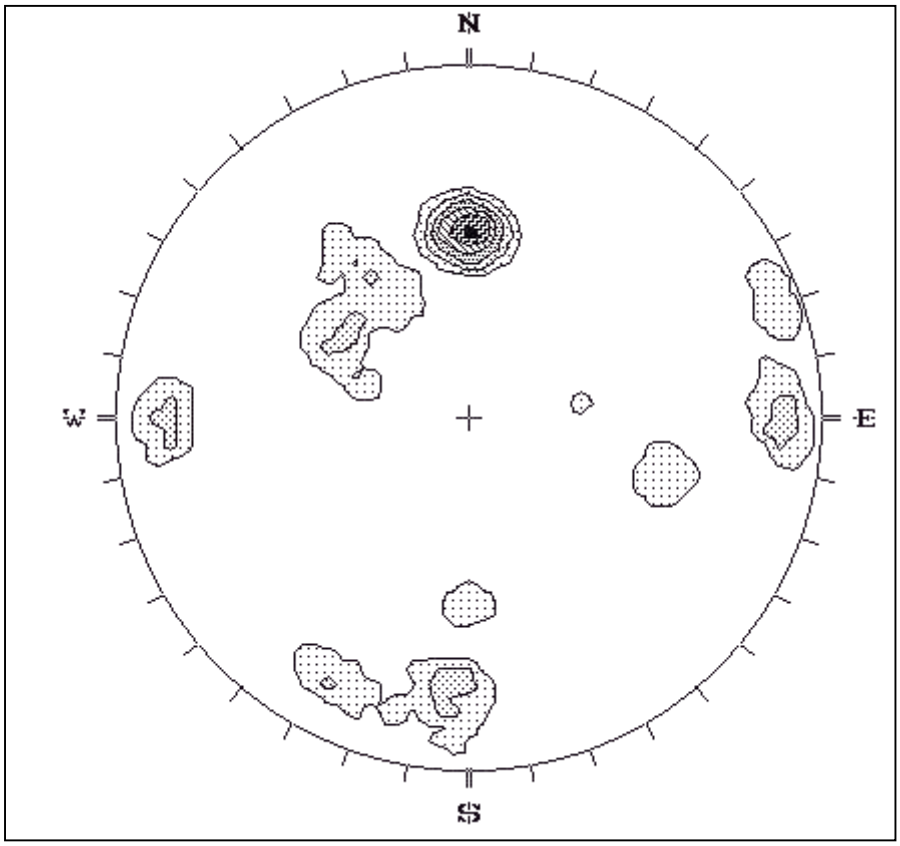

Figure 5.9 Pole plots at km 22+425. There are four pole clusters.

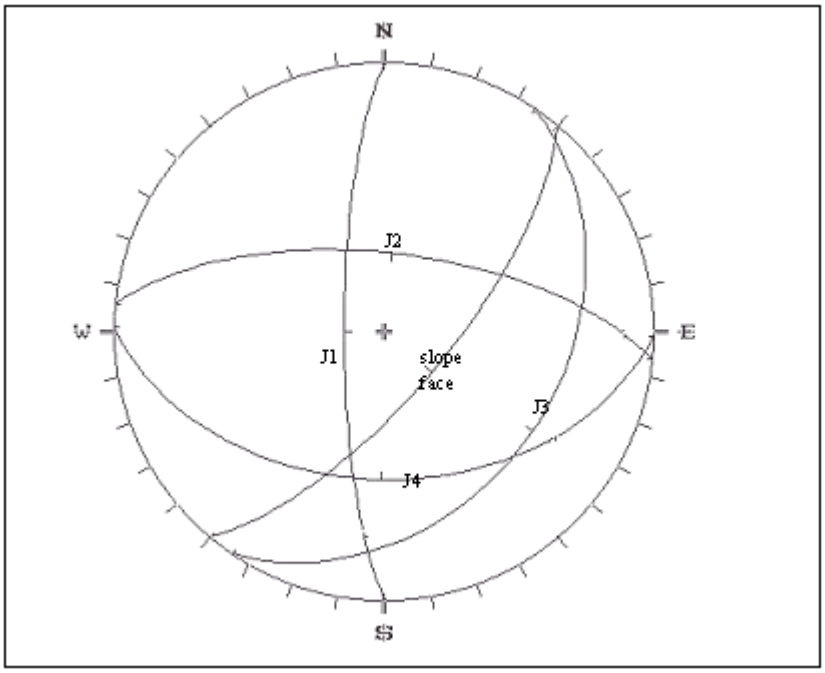

Figure 5.10 Representative plane plots at km 22+425. The dip of the slope face is greater than the dip of intersection between planes (J2 and J3, J1 and J4, J1 and J3, J4 and J2, and J3 and J4), but the actual wedge failures did not occur. This means that the friction angle is greater than the dip of the intersection between the planes.

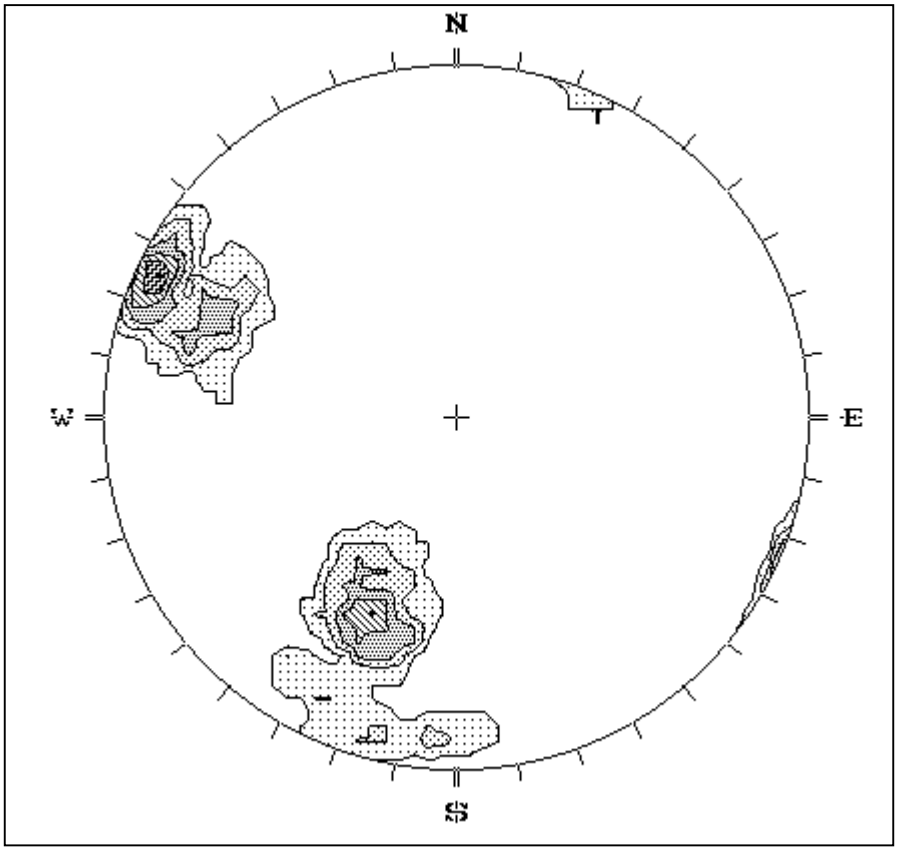

Figure 5.11 Pole plots at km 36+120. There are three representative pole plots.

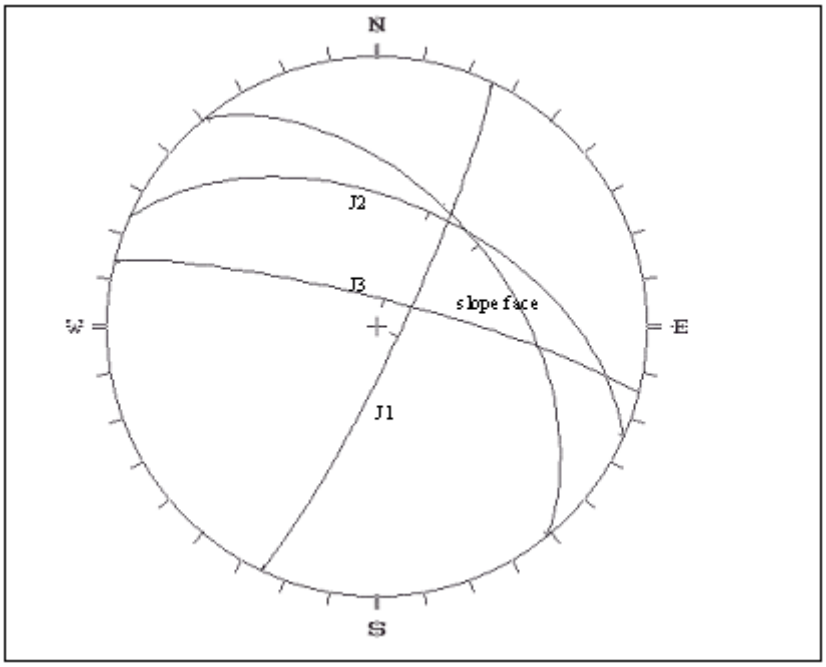

Figure 5.12 Representative plane plots at km 36+120. The dip of the slope face is less than the dip of failure plane (J2) and less than the dip of intersection between planes (J1 and J3); plane failure and wedge failure cannot occur.

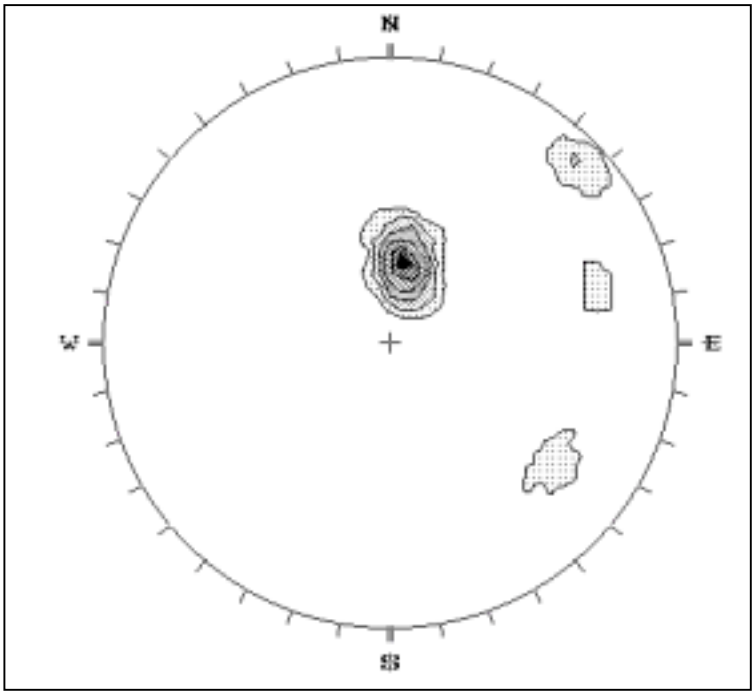

Figure 5.13 Pole plots at km 62+950. There are four representative pole clusters.

there are four joint sets. Figure 5.14 shows the plane plots that the dip of the slope face is greater than the dip of intersections between planes (J1 and J4, J1 and J3). This results in wedge form. However, the actual wedge failure cannot occur due to the friction angle of the rock is higher than the dip of intersection between the planes. The slope location at km 78+680 consists of 64 joint orientation measurements. The pole plots of the stereonet in Figure 5.15 shows five pole clusters. Figure 5.16 shows the representative plane plots at km 78+680 that the dip of the slope face is less than the dip of joint set 5 (J5) and less than the dip of intersections between planes (J2 and J5, J4 and J5), which means that plane failure and wedge failure cannot occur. However, rock falls have occurred at the site. This is probably because of loose blocks of highly weathered rock and the plane of joint set 1 gives rise to toppling failure. The sizes of rock falls are from few centimeters to boulders. Rock falls are found from the slope crest down to the slope toe. Some blocks roll off the ditch on the highway.

5.2.2 Results of calibrated shear strength parameters

The obtained C and ϕ of soil are 0.019 MPa and 23 degrees. For highly weathered rock, the C and ϕ are 0.021 MPa and 27 degrees.

5.2.3 Limit equilibrium analysis

Limit equilibrium analysis uses closed form solution of Bishop's simplified method (1955) to calculate the factor of safety of circular failures. For km 18+550, plane failure is calculated by closed form solution of Hoek and Bray (1981). The slope locations at km 16+450, 20+575, 21+225, 36+120, and 36+750 are analyzed. Table 5.1 shows the safety factor of each location (using the calibrated

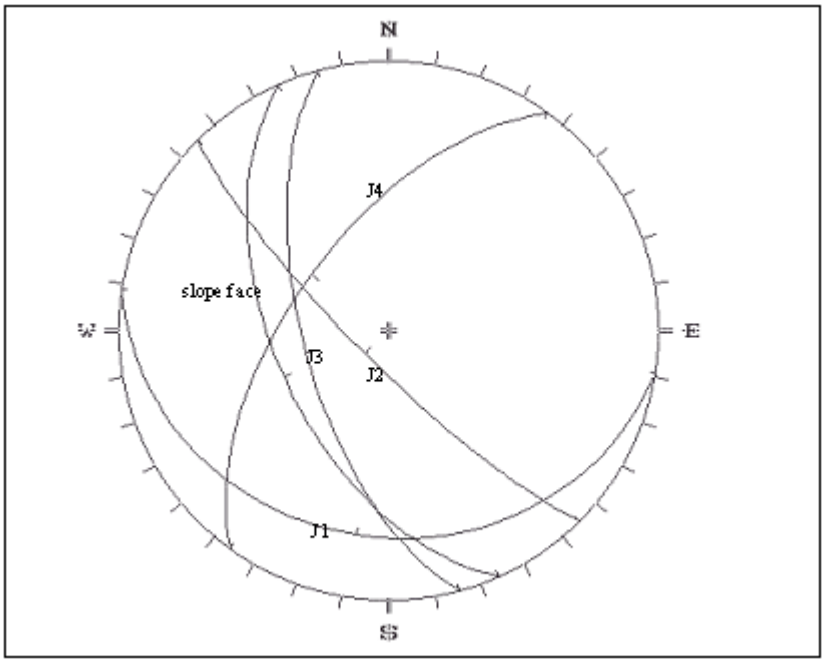

Figure 5.14 Representative plane plots at km 62+950. The dip of the slope face is greater than the dip of intersection between planes (J1 and J4), which means that wedge failure can occur. The actual wedge failure did not occur due to the friction angle is greater than the dip of the intersection between the planes.

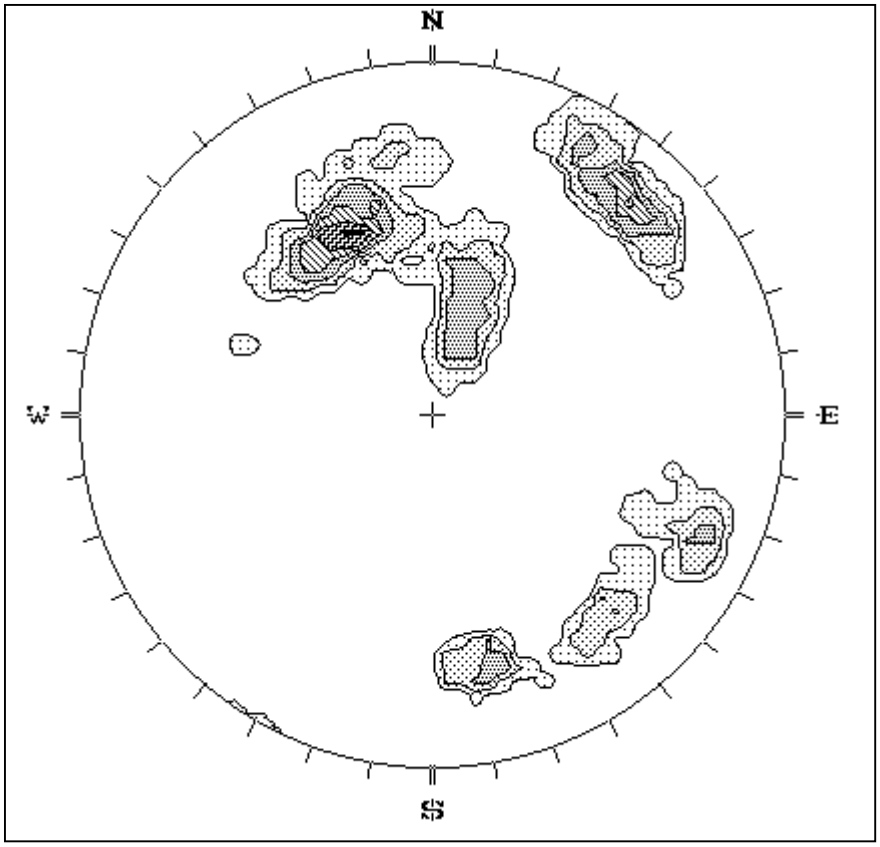

Figure 5.15 Pole plots at km 78+680. There are five representative pole clusters on the stereonet.

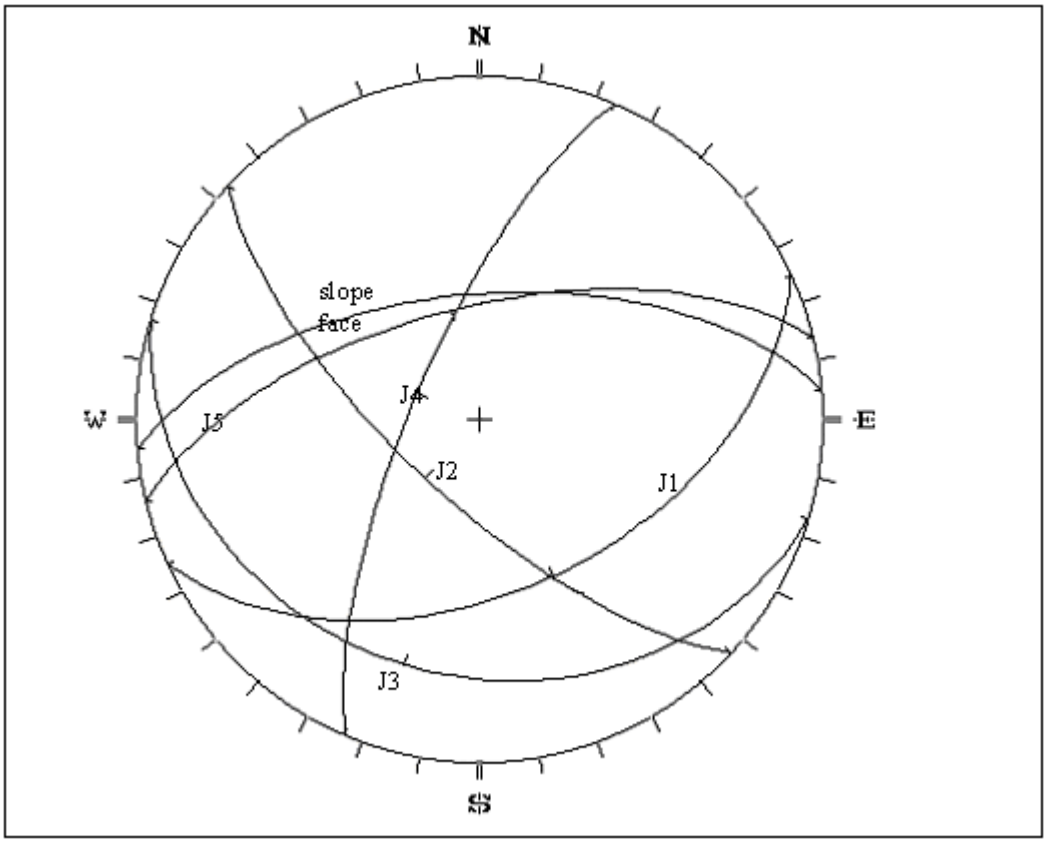

Figure 5.16 Representative plane plots at km 78+680. The dip of the slope face is less than the dip of failure plane (J5) and less than the dip of intersection between planes, which means that plane failure and wedge failures cannot occur. The plane of joint set 1 can give rise to toppling failure.

Table 5.1 Factor of safety of each location (using the calibrated shear strength parameters for calculation).

Location	F.S. of 1st failure sequence		F.S. of 2 nd failure sequence		F.S. of 3 rd failure sequence		Remarks
	Dry slope	Saturated slope	Dry slope	Saturated slope	Dry slope	Saturated slope	
Km 16+450	1.500	0.992	1.686	1.156	-	-	Ravelling
Km 17+000	N/A	N/A	N/A	N/A	N/A	N/A	Rock falls
Km 18+200	shotcrete	shotcrete	shotcrete	shotcrete	shotcrete	shotcrete	Stable
Km 18+550	1.374	0.979	3.996	3.562	-	-	Plane failure in the past, but now no daylight
Km 20+575	1.333	0.791	1.725	1.174	-	-	Circular failure
Km 21+225	1.029	0.539	1.329	0.810	1.499	1.002	Circular failure
Km 22+425	N/A	N/A	N/A	N/A	N/A	N/A	Stable
Km 36+120	1.051	0.550	1.613	1.103	-	-	Circular failure
Km 36+750	1.210	0.695	1.421	0.939	1.893	1.382	Circular failure
Km 62+950	N/A	N/A	N/A	N/A	N/A	N/A	Sandstone interbedded with siltstone
Km 78+680	N/A	N/A	N/A	N/A	N/A	N/A	Rock falls

shear strength parameters for the calculation). Some slope locations cannot be determined by the limit equilibrium such as km 17+000 and 78+680. The safety factors of the slope locations at km 22+425 and 62+950 cannot be determined because of their heterogeneity of rock. The slope location at km 18+200 is covered by shotcrete. The safety factor of the slope location at km 16+450 can be solved that the slope may occur circular failure.

The slope location at km 16+450 consists of completely (residual soil) to highly weathered shale. Erosion or ravelling initiates slope failure on the surface. Ravelling of soil/rock debris on the slope face is found from the upper to the lower slope faces (Figure 3.1). The rock fragments have a dimension of 8x10x12 centimeters. The slope failure causes the damage to the wire mesh. The safety factors of the first failure sequence are 1.500 for dry slope and 0.992 for fully saturated slope. The safety factors of the second failure sequence are 1.686 for dry slope and 1.156 for fully saturated slope.

The slope location at km 18+550 consists of slaty shale. From the evidence of the slip surfaces, the blocks of slaty shale slide down to the slope toe. This indicates that the slope face angle is greater than the failure plane angle, which results in plane slides in the past. At the time of field investigation, the slope face angle is reduced and becomes parallel to the angle of the failure plane, which results in stable slope. For the previous failures, the angle is presumably 52 degrees and the failure plane is 48 degrees. After the slope failure, the slope face angle is reduced to 48 degrees. Table 5.1 shows the safety factor of the first failure is 1.374 for dry slope, and 0.979 for fully saturated slope. Afterwards, the plane slides are unlikely.

The slope location at km 20+575 consists of highly weathered and heavily fractured shale. The circular failure leads to a massive failure. The failure surface appears on the upper slope (Figure 3.5a). Figure 3.5b shows the drained pipe, which is found at km 20+575 in the pile of rock debris. The safety factors of the first failure sequence are 1.333 for dry slope and 0.791 for fully saturated slope. The safety factors of the second failure sequence are 1.725 for dry slope and 1.174 for fully saturated slope.

The slope location at km 21+225 consists of highly weathered and heavily fractured shale. It shows a massive circular failure. The failure surface is from the slope crest to the mid-height of the slope face. The soil and rock debris piles on the slope toe and covers the ditch and the highway (Figure 3.6). The safety factors of the first failure sequence are 1.029 for dry slope and 0.539 for fully saturated slope. The safety factors of the second failure sequence are 1.329 for dry slope and 0.810 for fully saturated slope. The safety factors of the third failure sequence are 1.499 for dry slope and 1.002 for fully saturated slope.

The slope location at km 36+120 consists of highly weathered and heavily fractured shale. It shows a massive circular failure. Failure surface exposed after massive slope failure occurred (Figure 3.8). The rock fragments have a dimension of 8x10x12 centimeters. The safety factors of the first failure sequence are 1.051 for dry slope and 0.550 for fully saturated slope. The safety factors of the second failure sequence are 1.613 for dry slope and 1.103 for fully saturated slope.

The slope location at km 36+750 consists of highly weathered and heavily fractured shale. It shows a massive circular failure. Failure surface exposed

after massive slope failure occurred. The failure brought down both earthen and installed materials. The remaining shotcrete appears on the left side of the slope face (Figure 3.9). The safety factors of the first failure sequence are 1.210 for dry slope and 0.695 for fully saturated slope. The safety factors of the second failure sequence are 1.421 for dry slope and 0.939 for fully saturated slope. The safety factors of the third failure sequence are 1.893 for dry slope and 1.382 for fully saturated slope.

5.2.4 Intact rock strength estimates

The strength for the intact rock is estimated by field technique, based on the International Society of Rock Mechanics (Brown, 1981). Intact rocks at each slope location are tested by a geologic hammer and pocket knife.

Brown shale at km 16+450, 18+200, 20+575, 21+225, 36+120, and 36+750 can be peeled with a pocket knife with difficulty, shallow indentation made by firm blow with a geologic hammer. The uniaxial compressive strength of the intact shale is between 5 and 25 MPa. Gray shale at km 17+000 cannot be scraped or peeled with a pocket knife and it can be fractured with a single blow of a geologic hammer. The uniaxial compressive strength of the intact gray shale is between 25 and 50 MPa.

Slaty shale at km 18+550 can be peeled with a pocket knife with difficulty, shallow indentation made by firm blow with a geologic hammer. The uniaxial compressive strength of the intact slaty shale is between 5 and 25 MPa.

Sandstone at km 22+425 requires more than one blow of a geologic hammer to fracture it. The uniaxial compressive strength of the intact sandstone is between 50 and 100 MPa.

Sandstone interbedded with siltstone at km 62+950 cannot be scraped or peeled with a pocket knife and it can be fractured with a single blow of a geologic hammer.

Limestone at km 78+680 requires more than one blow of a geological hammer to fracture its hand specimen. The uniaxial compressive strength of the intact limestone is between 50 and 100 MPa.

5.3 Results of computer modeling

The results emphasize on the shear strength estimates of the Hoek and Brown criterion and the back analysis from Tables 5.2 through 5.4. Figures 5.17 through 5.21 show the sequence of the slope failures of km 18+550, 20+575, 21+225, 36+120, and 36+750. Appendix C shows the analysis of the rock strength using RocLab program (Figures C.1 through C.11).

5.3.1 Km 16+450

The uniaxial compressive strength of the intact shale in Table 5.2 is 15 MPa. The GSI is estimated as 30. The constant m_i of shale is 6. The disturbance factor is estimated as 0.85. These input parameters provide C = 0.051 MPa, ϕ = 22 degrees, with the unit weight of 22 kN/m^3.

5.3.2 Km 17+000

The uniaxial compressive strength of the intact gray shale is 35 MPa. The GSI for jointed shale is estimated as 30. The constant m_i of gray shale is 6. The disturbance factor of the rock mass is estimated as 0.85. These input parameters provide C = 0.074 MPa, ϕ = 28 degrees, with the unit weight of 22 kN/m^3.

Table 5.2 Shear strength parameters of the rock masses from Hoek and Brown criterion.

Slope location	Unit weight (γ) (kN/m^3)	Friction angle (ϕ) (degrees)	Cohesion (C) (MPa)	Remarks
Km 16+450	22	22	0.051	Brown shale σ_{ci} = 15 MPa GSI = 30 m_i = 6 D = 0.85
Km 17+000	22	28	0.074	Gray shale σ_{ci} = 35 MPa GSI = 30 m_i = 6 D = 0.85
Km 18+200	22	25	0.040	Brown shale σ_{ci} = 15 MPa GSI = 30 m_i = 6 D = 0.85
Km 18+550	22	20	0.061	Slaty shale σ_{ci} = 15 MPa GSI = 30 m_i = 6 D = 0.85
Km 20+575	22	26	0.038	Brown shale σ_{ci} = 15 MPa GSI = 30 m_i = 6 D = 0.85
Km 21+225	22	26	0.038	Brown shale σ_{ci} = 15 MPa GSI = 30 m_i = 6 D = 0.85
Km 22+425	25	58	0.449	Sandstone σ_{ci} = 75 MPa GSI = 60 m_i = 17 D = 0.85
Km 36+120	22	24	0.045	Brown shale σ_{ci} = 15 MPa GSI = 30 m_i = 6 D = 0.85
Km 36+750	22	26	0.038	Brown shale σ_{ci} = 15 MPa GSI = 30 m_i = 6 D = 0.85
Km 62+950	25	45	0.129	Brown shale σ_{ci} = 35 MPa GSI = 45 m_i = 12 D = 0.85
Km 78+680	26	50	0.554	Limestone σ_{ci} = 75 MPa GSI = 60 m_i = 8 D = 0.85

Table 5.3 Shear strength properties from the back analysis of dry slope (FS = 1).

Slope location	Material type	Unit weight (kN/m^3)	Friction angle (degrees)	Cohesion (MPa)	Remarks
Km 18+550	Rock	22	26	0.016	Back analysis of slaty shale from plane failure
Km 20+575	Soil	18	19	0.012	Back analysis of shale from circular failure
	Rock	22	20	0.014	
Km 21+225	Soil	18	24	0.014	Back analysis of shale from circular failure
	Rock	22	25	0.023	
Km 36+120	Soil	18	23	0.017	Back analysis of shale from circular failure
	Rock	22	25	0.021	
Km 36+750	Soil	18	20	0.013	Back analysis of shale from circular failure
	Rock	22	24	0.016	
Average shear strength properties	Soil	18	22	0.014	The average shear strength properties obtain from back analysis at mobilized strength.
	Rock	22	24	0.018	

Table 5.4 Shear strength properties from the back analysis of fully saturated slope (FS = 1).

Location	Material type	Unit weight (kN/m^3)	Friction angle (degrees)	Cohesion (MPa)	Remarks
Km 18+550	Rock	22	26	0.054	Back analysis of slaty shale from plane failure
Km 20+575	Soil	18	22	0.015	Back analysis of shale from circular failure
	Rock	22	22	0.039	
Km 21+225	Soil	18	23	0.024	Back analysis of shale from circular failure
	Rock	22	25	0.047	
Km 36+120	Soil	18	20	0.024	Back analysis of shale from circular failure
	Rock	22	25	0.052	
Km 36+750	Soil	18	20	0.016	Back analysis of shale from circular failure
	Rock	22	24	0.038	
Average shear strength properties	Soil	18	21	0.020	The average shear strength properties obtain from back analysis at mobilized strength.
	Rock	22	24	0.046	

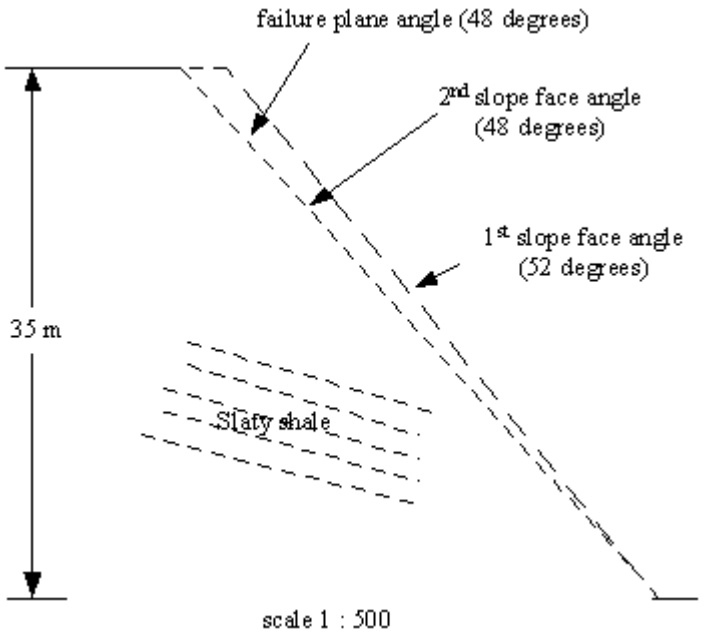

Figure 5.17 Sequence of the slope failure at km 18+550.

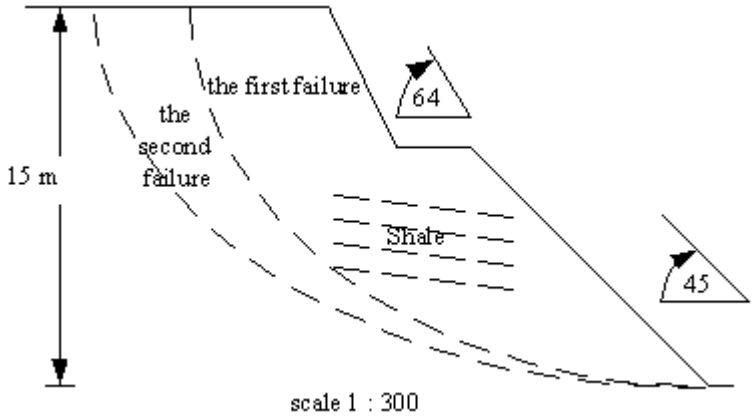

Figure 5.18 Sequence of the slope failure at km 20+575.

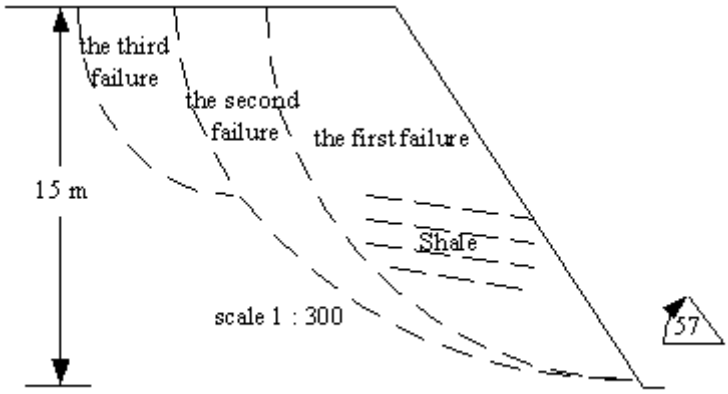

Figure 5.19 Sequence of the slope failure of km 21+225.

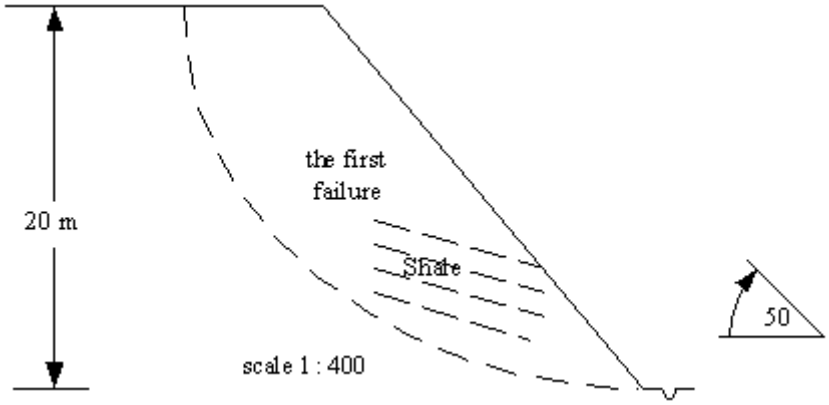

Figure 5.20 Sequence of the slope failure at km 36+120.

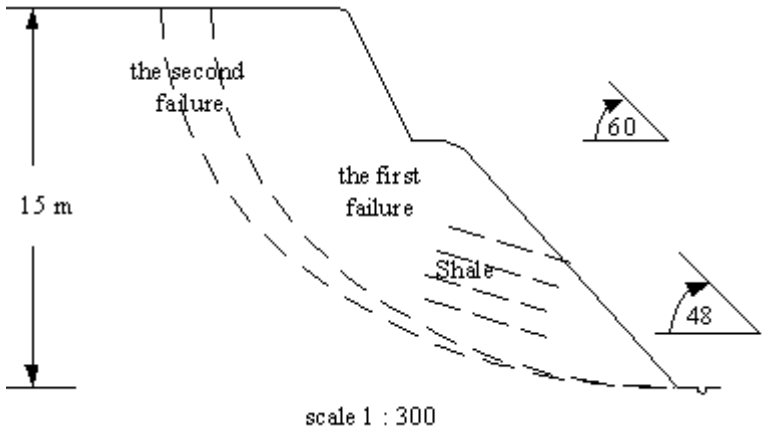

Figure 5.21 Sequence of the slope failure at km 36+750

5.3.3 Km 18+200

The uniaxial compressive strength of the intact shale in Table 5.2 is 15 MPa. The GSI for jointed shale is estimated as 30. The constant m_i of shale is 6. The disturbance factor is estimated as 0.85. These input parameters provide C = 0.040 MPa, ϕ = 25 degrees, with the unit weight of 22 kN/m^3. The shotcrete serves as an increase of the cohesion and the friction angle. This results in more stable slope.

5.3.4 Km 18+550

From Table 5.2, the uniaxial compressive strength of the intact shale is 15 MPa. The GSI for jointed slaty shale is estimated as 30. The constant m_i of slaty shale is 6. The disturbance factor of the rock mass D = 0.85. These input parameters provide C = 0.061 MPa, ϕ = 20 degrees, with the unit weight of 22 kN/m^3. Table 5.3 shows the shear strength parameters for dry slope with the safety factor of 1. For slaty shale, the cohesion and the friction angle are 0.016 MPa and 26 degrees, and the unit weight of shale is 22 kN/m^3. Table 5.4 shows the shear strength parameters for

f u l l y saturated slope with the safety factor of 1. For slaty shale, the cohesion and the friction angle are 0.054 MPa and 26 degrees, and the unit weight of slaty shale is 22 kN/m^3.

5.3.5 Km 20+575

The uniaxial compressive strength of the intact shale in Table 5.2 is 15 MPa. The GSI for jointed shale is estimated as 30. The constant m_i of shale is 6. The disturbance factor is estimated as 0.85. These input parameters provide C = 0.038 MPa, ϕ = 26 degrees, with the unit weight of 22 kN/m^3.

Table 5.3 shows the shear strength parameters for dry slope with the safety factor of 1. For soil, the cohesion and the friction angle are 0.012 MPa and 19 degrees, and the unit weight of soil is 18 kN/m^3. For highly weathered rock, the cohesion and the friction angle are 0.014 MPa and 20 degrees, and the unit weight of shale is 22 kN/m^3. Table 5.4 shows the shear strength parameters for fully saturated slope with the safety factor of 1. For soil, the cohesion and the friction are 0.015 MPa and 22 degrees, and the unit weight of soil is 18 kN/m^3. For highly weathered rock, the cohesion and the friction angle are 0.039 MPa and 22 degrees, and the unit weight of shale is 22 kN/m^3.

5.3.6 Km 21+225

The uniaxial compressive strength of the intact shale in Table 5.2 is 15 MPa. The GSI for jointed shale is 30. The constant m_i of shale is 6. The disturbance factor is estimated as 0.85. These input parameters provide the C = 0.038 MPa, ϕ = 26 degrees, with the unit weight of 22 kN/m^3.

Table 5.3 shows the shear strength parameters for dry slope with the safety factor of 1. For soil, the cohesion and the friction angle are 0.014 MPa and 24 degrees, and the unit weight of soil is 18 kN/m^3. For highly weathered shale, the cohesion and the friction angle are 0.023 MPa and 25 degrees, and the unit weight of shale is 22 kN/m^3. Table 5.4 shows the shear strength parameters of fully saturated slope with the safety factor of 1. For soil, the cohesion and the friction angle are 0.024 MPa and 23 degrees, and the unit weight of soil is 18 kN/m^3. For highly weathered shale, the cohesion and the friction angle are 0.047 MPa and 25 degrees, and the unit weight of shale is 22 kN/m^3.

5.3.7 Km 22+425

The uniaxial compressive strength of the intact sandstone in Figure 4.1 is 75 MPa. The GSI for jointed sandstone is estimated as 60. The constant m_i of sandstone is 17. The disturbance factor of the rock mass is 0.85. These input parameters provide C = 0.449 MPa, ϕ = 58 degrees, with the unit weight of 25 kN/m^3. This location cannot be calculated of the shear strength parameters by back analysis because of no slope failure.

5.3.8 Km 36+120

The uniaxial compressive strength of the intact shale in Table 5.2 is 15 MPa. The GSI for jointed shale is estimated as 30. The constant m_i of shale is 6. The disturbance factor is estimated is 0.85. These input parameters provide C = 0.045 MPa, ϕ = 24 degrees, with the unit weight of 22 kN/m^3.

Table 5.3 shows the shear strength parameters for dry slope with the safety factor of 1. For soil, the cohesion and the friction angle are 0.017 MPa and 23

degrees, and the unit weight of soil is 18 kN/m^3. For highly weathered shale, the cohesion and the friction angle are 0.021 MPa and 25 degrees, and the unit weight of shale is 22 kN/m^3. Table 5.4 shows the shear strength of fully saturated slope with the safety factor of 1. For soil, the cohesion and the friction angle are 0.024 MPa and 20 degrees, and the unit weight of soil is 18 kN/m^3. For highly weathered shale, the cohesion and the friction angle are 0.052 MPa and 25 degrees, and the unit weight of shale is 22 kN/m^3.

5.3.9 Km 36+750

The uniaxial compressive strength of the intact shale in Table 5.2 is 15 MPa. The GSI for jointed shale is estimated as 30. The constant m_i of shale is 6. The disturbance factor is estimated as 0.85. These input parameters provide C = 0.038 MPa, ϕ = 26 degrees, with the unit weight of 22 kN/m^3.

Table 5.3 shows the shear strength parameters for dry slope with the safety factor of 1. For soil, the cohesion and the friction angle are 0.013 MPa and 20 degrees, and the unit weight of soil is 18 kN/m^3. For highly weathered shale, the cohesion and the friction angle are 0.016 MPa and 24 degrees, and the unit weight of shale is 22 kN/m^3. Table 5.4 shows the shear strength parameters of fully saturated slope with the safety factor of 1. For soil, the cohesion and the friction angle are 0.016 MPa and 20 degrees, and the unit weight of soil is 18 kN/m^3. For highly weathered shale, the cohesion and the friction angle are 0.038 MPa and 24 degrees, and the unit weight of shale is 22 kN/m^3.

5.3.10 Km 62+950

The uniaxial compressive strength of the intact sandstone and siltstone is 35 MPa. The GSI for jointed sandstone interbedded with siltstone is 45. The constant m_i of the rock is 12. The disturbance factor of the rock mass is 0.85. These input parameters provide C = 0.129 MPa, ϕ = 45 degrees, with the unit weight of 25 kN/m^3.

5.3.11 Km 78+680

The uniaxial compressive strength (σ_{ci}) of the intact limestone in Table 5.2 is 75 MPa. The geological strength index (GSI) for jointed limestone is estimated as 60. The constant value (m_i) of limestone is 8. The disturbance factor of the rock mass is estimated as 0.85. These input parameters provide the cohesion (C) = 0.554 MPa, friction angle (ϕ) = 50 degrees, with the unit weight of 26 kN/m^3.

5.4 Discussions

Most rock slopes along Lomsak-Chumpae highway pose the possibility of failure due to the slope face angle is great enough to initiate subsequent failures during rainfall. Groundwater conditions affect the stability conditions, which means that dry slopes are more stable than fully saturated slopes. Few years after construction, some slope failures have been observed along Lomsak-Chumpae highway. Prior to the massive slope failure, the groundwater nearly reaches the upper slope face as indicated by the water stain near the cracks in the shotcrete. The massive failures are probably sudden. Fully saturated slopes in the computer modeling are conservative that the maximum water table is defined at the top of the slope face.

The determination of the average shear strength properties is to calculate the safety factor of each location. The SLOPE/W program is used for calibrating the representative shear strength properties considering the effects of groundwater conditions. The obtained C and ϕ of soil are 0.019 MPa and 23 degrees, and the γ of soil is 18 kN/m^3. For highly weathered rock, the C and the friction angle are 0.021 MPa and 27 degrees, and the unit weight of the rock is between 22 and 26 kN/m^3. These shear strength properties are close to the shear strength properties of the mobilized shear strength (FS =1). They indicate that the average safety factor of all slopes is close to 1. This implies the possibility of slope failures.

The shear strength estimates of Hoek and Brown criterion are in a good agreement with the fully saturated conditions from back analysis (at mobilized shear strength, FS = 1). The dry conditions show lower shear strength properties. Back analysis is suitable for the slope failures. The Hoek and Brown criterion provides the empirical formula for equivalent cohesion and friction angle. Therefore, back analysis can give more reliable shear strength properties than the Hoek and Brown criterion.

The friction angle from tilt test is higher than the friction angle from the back analysis due to the normal stress from tilt test is less than the actual normal stress from the field.

The slope failures may occur repeatedly in the future since the slope face angle is great enough to initiate subsequent failures during rainfall. Post-failures at km 21+225 and 36+750 are good examples for the future slope failures.

5.5 Verification of calibrated properties

The objectives of the verification of the shear strength properties are to verify the results of calibrated properties from the computer modeling. The Hoek and Brown criterion will be correlated with the back analysis method for various rock conditions (Hoek and Bray, 1981).

The shear strength properties of the Hoek and Brown criterion and fully saturated slope of back analysis at km 16+450, 17+000, 18+200, 18+550, 20+575, 21+225, 36+120, and 36+750 are in the range or close to the shear strength properties of disturbed weathered soft rock (between 0.04 and 1 MPa for cohesion and between 15 and 25 degrees for friction angle).

The shear strength properties of the Hoek and Brown criterion and fully saturated slope of back analysis at km 22+425, 62+950 and 78+680 are in the range of the shear strength properties of undisturbed rock (over 0.2 MPa for cohesion and over 25 degrees for friction angle).

CHAPTER VI

RECOMMENDED STABILIZATION

6.1 Introduction

The objective of this chapter is to propose the stabilization methods for preventing future slope failures along Lomsak-Chumpae highway. The slope characteristics such as rock type, slope height, slope orientation, number of joint sets, joint orientation, joint spacing, joint aperture, filled material in rock joints, JRC, groundwater conditions, existing supports, intact rock strength, and stability condition are considered for determining the types of rock slope supports. Presented in this chapter are the design approaches and the specifications of the recommended supports for each location.

6.2 Design approaches for rock supports

Two approaches are used to derive the stabilization methods: 1) Conventional approach and 2) Bieniawski's approach.

6.2.1 Conventional approach

The conventional approach gives the widely used slope stabilization method taken from numerous published case studies.

6.2.1.1 Design process

The design process considers the slope characteristics and modes of failure to derive design solutions and design components. The slope characteristics along Lomsak-Chumpae highway can be classified into two cases: (1) blocky/bedded rock and, (2) heavily jointed rock. Tables 6.1 and 6.2 list the slope characteristics and modes of failure, parameters considered, design solutions, and design components.

Based on the slope characteristics and modes of failure, the design processes of blocky/bedded rock and heavily jointed rock select the most suitable design solutions, and design components for rock supports (Chen and Collopy, 1999). Both design solutions comprise (1) rock bolts, (2) rock bolts and wire mesh, (3) rock bolts, wire mesh, and drained pipes, (4) drained pipes, (5) modified slope shape, (6) modified slope shape and rock bolts, (7) modified slope shape, rock bolts, and wire mesh, (8) modified slope shape, rock bolts, wire mesh, and drained pipes. Both parameters considered include dip direction of slope face, average joint spacing, slope height, slope length, slope face angle, and rock unit weight. Both design components include rock bolts, cement, steel plates, wire mesh, drained pipes, and method of excavations.

The specifications for the recommended supports for blocky/bedded rock and heavily jointed rock are based on slope characteristics and modes of failure (Chen and Collopy, 1999). They consist of design specifications and design construction.

Table 6.1 Design process for rock supports of blocky/bedded rock.

Slope characteristics and modes of failure	Design solutions	Parameters considered	Design components
Blocky and bedded rock with plane, wedge, and toppling failures	Solution: 1 Using rock bolts only	1.Dip direction 2. Average joint spacing 3. Slope height 4. Slope length 5. Slope face angle 6. Rock unit weight	1. Rock bolts 2. Cement 3. Steel plates
	Solution: 2 Using rock bolts and wire mesh	1.Dip direction 2. Average joint spacing 3. Slope height 4. Slope length 5. Slope face angle 6. Rock unit weight	1. Rock bolts 2. Cement 3. Steel plates 4. Wire mesh
	Solution: 3 Using rock bolts, wire mesh, and drained pipes	1. Dip direction 2. Average joint spacing 3. Slope height 4. Slope length 5. Slope face angle 6. Rock unit weight	1. Rock bolts 2. Cement 3. Wire mesh 4. Steel plates 5. PVC pipes
	Solution: 4 Using drained pipes only	1.Slope height 2. Dip direction	1. PVC pipes

Table 6.2 Design process for rock supports of heavily jointed rock.

Slope characteristics and modes of failure	Design solutions	Parameters considered	Design components
Heavily jointed rock with circular, plane, wedge, and toppling failures	Solution: 1 Using modified slope shape only	1.Slope height 2. Slope face angle	1. Backhoe
	Solution: 2 Using modified slope shape and rock bolts	1.Slope height 2. Slope face angle	1. Backhoe 2. Rock bolts 3. Steel plates 4. Cement
	Solution: 3 Using modified slope shape, rock bolts, and wire mesh	1. Slope height 2. Slope face angle 3. Average joint spacing	1. Backhoe 2. Rock bolts 3. Steel plates 4. Cement 5. Wire mesh
	Solution: 4 Using modified slope shape, rock bolts, wire mesh, and drained pipes	1. Slope height 2. Slope face angle 3. Average joint spacing	1. Backhoe 2. Rock bolts 3. Steel plate 4. Cement 5. Wire mesh 6. PVC pipes

For blocky/bedded rock as classified for some locations along Lomsak-Chumpae highway, the design specifications include (1) rock bolts, (2) wire mesh, and (3) drained pipes.

For rock bolts, fully grouted cement should be used and grout pressure should be between 150 and 200 kN/m^2 (Douglas and Arthur, 1983). The grout should be allowed to develop an adequate strength after 24 hours, before tensioning takes place (Douglas and Arthur, 1983). The diameter of the bolt depends on the working load. Normally, the working load of bolt with 25 mm diameter is between 160 and 400 kN (Williams Form Engineering Corp, 2002). This is enough for general slope. The bolt length should be 2-3 times of the joint spacing, but less than 3 m (Douglas and Arthur, 1983). The total tension (T_{total}) is modified from Hoek and Bray (1981):

$$T_{total} = (F \cdot W \cdot \text{Sin}\,\Psi_p - W \cdot \text{Cos}\,\Psi_p \cdot \tan\phi + U \cdot \tan\phi)/(\text{Cos}\,\beta + \text{Sin}\,\beta \cdot \tan\phi) \quad (5.1)$$

where F = safety factor, W = weight of slope, ϕ = friction angle, U = uplift pore pressure, β = angle of installed bolt to the plane, and Ψ_p = angle of failure plane.

The relationship between β, F, and ϕ from Hoek and Bray (1981) is

$$\beta = \tan^{-1}(1/F) \cdot \tan\,\phi \quad (5.2)$$

where F = safety factor, and ϕ = friction angle.

The weight of slope is calculated from Hoek and Bray (1981) as:

$$W = 0.5 \cdot \gamma_{rock} \cdot H^2 \cdot (\text{Cot}\,\Psi_p - \text{Cot}\,\Psi_f) \quad (5.3)$$

where γ_{rock} = unit weight of rock, H = slope height, Ψ_p = angle of failure plane, and Ψ_f = angle of slope face.

The uplift pore pressure (U) can also be calculated as:

$$U = 1/4 \cdot \gamma_w \cdot H_w^2 \cdot \text{Cosec } \Psi_p \quad (5.4)$$

where γ_w = unit weight of water, H_w = the height of water in slope, Ψ_p = failure plane angle.

Thompson et al. (1999) suggested that the opening mesh should be less than the block sizes.

The drained pipes should be installed at 5-10° from horizontal to drain groundwater effectively (Romana, 1993). The drained pipe spacing should be about 2 meters. The drained pipes can be made of fully perforated plastic PVC to allow groundwater flow into the pipes. The minimum length should be equal to the slope height to drain groundwater from the back slope out through the slope face (Hoek and Brown, 1981). They should be wide enough with a minimum diameter of 6.5 cm to drain groundwater effectively and should be wrapped with filter to prevent debris clog.

The specifications of the recommended supports for heavily jointed rock consist of the design specifications and design construction. The design specifications are provided for all rock supports: (1) modified slope shape, (2) rock bolts, (3) wire mesh, and (4) drained pipes.

The slope height should be cut for a single bench and the width of the bench should be equal or greater than 4 m (Miller et al., 2000). The specifications

for the recommended supports (bolts and drained pipes) of heavily jointed rock are similar to those of blocky and bedded rock.

The design constructions for both blocky/bedded rock and heavily jointed rock are identical. The procedures of design construction are from Douglas and Arthur (1983) as follows: (1) clear slope face and rock scaling (2) select bolt location (3) drill holes for rock bolts by any types of suitable capacity (small hand-held drill to sophisticated hydraulic or pneumatic multiples boom jumps), (4) flush out with water under pressure and/or compressed air, (5) install wire mesh, (6) insert rock bolts, (7) grout and air vent tubes, (8) grout point anchor, (9) tension bolts (using hydraulic jack or torque wrench), (10) secondary grout, (11) make a drained holes, (12) insert drained pipes.

6.2.1.2 Design recommendations for each location

The design solution for each site along Lomsak-Chumpae highway depends on the slope characteristics and modes of failure.

Ravelling on the slope face at km 16+450 causes loosed debris on the upper through the lower slope face. Pre-existing supports including wire mesh and rock bolts are damaged. Soil/rock debris has been occasionally found in the slope toe, especially in rainy season. Therefore, the slope should be benching. The width of bench is 4 m. The wire mesh opening is 5 cm. The long drained pipes should be 25 m long. They should be made of fully perforated plastic PVC with 6.5 cm in diameter wrapped by geotextile filter or other filters. The drained pipes should be installed with an angle of 5-10 degrees from horizontal with 2 meters spacing..

The slope face at km 17+000 and km 78+680 should be covered with wire mesh to prevent free fall of rock blocks. The opening of the wire mesh installed should be small enough to retain loose blocks, and acting as a curtain to prevent falling rock blocks rolling off the slope face. The sizes of rock blocks vary from pebbles to large boulders (wire mesh size<block sizes). Therefore, the wire mesh should have 5 cm opening. The mesh should be used in conjunction with rock bolts that it is tied back to the rock face with bolts. The bolt length should be 50 cm (2-3 times joint spacing) and the diameter of bolt should be 2.5 cm. The spacing of rock bolts should be 2 m (2 times joint spacing).

The rock slope at km 18+200 is stable. However, the drained pipes should be installed with an angle of 5-10 degrees from horizontal. The spacing of drained holes should be 2 m. The pipes should be 20 m long and should be made of fully perforated plastic PVC with 6.5 cm in diameter wrapped by geotextile filter or other filters.

Slope location at km 18+550 shows plane slides on the bedding plane owing to the angle of bedding planes is less than the angle of the slope face. The tension of the rock bolt calculated from the closed form solution is 2320 kN. This tension is presumably on the angle of the failure plane with 45 degrees, and the angle of the slope face is 48 degrees. However, the rock supports may be installed by spot bolts and wire mesh for preventing minor slides.

The slopes at km 20+575, 21+225, 36+120, and 36+750 show the massive circular failure. This failure brought down both earthen and supported material. Part of shotcrete remains on the slope face. The slope height should be cut

to create a bench of 4 m wide. The slope should be cut to create 45° slope face (Miller et al., 2000). Systematic fully grouted rock bolts should be installed on the slope toe. The minimum bolt length should be 2 m. The diameter of bolt should be 2.5 cm. The drained pipes should be 15 m long (length of drained pipe = slope height). They should be made of fully perforated plastic PVC with 6.5 cm in diameter wrapped by geotextile filter or other filters. The drained pipes should be installed with an angle of 5-10° from horizontal with 2 meters spacing. The wire mesh opening should be small enough to retain loose blocks, and acting as a curtain to control falling rock blocks rolling off the rock face. The sizes of rock blocks vary from pebbles to large boulders. Therefore, the wire mesh opening should be 5 cm.

The slope at km 22+425 is stable. It is not necessary to use rock supports. In addition, pre-existing supports such as rock bolt, wire mesh, and gabion wall are enough for preventing future slope failure.

6.2.2 Bieniawski's approach

6.2.2.1 Design process

Bieniawski (1989) provides the Slope Mass Rating (SMR) system for field guidelines and recommendations on rock supports, which allows a systematic use of a geomechanical classification for slopes.

The SMR classification is a development of the Bieniawski 'Rock Mass Rating' (RMR) system that can be used as a tool for the preliminary assessment of slope stability. It gives some simple rules about instability modes and the required rock supports. It cannot be a substitute for detailed analysis of each slope, which must combine both good common engineering and sound analytical method. Here, the Q

values of the studied slopes obtained from Changsuwan (1984) are converted to RMR values. The Tunneling Quality (Q) and RMR are used in deriving solution to the problem. It has been found that the equation RMR = $9\log_e Q+44$ proposed by Bieniawski (1976) adequately describes the relationship between the two systems.

The proposed SMR is obtained from RMR by subtracting a factorial adjustment factor depending on the joint-slope relationship and adding a factor depending on the method of excavation.

$$SMR = RMR+(F_1 \cdot F_2 \cdot F_3)+F_4 \quad (5.5)$$

F_1 depends on parallelism between joints and slope face strikes. Its range is from 1.00 (when both are near parallel) to 0.15 (when the angle between them is more than $30°$ and the failure probability is very low). F_2 refers to joint dip angle in the planar mode of failure. In a sense, it is a measure of the probability of joint shear strength. Its values vary from 1.00 (for joint dipping more than $45°$) to 0.15 (for joint dipping less than $20°$). F_3 reflects the relationship between the slope face and joint dip. In the planar mode of failure, it refers to the probability that joints 'daylight' in the slope face. F_4 refers to the adjustment factor for the method of excavation. Tables 6.3 and 6.4 show the adjustments rating for joints and the adjustments rating for methods of excavation of slopes. For Table 6.3, P is plane failure; T is toppling failure; α_j is joint dip direction; α_s is slope dip direction; β_j is joint dip angle; and β_s is slope dip angle.

Table 6.5 shows the relationship between Q, RMR and SMR of all slope locations. Some locations such as km 16+450, 18+200, and 36+750 have no

SMR values. Slope locations at km 16+450 and 36+750 have no joint measurements; slope location at km 18+200 is covered by shotcrete.

Afterwards, the SMR is classified as a quality of rock mass. Tentative descriptions of the SMR classes are given in Table 6.6.

Table 6.7 shows the relationship of SMR and rock supports, which provide support measures for each stability class.

Table 6.3 Adjustments rating for joints (Bieniawski, 1989).

Case	Very favorable	Favorable	Fair	Unfavorable	Very unfavorable
P $\lvert\alpha_j - \alpha_s\rvert$ T $\lvert (\alpha_j - \alpha_s) - 180^\circ \rvert$	>30°	20-30°	10-20°	5-10°	5°<
P/T F_1	0.15	0.40	0.70	0.85	1.00
P $\lvert\beta_j\rvert$	20°<	20-30°	30-35°	35-45°	>45°
P F_2	0.15	0.40	0.70	0.85	1.00
T F_2	1	1	1	1	1
P $\beta_j - \beta_s$	>10°	0-10°	0°	-10 to 0°	-10°<
T $\beta_j + \beta_s$	110°<	110-120°	>120°	-	-
P/T F_3	0	-6	-25	-50	-60

Table 6.4 Adjustments rating for methods of excavation of slopes.

Method	Natural Slope	Pre-splitting	Smooth Blasting	Blasting or Mechanical	Deficient Blasting
F_4	+15	+10	+8	0	-8

Table 6.5 The values among Q, RMR, and SMR.

Slope location	Q	RMR	F_1	F_2	F_3	F_4	SMR
Km 16+450	1.47	47.47	N/A	N/A	N/A	N/A	N/A
Km 17+000	1.47	47.47	0.85	1	-6	0	42.37
Km 18+200	0.94	43.44	shotcrete	shotcrete	shotcrete	shotcrete	shotcrete
Km 18+550	0.54	38.45	0.85	0.85	-25	0	20.39
Km 20+575	0.21	29.95	0.4	1	0	0	29.95
Km 21+225	0.81	42.10	0.15	1	-6	0	41.2
Km 22+425	6.56	60.93	0.85	0.7	0	0	60.93
Km 36+120	0.98	43.82	0.4	1	-25	0	40.07
Km 36+750	0.98	43.82	N/A	N/A	N/A	N/A	N/A
Km 62+950	3.50	55.27	0.85	1	-6	0	50.17
Km 78+680	2.62	52.67	0.85	1	0	0	52.67

Table 6.6 Tentative descriptions of SMR classes (Bieniawski, 1989).

Class	SMR	Description	Support
I	81-100	Very good	None
II	61-80	Good	Occasional
III	41-60	Fair	Systematic
IV	21-40	Poor	Important/Corrective
V	0-20	Very poor	Re-excavation

Table 6.7 Recommended support measures for each stability class (Bieniawski, 1989).

Class	SMR	Description	Rock Supports
Ia	91-100	Very good	None
Ib	81-90	Very good	None or Scaling
IIa	71-80	Good	None or Toe ditch or fence) Spot bolts
IIb	61-70	Good	Toe ditch or fence. Nets Spot or systematic bolts
IIIa	51-60	Fair	Toe ditch and/or nets, Spot or systematic bolts, spot shotcrete
IIIb	41-50	Fair	Toe ditch and/or nets, Systematic bolts, anchors, systematic shotcrete, Toe wall
IVa	31-40	Bad	Anchors, systematic, Toe wall, shotcrete, drainage or re-excavation
IVb	21-30	Poor	Systematic reinforced shotcrete, Toe wall, deep drainage, re-excavation
Va	11-20	Very poor	Gravity or anchored wall, re-excavation

6.2.2.2 Design recommendations for each location

According to the design criteria of Bieniawski (1989), the rock supports for each location can be summarized as follows.

The slope location at km 17+000 shows rock falls with SMR values equal 42.37, which is classified as fair (class IIIb). The recommended rock supports include toe ditch or wire mesh, systematic bolts/anchors, systematic shotcrete, and toe wall.

The slope location at km 18+550 contains plane failure with SMR values equal 38.45, which is classified as poor (class IVa). The recommended rock supports include systematic anchors, toe wall, shotcrete, drainange, or re-excavation.

The slope location at km 20+575 shows circular failure with SMR values equal 29.95, which is classified as poor (class IVb). The recommended rock supports include systematic reinforced shotcrete, toe wall, deep drainage, and re-excavation.

The slope location at km 21+225 shows circular failure with SMR values equal 41.2, which is classified as fair (class IIIb). The recommended rock supports include toe ditch, wire mesh, systematic bolts/anchors, systematic shotcrete, and toe wall.

The slope location at km 22+425 is stable now. SMR values equal 60.93, which is classified as good (class IIb). The recommended rock supports include toe ditch or fence, wire mesh, spot or systematic bolts.

The slope location at km 36+120 and 36+750 show circular failure with SMR values equal 40.07, which is classified as poor (class IVa). The recommended rock supports include systematic anchors, toe wall, shotcrete, drainage, or re-excavation.

The slope location at km 62+950 is stable. SMR values equal 50.17, which is classified as fair (class IIIb). The recommended rock supports include toe ditch or wire mesh, systematic bolts/anchors, systematic shotcrete, and toe wall.

The slope location at km 78+680 has shown rock falls with SMR values equal 52.67, which is classified as fair (class IIIa). The recommended rock supports include toe ditch, wire mesh, systematic bolts, or spot shotcrete.

6.3 Discussions

Two-design processes for rock supports, conventional approach and Bieniawski's approach, are compared. The conventional approach is conservative than the Bieniawski' approach. The Bieniawski's approach is a broad recommended rock supports, but the conventional approach is more specific for the study slopes. The cost of rock supports for conventional approach is probably cheaper than that of the Bieniawski's approach due to the extensive supports of Bieniawski's approach such as toe ditch, wire mesh, rock bolt, rock anchor, shotcrete, drained hole, toe-wall, and re-excavation. The conventional approach is more convenient to install rock supports than Bieniawski's approach.

CHAPTER VII

CONCLUSIONS AND RECOMMENDATIONS FOR FUTURE STUDIES

7.1 Conclusions

The main objective of this research is to investigate the slope failure and to propose remedial measures to prevent further failure along Lomsak-Chumpae highway, Thailand. The research has been conducted on 11 slope locations from km 16+450 to km 78+680. The research effort starts with desktop study and collection of existing information from the relevant books, journals, and proceedings. Field investigation has been conducted on stable and unstable slopes along the highway to understand their recent massive failures. The collected data are slope geometry, joint conditions and orientation, performance of the existing supports (if any), modes of failure, rock conditions, and groundwater conditions.

The Hoek and Brown criterion and the Mohr-Coulomb criterion are used for estimating the shear strength properties of the rock mass. The Hoek and Brown criterion uses RocLab program for determining the shear strength properties of the rock mass. The relevant parameters are fed into the RocLab program to obtain C and ϕ values. The SLOPE/W program uses to calibrate and back-calculate the shear strength properties of soil and rock and to determine the safety factor for pre-failure and post-failure of the slope at each location.

The slope characteristics at km 16+450, 17+000, 18+200, 18+550, 20+575, 21+225, 36+120 and 36+750 are similar. The rock is highly weathered and heavily fractured shale belonging to the Nam Duk Formation in the Middle Permian. The slope face angles vary from 45 to 72 degrees.

Most slope locations have three joint sets. The average joint spacing is between 5 and 20 cm. The joint apertures are between 0.1 and 1 cm. Filled materials in the rock joints are mostly clay. The JRC is estimated as 1 to 5. All rock joints are dry. The existing supports are usually damaged by slope failures. Field-determined intact rock strength is between 5 and 25 MPa, which is classified as weak rock, except km 17+000 with medium strong rock (25-50 MPa) due to less weathered and fractured than those of km 16+450, 17+000, 18+200, 18+550, 20+575, 21+225, 36+120, and 36+750.

Different slope characteristics from the above are km 22+425, 62+950, and 78+680. The joint spacings are between 5 and 30 cm. The JRC is estimated as 3 to 5. The joint apertures are between 0.1 and 1 cm. Filled material in rock joints is mostly clay. All rock joints are dry. Field-determined intact rock strength is between 50 and 100 MPa, which are classified as strong rock, except km 62+950 with medium strong rock (25-50 MPa).

The results of field investigation indicate three stable slopes, and eight unstable slopes. The stable slopes include km 18+200, 22+425, and 62+950. The unstable slopes include km 16+450, 17+000, 18+550, 20+575, 21+225, 36+120, 36+750 and 78+680. The slope location at km 18+550 shows plane failure; km 20+575, 21+225, 36+120, and 36+750 show circular failures; km 17+000 and 78+680 show minor rock falls; km 16+450 shows ravelling of rock debris.

The calibrated properties provide the shear strength properties for the safety factor calculation of each slope. For soil, the obtained C and ϕ are 0.019 MPa and 23 degrees. For the rock mass, C and ϕ are 0.021 MPa and 27 degrees. The shear strengths estimated from Hoek and Brown criterion are in good agreement with the back-calculated strengths under saturated condition.

Most rock slopes along Lomsak-Chumpae highway pose the possibility of failure due to the slope face angle is great enough to initiate subsequent failures during rainfall. Groundwater conditions in the analysis are divided into two cases: dry conditions and fully saturated conditions. The slope failures are likely to occur repeatedly in some locations (such as km 21+225 and 36+750) since the slope face angle is great and the rock mass weathers rapidly.

Two approaches are used to derive the stabilization methods: (1) conventional approach and (2) Bieniawski's approach. For the conventional approach, the design process for rock supports can be classified into two cases: (1) blocky/bedded rock with potential plane, wedge, and toppling failures; and (2) heavily jointed rock with potential circular, plane, wedge, and toppling failures. The designed slope supports depend on the slope characteristics and modes of failure. For the Bieniawski's approach, the design process for rock supports relies on SMR values, which are used to determine the rock supports for each stability class.

The rock supports of conventional approach are more conservative, specific uses, and convenient than those of Bieniawski's approach.

7.2 Discussions

The results of field investigation indicate that the failure mechanisms are complex due to the heterogeneity of the materials, the irregularity of the slope profile, and the fluctuation of groundwater in the rock mass and the overlying soil. Various combinations of several modes of failure have been found e.g., plane and wedge slides, block toppling and circular failures. Soon after the construction, rapid weathering and surface run-off have been the main factors for initial and minor failures. The occurrence of these progress failures usually associates with heavy rainfall. The weathering, erosion, and groundwater pressure probably have not been taken into consideration in the original slope design and in the later stabilization schemes. The application of full-face shotcrete induces poor drainage system, which likely contributes to the subsequent massive failure of these slopes. The drained holes are very short and cannot drain groundwater effectively. These result in pore pressure built up behind the slope face and subsequently induces the slides of rock mass and the upper soil. Recommendations for slope stabilization are based on the design criteria for rock support and the specifications of the recommended support. These lead to suitable rock supports of each location. The appropriate length drained pipes are the main remedial method to stabilize most slopes. Some slopes require wire mesh and rock bolts to prevent future failure. .

7.3 Recommendations for future studies

Direct shear testing is needed to obtain the shear strength properties because it can provide more reliable data. Holes drilling should be performed to determine actual depths of soil, highly weathered zone, and fresh intact rock zone. Some

undisturbed core specimens of shale, sandstone, and siltstone should be obtained for direct shear testing in the laboratory. The obtained shear strength properties from laboratory should be correlated with the back-calculated strength of Mohr-Coulomb criterion and rock mass shear strength estimates of Hoek and Brown criterion. Geotechnical instruments such as piezometer and inclinometer may be installed for monitoring pore pressure and deformation of the rock mass. Wide crackmeter should be used to monitor existing crack and movement of the rock masses. Original slope profile and post-failure profiles should be used into SLOPE/W program for a more rigorous and accurate slope stability calculation.

REFERENCES

Abramson, L. W., Lee, T. S., Sharma, S. and Boyce, G. M. (1995). **Slope Stability and Stabilization Methods.** New York : John Wiley & Sons.

Al-Homoud, A. S., Tal, A. B. and Taqieddin, S. A. (1997). A comparative study of slope stability methods and mitigative design of a highway embankment landslide with a potential for deep-seated sliding. **Journal of Engineering Geology**. 47: 157-173.

Barton, N., and Choubey, V. (1977). The shear strength of rock joints in theory and practice. In **Proceeding of Mechanics.** (Vol. 10, pp. 1-54). New York: Pergamon.

Bhatta, N. R. (1992). **Analysis of Slope Movment at right abutment of Mae Song Dam**. M.S. thesis, Asian Institute of Technology, Thailand.

Bieniawski, Z. T. (1976). Rock mass classification in rock engineering. In **Proceeding of Exploration for Rock Engineering.** (pp. 97-106). Cape Town: Balkema.

Bieniawski, Z. T. (1989). **Engineering Rock Mass Classifications.** New York: Wiley.

Bishop, A. W. (1955). The use of the slip circle in the stability analysis of earth slopes. In **Proceeding of Geotechnique.** (Vol. 5., pp. 7-17). New York: Oxford University.

Brown, E. T. (1981). **Rock Characterization Testing and Monitoring: ISRM Suggested Methods**. The Commission on Rock Testing Methods, International Society for Rock Mechanics, New York: Pergamon.

Changsuwan, S. (1984). **Survey of Slope Cutting, Lomsak-Chumpae Highway, Phetchabun Province**. Materail & Research Division, Department of Highway, Bangkok, Thailand.

Chen, D., and Collopy, D. (1999). Rock bolting practice and the geotechnical management system at Darlot Gold Mine. In **Proceedings of the International Symposium on Ground Support Kalgoorlie** (pp. 267-275). Rotterdam: Balkema.

Cheng, Y. and Liu, S. (1990). Power caverns of the Mingtan Pumped Storage Project, Taiwan. In J. A. Hudson (ed.). **Comprehensive Rock Engineering** (pp. 111-132). Oxford: Pergamon.

Chonglakmani, C., and Sattayarak, N. (1978). Stratigraphy of the Huai Hin Lat Formation (Upper Triassic) in Northern Thailand. In **the Third Regional Conference on Geology and Mineral Resources of Southeast Asia (**pp. 739-762). Bangkok, Thailand: Department of Mineral resources.

Douglas, T. H., and Arthur, L. J. (1983). **A guide to the use of rock reinforcement.** London: Construction Industry Research and Information Association.

Elleboudy, A. M. (1999). Geoenvironment factors influencing the deterioration of shale in a rock slope. In **Proceedings of the International Symposium on Slope Stability Engineering, Shikoku, Japan**. (Vol. 1, pp. 103-108). Rotterdam, Netherlands: Balkema.

Enoki, M. and Kokubu, A. A. (1999). Relation between slope stability and groundwater flow caused by rainfalls. In **Proceedings of the International Symposium on Slope Stability Engineering, Shikoku, Japan**. (Vol. 1, pp. 429-434). Rotterdam, Netherlands: Balkema.

Farquhar, Q. C. (1980). Geological process affecting the stability of rock slopes along Massachusetts highways. **Journal of Engineering Geology**. 16: 135-145.

Fiorillo, F. (2003). Geological features and landslide mechanisms of an unstable coastal slope (Petacciato, Italy). **Journal of Engineering Geology**. 67: 255-267.

Fuenkajorn, K. and Thongthiangdee, P. (2002). Slope failure along Lomsak-Chumpae highway, Thailand. In **Third International Conference on Landslides, Slope Stability & The Safety of Infra-structures**. (pp. 205-212). Singapore: CI-Premier.

Fujita, T. (1999). Geological Characteristics of landslides of the soft rock type, Central Japan. In **Proceedings of the International Symposium on Slope Stability Engineering, Shikoku, Japan**. (Vol. 1, pp. 169-174). Rotterdam, Netherlands: Balkema.

Geo-Slope International. (1995). **User's Guide of Slope/w for slope stability analysis, version 3**. Alberta, Canada: Geo-Slope International.

Grasselli, G. and Egger, P. (2000). 3D surface characterization for the prediction of the shear strength of rough joint. In DGGT (ed.). **Eurock 2000** (pp. 281-286). Germany: Balkema.

Helgstedt, M. D. (1997). **An Assessment of the In-Situ Shear Strength of Rock Masses and Discontinuities**. Master's Thesis: 178 CIV, Division of Rock Mechanics, Lulea University of Technology.

Helmcke, D. (1982). **On the Variscan Evolution of Central Mainland Southeast Asia**. Belgium: Earth Evolution Sciences.

Highway district of Phetchabun province. (2002). **Rainfall and Transportation data of Amphoe Lomsak**. Department of Highway, Bangkok, Thailand.

Hoek, E. (1983). Strength of jointed rock masses, 23 rd Rankine Lecture. **Journal of Geotechnique** 33: 187-223.

Hoek, E. (1990). Estimating Mohr-Coulomb friction and cohesion values from the Hoek-Brown failure criterion. **International Journal of Rock Mechanics and Mining Science.** 12 (3): 227-229.

Hoek, E. (1994). Strength of rock and rock masses. **ISRM News Journal.** 2 (2): 4-16.

Hoek, E. (2000). **Practical Rock Engineering-Hoek's 2000 edition**[On-line]. Available: http://www.rocscience.com.

Hoek, E. and Bray, J. W. (1981). **Rock Slope Engineering**. The Institute of Mining and Metallurgy, London.

Hoek, E. and Brown, E. T. (1980). **Underground Excavations in Rock.** The Institute of Mining and Metallurgy, London.

Hoek, E. and Brown, E. T. (1988). The Hoek-Brown failure criterion-a 1988 update. In **Proceeding of 15th Canadian Rock Mechanics Symposium.** (pp. 31-38). Toronto, Canada: Civil Engineering Department, University of Toronto.

Hoek, E. and Brown, E. T. (1997). Practical estimates of rock mass strength.

International Journal of Rock Mechanics and Mining Science. 34(8): 1165-1186.

Hoek, E., and Marinos, P. (2000). Predicting Tunnel Squeezing. In **Proceeding of Tunnels and Tunnelling International,** Part 1-November 2000, Part 2-December 2000. (pp. 34-36).

Hoek, E., Carranza-Torres, C. T., and Corkum, B. (2002). Hoek-Brown failure criterion-2002 edition. In **Proceeding of North American Rock Mechanics Society meeting in Toronto in July 2002.** (pp. 267-273).

Hoek, E., Keiser, P. K., and Bawden, W. F. (1995). **Support of underground excavations in hard rock.** Rotterdam: Balkema.

Hoek, E., Marinos, P. and Benissi, M. (1998). Applicability of the Geological Streng Index (GSI) classification for very weak and sheared rock masses, the case of Athens Schist Formation. **Bulletin of Engineering Geology and Environment.** 57(2): 151-160.

Hoek, E., Woods, D., and Shah, S. (1992). A modified Hoek-Brown criterion for jointed rock masses. In **Proceeding of Rock Characterization, Symposium International Society of Rock Mechanics: Eurock '92.** (pp. 209-213). London: British Geotech Society.

Huang, T. H. and Doong, Y. S. (1990). **Anisotropic shera strength of rock joints, in Rock joints, Barton & Stephansson eds.** Norway: Balkema.

Ishii, T., Yatabae, R., Yaki, N. and Yokota, K. (1999). Influence of clay minerals on strength characteristics of landslide clay in Mikabu. In **Proceedings of the International Symposium on Slope Stability Engineering, Shikoku, Japan,** (Vol. 1, pp. 697-700). Rotterdam, Netherlands: Balkema.

Jamaludin, A. and Hussein, A. N. (1999). Stabilization and remedial works on some failed slopes along the East-West highway, Malaysia. In **Proceedings of the International Symposium on Slope Stability Engineering, Shikoku, Japan,** (Vol. 2, pp. 943-948). Rotterdam, Netherlands: Balkema.

Jiang, J. C. and Yamagami, T. (2002). Back analysis of strength parameters from slope failures with a weak layer. In **Third International Conference on Landslides, Slope Stability & The Safety of Infra-structures**. (pp. 275-282). Singapore: CI-Premier.

Jiang, J. C., Yamagami, T. and Ueta, Y. (1999). Back analysis of unsaturated shear strength from a circular slope failure. In **Proceedings of the International Symposium on Slope Stability Engineering, Shikoku, Japan,** (Vol. 1, pp. 305-310). Rotterdam, Netherlands: Balkema.

Jing, L., Nordlund, E. and Stephansson, O. (1992). An experimental study on the anisotropy and stress dependency of the shear streng and deformability of rock joints. **International Journal of Rock Mechanics and Mining Science.** 29 (6): 542-565.

Kabir, M. H. and Hamid, A. M. (1999). Design and constructional aspects of an anchored slope and gabion revetment system. In **Proceedings of the International Symposium on Slope Stability Engineering, Shikoku, Japan,** (Vol. 2, pp. 901-906). Rotterdam, Netherlands: Balkema.

Kitagawa, R. (1999). Weathering mechanism and slope failures of granitic rocks in Southwest Japan-Effect of hydrothermal activities. In **Proceedings of the International Symposium on Slope Stability Engineering, Shikoku, Japan,** (Vol. 1, pp. 109-114). Rotterdam, Netherlands: Balkema.

Kumar, P. (1998). Shear Failure Envelope of Hoek-Brown criterion for Rockmass. **Journal of Tunnelling and Underground Space Technology**. 13 (4): 453-458.

Ladanyi, B. and Archambault, G. (1970). Simulation of shear behaviour of a jointed rock mass. In **Proceeding of 11 th U. S. Symposium on Rock Mechanics**. (pp. 105-125). New York: Society of Mining Engineers, AIME.

Lan, H. X., Hu, R. L., Yue, Z. Q., Lee, C. F. and Wang, S. J. (2002). Engineering and geological characteristics of granite weathering profiles in south China. **Journal of Asian Earth Sciences**. 01: 1-2.

Lanaro, F., Jing, L. and Stephansson, O. (1998). 3-D-laser measurements and representation of roughness of rock fractures, in Mechanics of In **Proceedings of the Seventh International IAEG Congress.** (pp. 2827-2935). Rotterdam, Netherlands: Balkema.

Lee, Y. H., Carr, J. R., Barr, D. J. and Haas, C. J. (1990). The fractal dimension as a measure of the roughness of rock discontinuity profiles. **International Journal of Rock Mechanics and Mining Science.** 453-464.

Lorig, L. and Varona, P. (2001). Practical slope stability analysis using finite-different codes. In W. A. Hustrulid, M. J. McCarter and D. J. A. Van Zyl (eds.). **Slope Stability in Surface Mining.** (pp. 239-250). Littleton: Society for Mining, Metallurgy and Exploration.

Lorman, W. R. (1968). **Engineering properties of shotcrete.** Pit slope manual (Chapter 6: Mechanical Support), Mines and Resources, Canada.

Maharaj, R. J. (1999). Site investigation of weathered expansive mud rock slopes: Implications for slope instability and slope stabilization. In **Proceedings of**

the International Symposium on Slope Stability Engineering, Shikoku, Japan (Vol. 1, pp. 115-120). Rotterdam, Netherlands: Balkema.

Marinos, P. and Hoek, E. (2000). GSI-A geologically friendly tool for rock mass strength estimation. In **Proceeding of GeoEng2000 Conference** (pp. 1422-1440). Melbourne, Australia: Technomic.

Marinos, P. and Hoek, E. (2001). Estimating the geotechnical properties of heterogeneous rock masses such as flysh. In **the Bulletin of the International Association of Engineering Geologists** (pp. 85-92). Canada: University of Toronto.

Michalowski, R. L. and You, L. (1999). Displacements of slope subjected to seismic loads. In **Proceedings of the International Symposium on Slope Stability Engineering, Shikoku, Japan,** (Vol. 1, pp. 637-640). Rotterdam, Netherlands: Balkema.

Miller, S. M., Girard, J. M., and McHugh, E. (2000). Computer modeling of catch benches to mitigate rockfall hazards in open pit mines. In **Proceedings of the Fourth North American Rock Mechanics Symposium Narms 2000, Washington, USA** (pp. 539-545). Rotterdam: Balkema.

Nakano, J., Miki, H., Kohashi, H. and Fujii, A. (1999). Reduction of land cutting effects by the application of lightweight embankments. In **Proceedings of the International Symposium on Slope Stability Engineering, Shikoku, Japan,** (Vol. 2, pp. 955-958). Rotterdam, Netherlands: Balkema.

Nawari, N. O. and Liang, R. (1999). Fuzzy-based stability investigation of sliding rock masses. In **Proceedings of the International Symposium on Slope**

Stability Engineering, Shikoku, Japan, (Vol. 1, pp. 335-360). Rotterdam, Netherlands: Balkema.

Omar, H., Daud, M., Zohadie, M. B., Abmalik, R. and Maail, S. (2002). Geological factors contributing to slope failure-Post Selim Highway case study. In **Third International Conference on Landslides, Slope Stability & The Safety of Infra-structures**. (pp. 365-372). Singapore: CI-Premier.

Patton, F. D. (1966). Multiple modes of shear failure in rock. In **the first Congress of International Society of Rock Mechanics.** (pp. 509-513).

Pierce, M., Brandshaug, T., and Ward, M. (2001). Slope stability assessment at the Main Cresson Mine. In W. A. Hustrulid, M. J. McCarter and D. J. A. Van Zyl (eds.). **Slope Stability in Surface Mining** (pp. 239-250). Littleton: Society for Mining, Metallurgy and Exploration.

Popescu, M. E. (2002). Landslide causal factors and landslide remediatial options. In **Third International Conference on Landslides, Slope Stability & The Safety of Infra-structures**. (p. 78). Singapore: CI-Premier.

Reading, T. J. (1966). **Shotcreting**. Pit slope manual (Chapter 6: Mechanical Support), Mines and Resources, Canada.

Reeves, M. J. (1985). Rock surface roughness and frictional strength. **International Journal of Rock Mechanics and Mining Science.** 22(6): 429-442.

Rock Engineering Group. (1989). **User's Guide of Dips program : Plotting, Analysis and Presentation of Structural Data, Using Spherical Projection Techniques**. Canada: Rocscience Inc.

Romana, M. R. (1993). A geomechanics classification for slopes: Slope Mass Rating. In **Comprehensive Rock Engineering** (Vol. 3, pp. 575-599). Hudson: Pergamon.

Sakurai, S. and Nagayama, T. (1999). A back analysis in assessing the stability of slopes by means of surface measurements. In **Proceedings of the International Symposium on Slope Stability Engineering, Shikoku, Japan,** (Vol. 1, pp. 339-344). Rotterdam, Netherlands: Balkema.

Schaefer, V. R. (2002). Residual strength and back analysis of slope in Pierre Shale. In **Third International Conference on Landslides, Slope Stability & The Safety of Infra-structures**. (pp. 407-414). Singapore: CI-Premier.

Seidal, J. P. and Haberfield, C. M. (1995). **The use of fractal geometry in a joint shear model, in Mechanics of jointed and faulted rock**. Vienna: Balkema.

Sjoberg, J., Sharp, J. C. and Malorey, D. J. (2001). Slope stability at Aznalcollar. In W. A. Hustrulid, M. J. McCarter and D. J. A., Van Zyl (eds.). **Slope Stability in Surface Mining.** (pp. 183-202). Littleton: Society for Mining, Metallurgy and Exploration.

Sonmez, H. and Ulusay, R. (1999). Modifications to the geological strength index (GSI) and their applicability to stability of slopes. **International Journal of Rock Mechanics and Mining Sciences**. 36: 743-760.

Sonmez, H., Ulusay, R. and Gokceoglu, C. (1998). A practical Procedure for the Back Analysis of Slope Failures in Closely Jointed Rock Masses. **International Journal of Rock Mechanics and Mining Sciences**. 35 (2): 219-233.

Stillborg, B. (1994). **Professional users handbook for rock bolting**. Clausthal-Zellerfeld: Trans Tech Publications.

Suorineni, F. T., Tannant, D. D. and Keiser, P. K. (1999). Determination of fault-related sloughage in open stopes. **International Journal of Rock Mechanics and Mining Sciences**. 36: 891-906.

Thompson, A. G., Winsor, C. R., and Cadby, G. W. (1999). Performance assessment of mesh for ground control applications. In **Proceedings of the International Symposium on Ground Support Kalgoorlie** (pp. 119-130). Rotterdam: Balkema.

Tse, R. and Cruden, D. M. (1979). Estimating joint roughness coefficients. In **International Journal of Rock Mechanics and Mining Science.** 16: 303-307.

Wannakao, L., Archwichai, L., Buaphan, C., Wannakao, P. and Muangnoicharoen, N. (1985). **The Study of Rock Slope Stability at km 18-24 along Lomsak-Chumpae highway.** Department of Geotechnology, Khon Kaen University, Thailand.

Williams Form Engineering Corp. (2002). **Spin-Lock Mechanical Rock Anchor Systems.** USA.

Xie, H. P., Wang, J. A. and Kwasniewski, M. A. (1999). Multifractal characterization of rock fracture surfaces. **International Journal of Rock Mechanics and Mining Science.** 36: 19-27.

Xie, H. P., Wang, J. A. and Xie, W. H. (1997). Fractal effects of surface roughness on the mechanical behavior of rock joints. In **Proceeding of Chaos Solution and Fractals.** (Vol. 8, pp. 221-252).

Zhao, J. (2000). Applicability of Mohr-Coulomb and Hoek-Brown strength criteria to the dynamic strength of brittle rock. **International Journal of Rock Mechanics and Mining Sciences**. 37: 1115-1121.

APPENDIX A

RAINFALL DATA

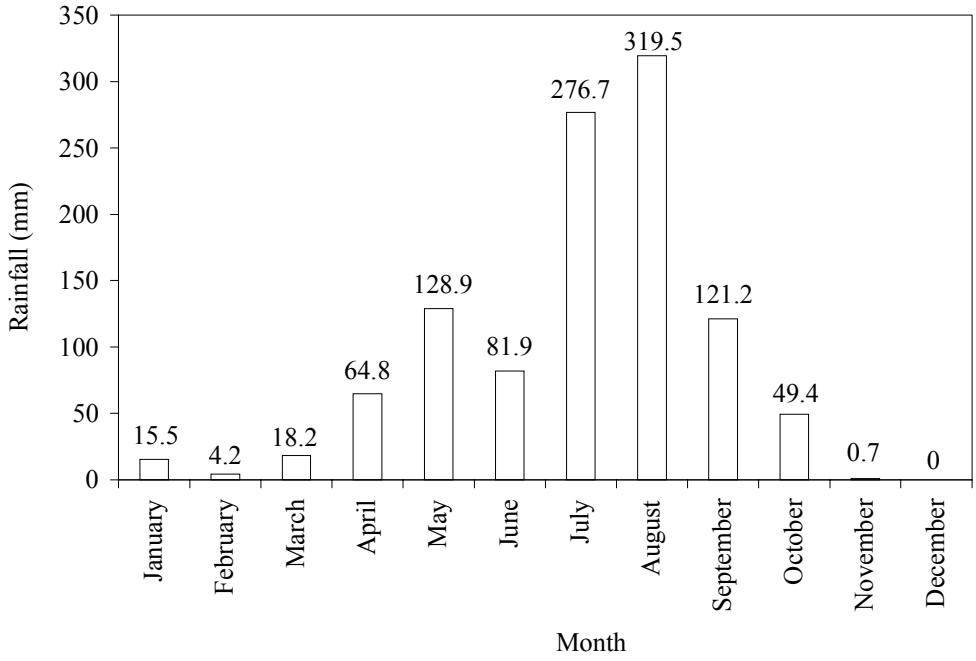

Figure A.1 Rainfall data in 1995 of Lomsak-Chumpae highway, Thailand.

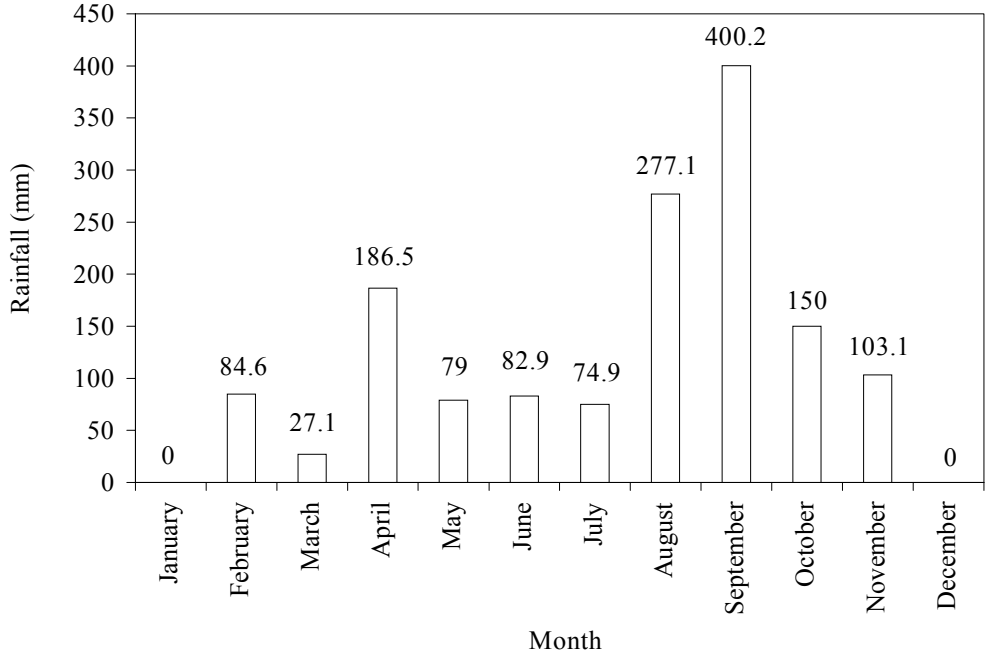

Figure A.2 Rainfall data in 1996 of Lomsak-Chumpae highway, Thailand.

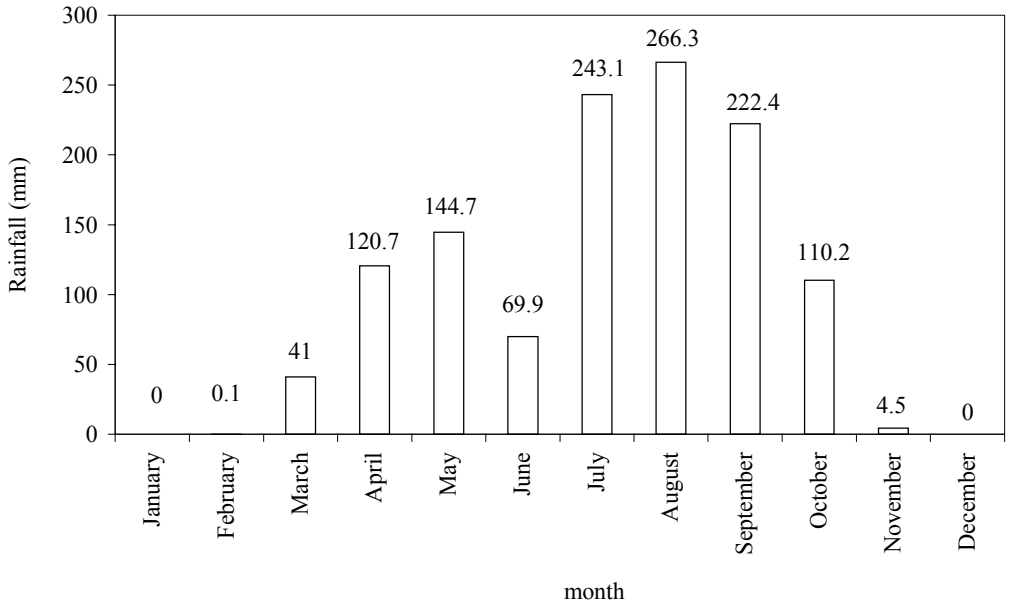

Figure A.3 Rainfall data in 1997 of Lomsak-Chumpae highway, Thailand.

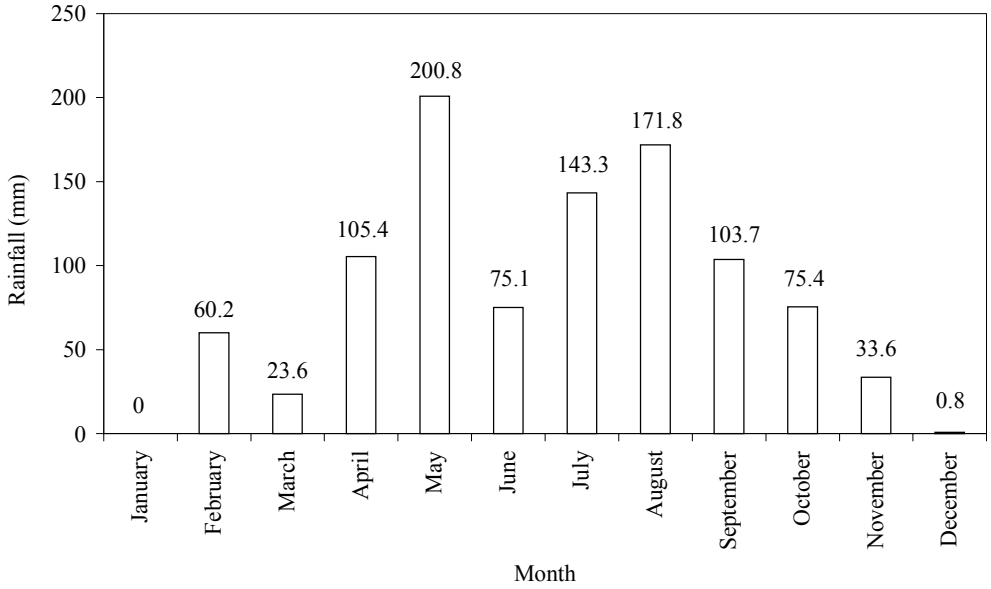

Figure A.4 Rainfall data in 1998 of Lomsak-Chumpae highway, Thailand.

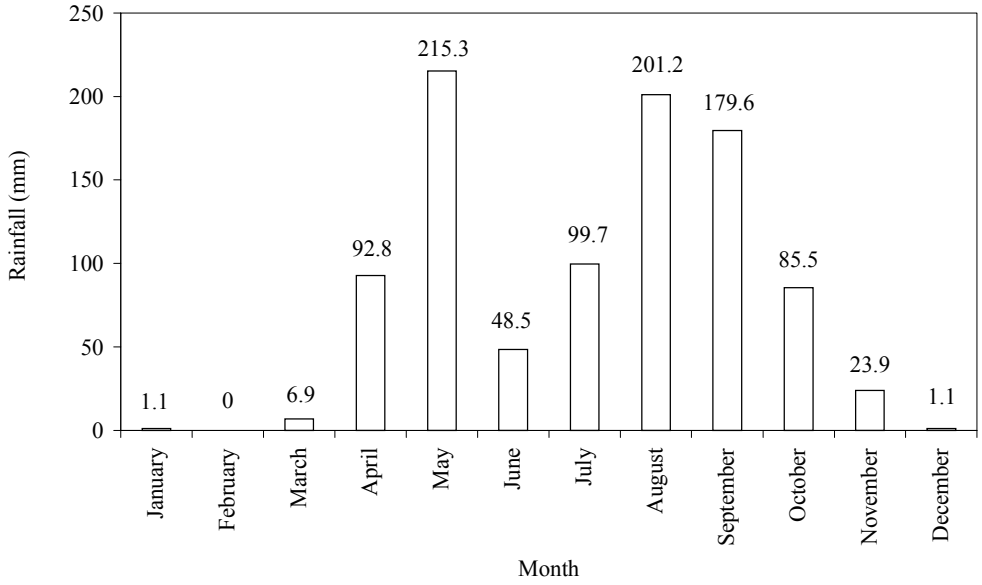

Figure A.5 Rainfall data in 1999 of Lomsak-Chumpae highway, Thailand.

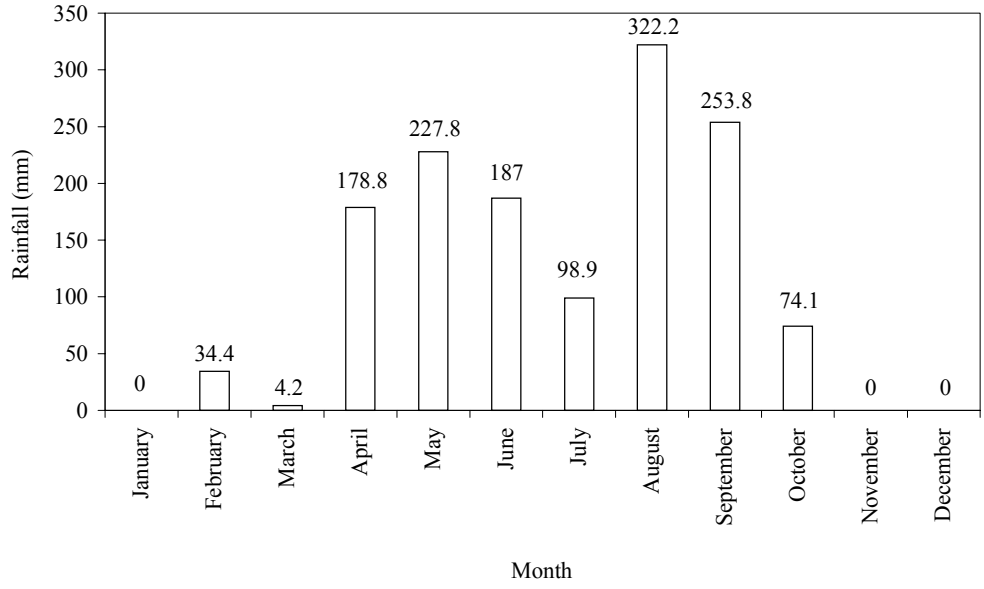

Figure A.6 Rainfall data in 2000 of Lomsak-Chumpae highway, Thailand.

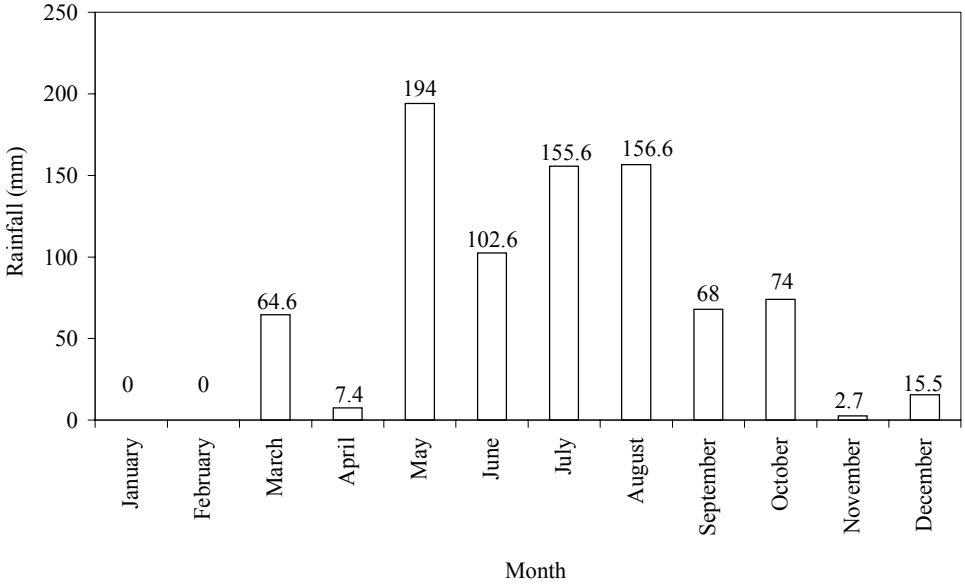

Figure A.7 Rainfall data in 2001 of Lomsak-Chumpae highway, Thailand.

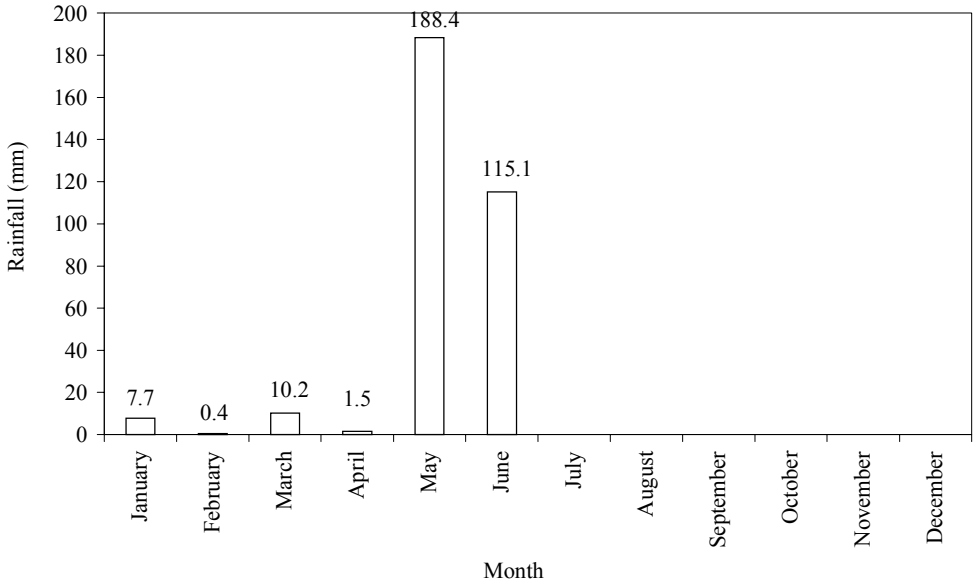

Figure A.8 Rainfall data in 2002 of Lomsak-Chumpae highway, Thailand.

APPENDIX B

TRANSPORTATION DATA

Table B.1 Average annual daily traffic on highway 1995.

No	Route Control	Location name	Km.	Car	Light bus	Heavy bus	Light truck	Medium truck	Heavy truck	Total	Bicycle	Motorcycle	Total	District
1	12	Km. 90+500 (Phitsanulok district junction) to Camp Son	94+000	505	112	83	1164	144	74	2082	3	328	331	Phetchabun
2	12	Junction of Camp Son to Junction of Lomsak	120+000	691	104	63	1615	172	102	2747	2	362	364	Phetchabun
3	12	Km. 130+000 to km. 130+545	130+300	51	1	11	225	25	29	342	2	170	172	Phetchabun
4	12	Junction of Lomsak to Ban Pakchong	2+000	534	133	60	1650	134	98	2609	36	1313	1349	Phetchabun
5	12	Ban Pakchong to Namnao National Park	27+500	575	152	164	757	222	102	1972	3	228	231	Phetchabun
6	12	Namnao National Park to km.73+200 (Namnao National Park)	53+100	822	138	164	642	226	132	2124	0	198	198	Phetchabun

Table B.2 Average annual daily traffic on highway 1996.

No	Route Control	Location name	Km.	Car	Light bus	Heavy bus	Light truck	Medium truck	Heavy truck	Total	Bicycle	Motorcycle	Total	District
1	12	Km. 90+500 (Phitsanulok district junction) to Camp Son	94+000	425	160	69	1675	173	79	2581	2	504	506	Phetchabun
2	12	Junction of Camp Son to Junction of Lomsak	120+000	729	160	58	2049	167	58	3221	7	467	474	Phetchabun
3	12	Km. 130+000 to km. 130+545	130+300	146	2	2	250	24	28	452	5	210	215	Phetchabun
4	12	Km. 130+200 to km. 130+750	130+500	183	13	14	844	153	97	1304	11	532	543	Phetchabun
5	12	Junction of Lomsak to Ban Pakchong	2+000	1156	258	151	2235	202	43	4045	125	1781	1906	Phetchabun
6	12	Ban Pakchong to Namnao National Park	27+500	617	61	58	680	105	26	1547	3	243	246	Phetchabun
7	12	Namnao National Park to km.73+200 (Namnao National Park)	53+100	268	44	127	892	93	20	1444	4	107	111	Phetchabun

Table B.3 Average annual daily traffic on highway 1997.

No	Route Control	Location name	Km.	Car	Light bus	Heavy bus	Light truck	Medium truck	Heavy truck	Total	Bicycle	Motorcycle	Total	District
1	12	Km. 90+500 (Phitsanulok district junction) to Camp Son	94+000	808	73	64	2138	164	106	3353	-	662	662	Phetchabun
2	12	Junction of Camp Son to Junction of Lomsak	120+000	742	113	65	2241	201	166	3528	-	526	526	Phetchabun
3	12	Km. 130+000 to km. 130+545	130+300	289	12	12	95	26	11	445	2	294	296	Phetchabun
4	12	Km. 130+200 to km. 130+750	130+500	167	20	14	509	94	31	835	19	392	411	Phetchabun
5	12	Junction of Lomsak to Ban Pakchong	2+000	1480	534	135	2611	495	306	5561	82	2074	2156	Phetchabun
6	12	Ban Pakchong to Namnao National Park	27+500	479	55	60	953	131	56	1734	1	375	376	Phetchabun
7	12	Namnao National Park to km.73+200 (Namnao National Park)	53+100	455	21	54	1018	91	25	1664	6	154	160	Phetchabun

Table B.4 Average annual daily traffic on highway 1998.

No	Route Control	Location name	Km.	Car	Light bus	Heavy bus	Light truck	Medium truck	Heavy truck	Total	Bicycle	Motorcycle	Total	District
1	12	Km. 90+500 (Phitsanulok district junction) to Camp Son	94+000	607	55	56	1883	164	44	2809	17	727	744	Phetchabun
2	12	Junction of Camp Son to Junction of Lomsak	120+000	740	93	74	2174	239	161	3481	0	504	504	Phetchabun
3	12	Km. 130+000 to km. 130+545	130+300	38	13	2	131	11	15	210	6	149	155	Phetchabun
4	12	Km. 130+200 to km. 130+750	130+500	286	86	33	750	70	48	1273	7	499	506	Phetchabun
5	12	Junction of Lomsak to Ban Pakchong	2+000	394	146	48	2761	97	44	3490	17	1548	1565	Phetchabun
6	12	Ban Pakchong to Namnao National Park	27+500	865	126	59	768	169	36	2023	2	400	402	Phetchabun
7	12	Namnao National Park to km.73+200 (Namnao National Park)	53+100	634	38	54	1036	189	48	1999	0	270	270	Phetchabun

Table B.5 Average annual daily traffic on highway 1999.

No	Route Control	Location name	Km.	Car	Light bus	Heavy bus	Light truck	Medium truck	Heavy truck	Total	Bicycle	Motorcycle	Total	District
1	12	Km. 90+500 (Phitsanulok district junction) to Camp Son	94+000	585	234	66	2268	215	69	3437	0	1183	1183	Phetchabun
2	12	Junction of Camp Son to Junction of Lomsak	120+000	1061	187	96	2790	311	198	4643	7	1323	1330	Phetchabun
3	12	Km. 130+000 to km. 130+545	130+300	190	46	8	378	43	41	706	20	627	647	Phetchabun
4	12	Km. 130+200 to km. 130+750	130+500	293	40	10	649	51	21	1064	32	816	848	Phetchabun
5	12	Junction of Lomsak to Ban Pakchong	2+000	592	95	54	2297	86	51	3175	34	3064	3098	Phetchabun
6	12	Ban Pakchong to Namnao National Park	27+500	585	100	107	1328	195	92	2407	12	568	580	Phetchabun
7	12	Bypass Khon Kaen	8+600	11649	404	630	320	770	397	14170	59	6823	6882	Phetchabun
8	12	Namnao National Park to km.73+200 (Namnao National Park)	53+100	1341	119	120	430	160	75	2245	2	306	308	Phetchabun

Table B.6 Average annual daily traffic on highway 2000.

No	Route Control	Location name	Km.	Car	Light bus	Heavy bus	Light truck	Medium truck	Heavy truck	Total	Bicycle	Motorcycle	Total	District
1	12	Km 90+500 (Phitsanulok district junction) to Camp Son	94+000	537	116	96	1559	176	84	2568	9	400	409	Phetchabun
2	12	Junction of Camp Son to Junction of Lomsak	120+000	655	84	64	2581	163	108	3655	2	293	295	Phetchabun
3	12	Junction of Lomsak to Ban Pakchong	2+000	581	141	63	3256	155	80	4276	13	1579	1592	Phetchabun
4	12	Ban Pakchong to Namnao National Park	27+500	903	45	74	438	74	21	1555	12	175	197	Phetchabun
5	12	Namnao National Park to km.73+200 (Namnao National Park)	53+100	594	69	81	693	111	55	1603	0	92	92	Phetchabun

APPENDIX C

ANALYSIS OF ROCK MASS SHEAR STRENGTH

USING ROCLAB

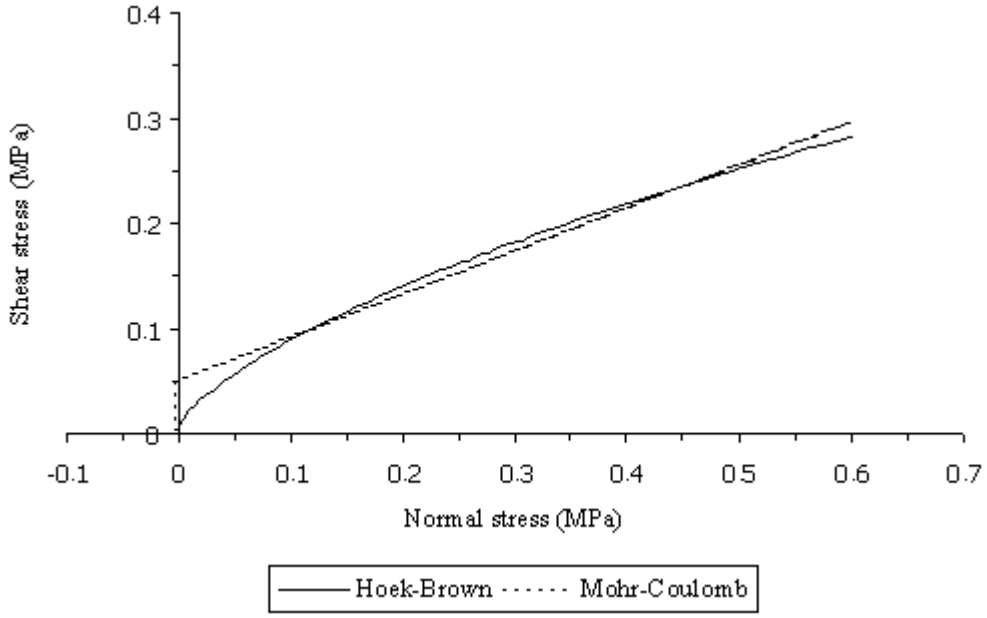

Figure C.1 The estimates of the shale shear strength by using RocLab program at km 16+450. Hoek-Brown and equivalent Mohr-Coulomb failure envelope are plotted in shear-normal stress. The cohesion and the friction angle are 0.051 MPa and 22 degrees.

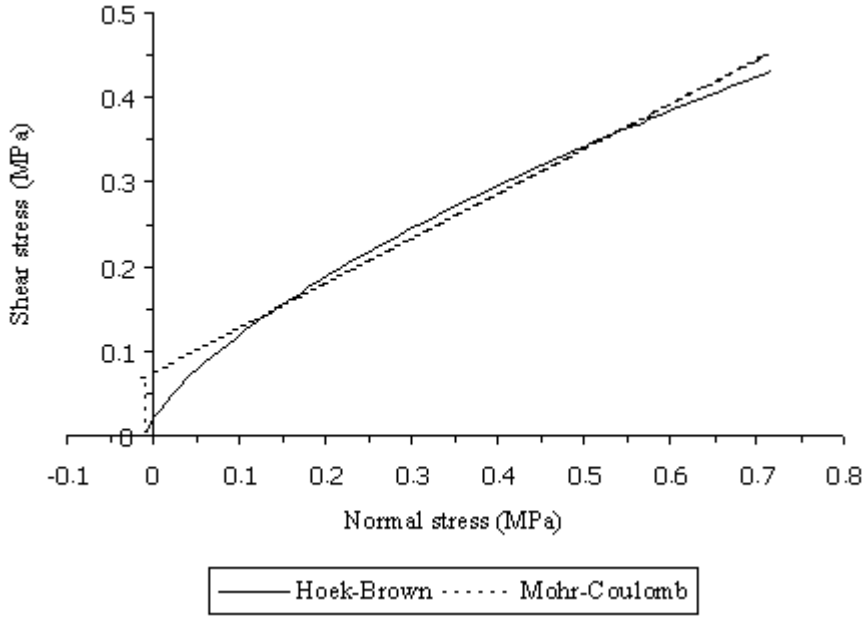

Figure C.2 The estimates of the shale shear strength by using RocLab program at km 17+000. Hoek-Brown and equivalent Mohr-Coulomb failure envelope are plotted in shear-normal stress. The cohesion and the friction angle are 0.074 MPa and 28 degrees.

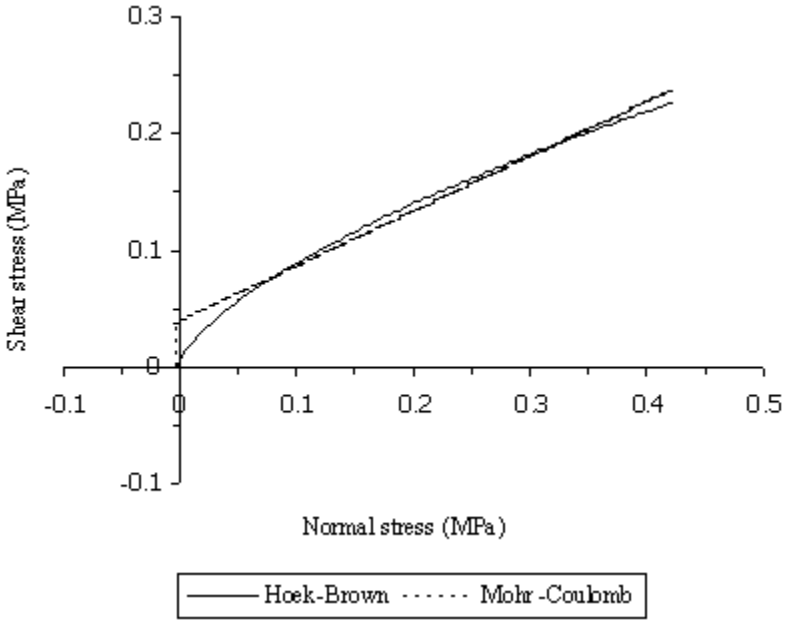

Figure C.3 The estimates of the shale shear strength by using RocLab program at km 18+200. Hoek-Brown and equivalent Mohr-Coulomb failure envelope are plotted in shear-normal stress. The cohesion and the friction angle are 0.040 MPa and 25 degrees.

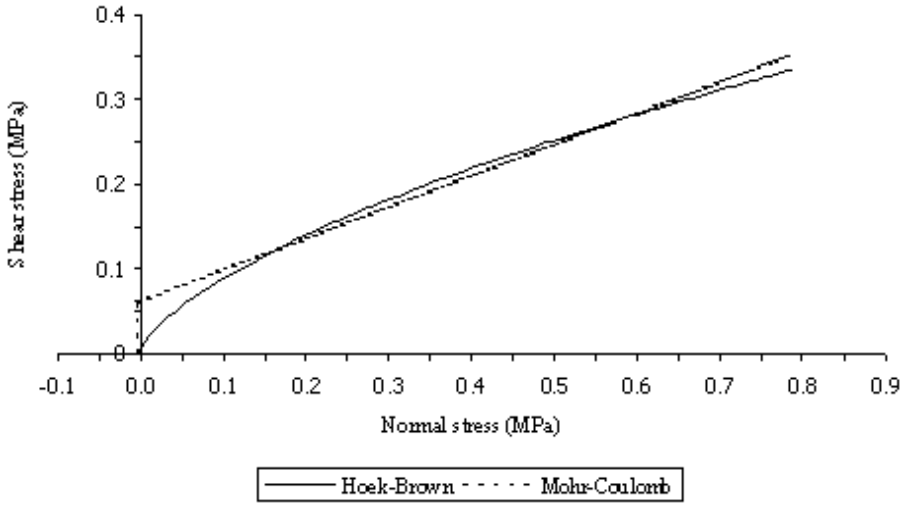

Figure C.4 The estimates of the slaty shale shear strength by using RocLab program at km 18+550. Hoek-Brown and equivalent Mohr-Coulomb failure envelope are plotted in shear-normal stress. The cohesion and the friction angle are 0.061 MPa and 20 degrees.

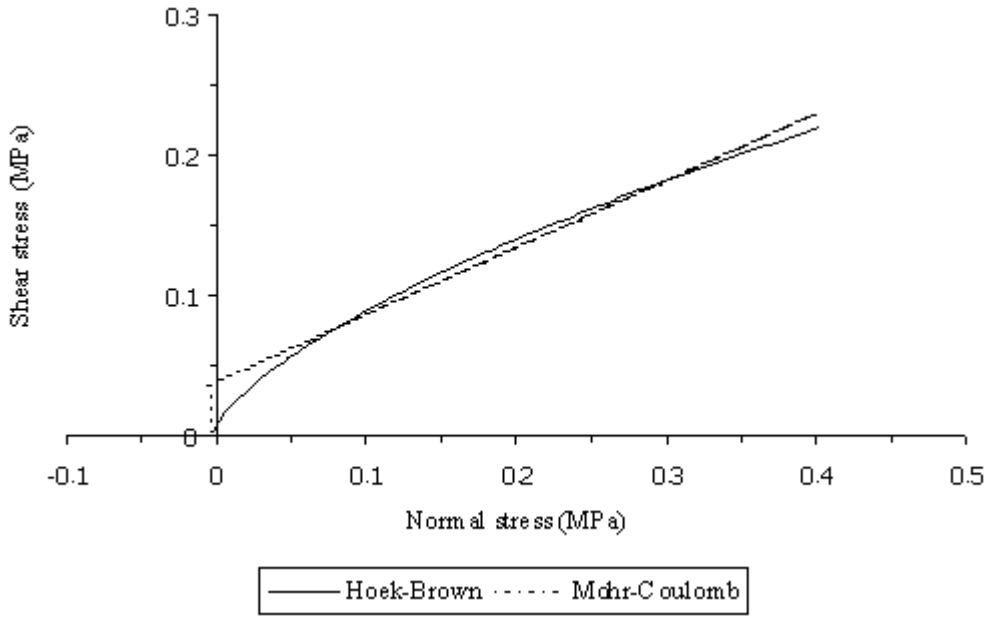

Figure C.5 The estimates of the shale shear strength by using RocLab program at km 20+575. Hoek-Brown and equivalent Mohr-Coulomb failure envelope are plotted in shear-normal stress. The cohesion and the friction angle are 0.038 MPa and 26 degrees.

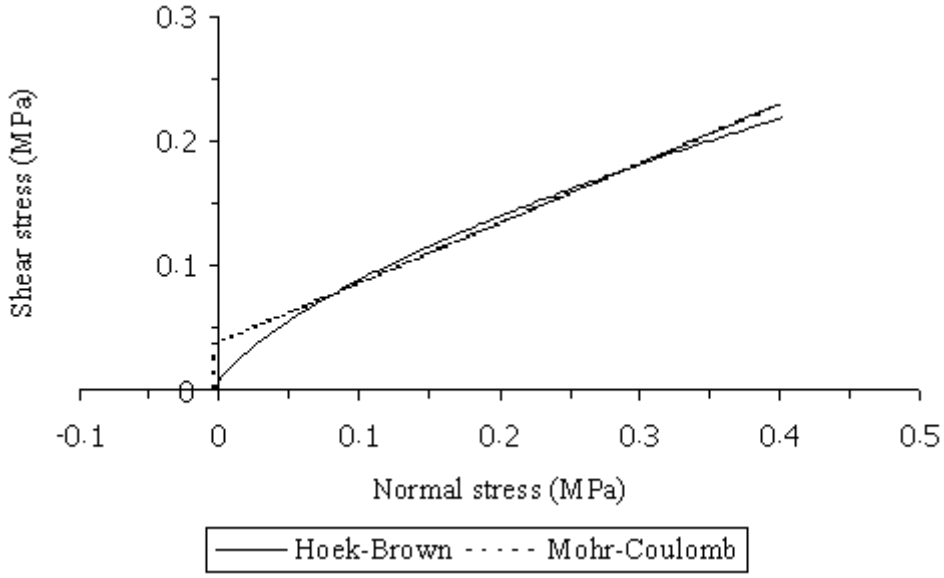

Figure C.6 The estimates of the shale shear strength by using RocLab program at km 21+225. Hoek-Brown and equivalent Mohr-Coulomb failure envelope are plotted in shear-normal stress. The cohesion and the friction angle are 0.038 MPa and 26 degrees.

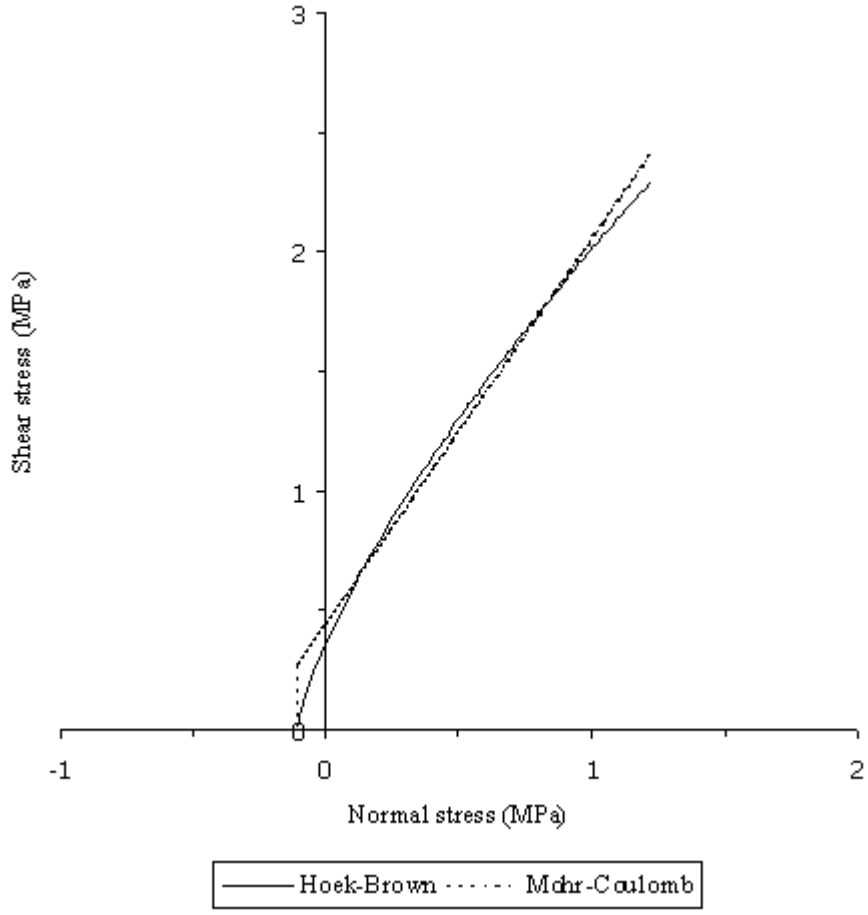

Figure C.7 The estimates of the sandstone shear strength by using RocLab program at km 22+425. Hoek-Brown and equivalent Mohr-Coulomb failure envelope are plotted in shear –normal stress. The cohesion and the friction angle are 0.449 MPa and 58 degrees.

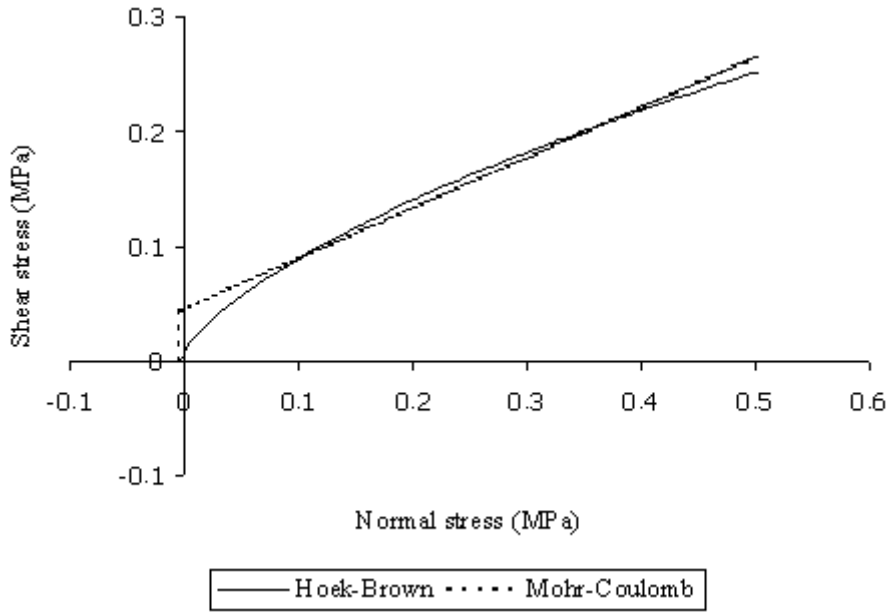

Figure C.8 The estimates of the shale shear strength by using RocLab program at km 36+120. Hoek-Brown and equivalent Mohr-Coulomb failure envelope are plotted in shear-normal stress. The cohesion and the friction angle are 0.045 MPa and 24 degrees.

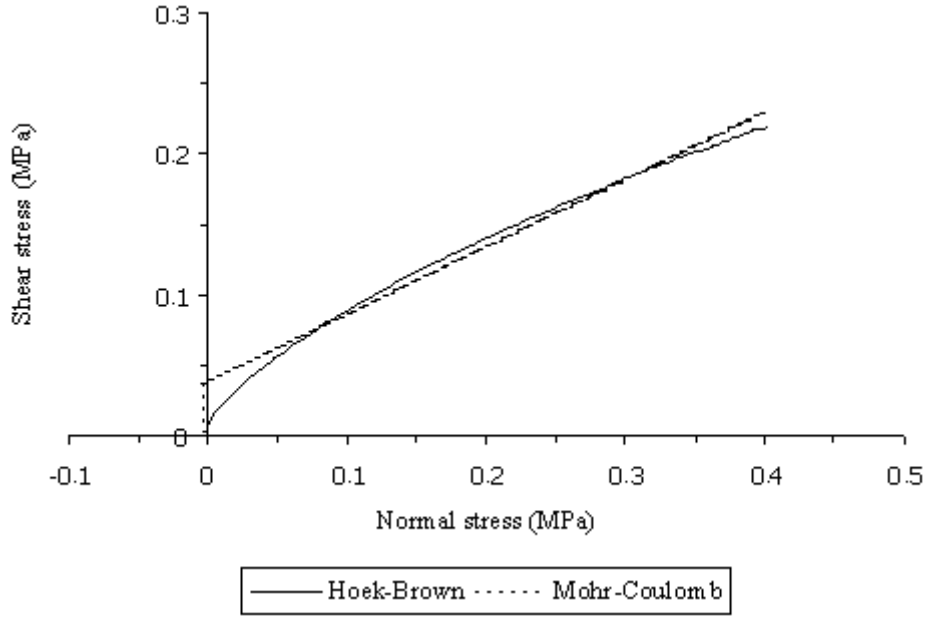

Figure C.9 The estimates of the shale shear strength by using RocLab program at km 36+750. Hoek-Brown and equivalent Mohr-Coulomb failure envelope are plotted in shear-normal stress. The cohesion and the friction angle are 0.038 MPa and 26 degrees.

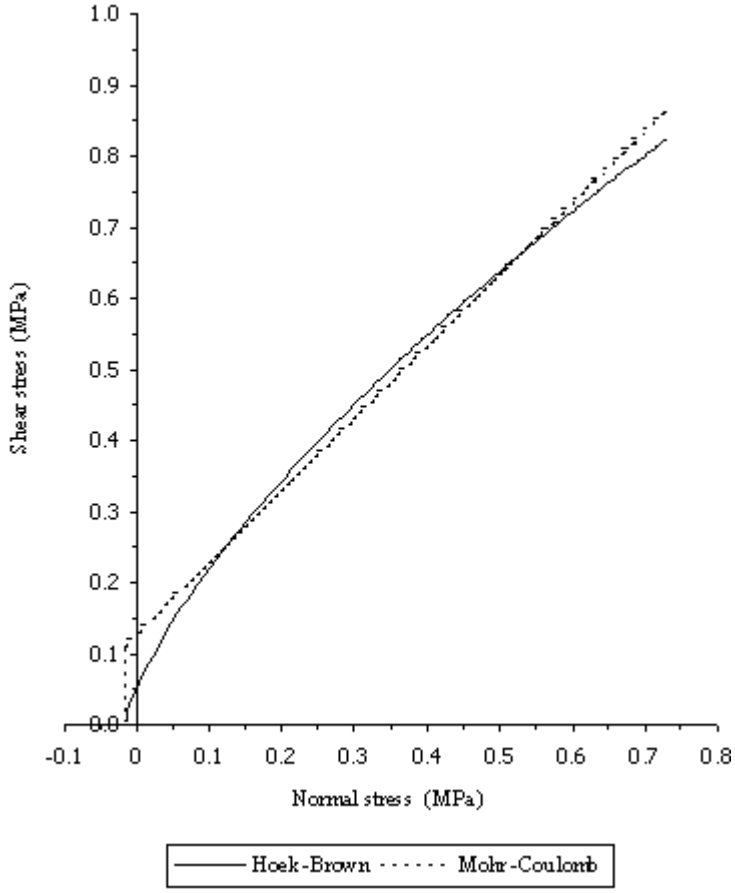

Figure C.10 The estimates of the sandstone interbedded with siltstone shear strength by using RocLab program at km 62+950. Hoek-Brown and equivalent Mohr-Coulomb failure envelope are plotted in shear-normal stress. The cohesion and the friction angle are 0.129 MPa and 45 degrees.

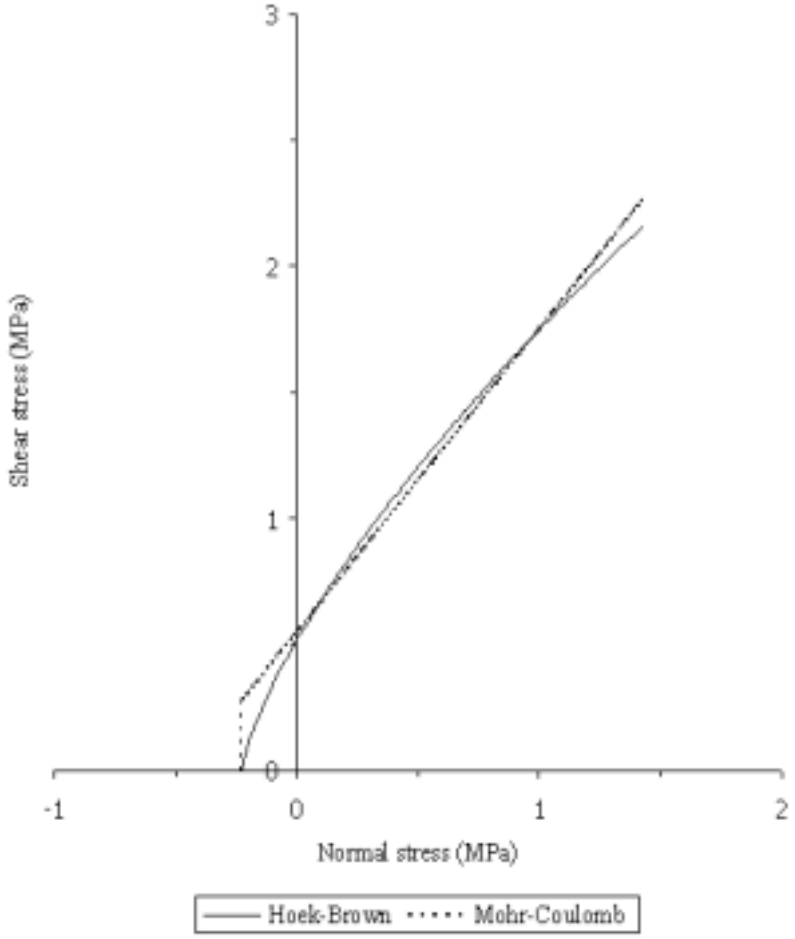

Figure C.11 The estimates of the limestone shear strength by using RocLab program at km 78+680. Hoek-Brown and equivalent Mohr-Coulomb failure envelope are plotted in shear-normal stress. The cohesion and the friction angle are 0.554 MPa and 50 degrees.

BIOGRAPHY

Mr. Parinya Thongthiangdee was born on the 2nd of January 1969 in Ubon Ratchathani province. He earned his Bachelor's Degree in Geotechnology, Department of Geotechnology, Faculty of Technology, Khon Kaen University (KKU) in 1992. After graduation, he has been employed under the position of engineering geologist by the GMT Corporation Ltd. He has been promoted to be a head of the foundation investigation section. From 1999 to 2003, he studied for his Master's Degree in the School of Geotechnology, Institute of Engineering at Suranaree University of Technology (SUT) with the major in Geological Engineering. His expertise is in the areas of soil and rock mechanics, field-testing and geotechnical instrumentation.